GEORG-AUGUST-UNIVERSITÄT
GÖTTINGEN

Dissertation

Ablation of cell-specific cholesterol synthesis affects cerebral β-amyloidosis

for the award of the degree
“Doctor rerum naturalium”
of the Georg-August-Universität Göttingen

within the doctoral program Biology
of the Georg-August University School of Science (GAUSS)

submitted by

Lena Spieth

from Ludwigsburg

Göttingen, 2022

Thesis Advisory Committee

Dr. Gesine Saher (1st Reviewer)
Department of Neurogenetics, Max Planck Institute for Multidisciplinary Sciences

Prof. Dr. Thomas Bayer (2nd Reviewer)
Division of Molecular Psychiatry, University Medical Center Göttingen

Prof. Dr. Dr. Hannelore Ehrenreich
Department of Clinical Neuroscience, Max Planck Institute for Multidisciplinary Sciences

Extended Examination Board

Prof. Dr. Rüdiger Behr
Degenerative Diseases, German Primate Center, Göttingen

Prof. Susann Boretius
Functional Imaging, German Primate Center, Göttingen

Dr. Nico Posnien
Developmental Biology, University Medical Center Göttingen

Date of Oral Examination
02.05.2022

Declaration

I hereby declare that I wrote this PhD thesis with the title “Ablation of cell-specific cholesterol synthesis affects cerebral β-amyloidosis” independently with no other contributory sources and aids than quoted.

Göttingen, March 2022

Lena Spieth

Table of content

Abstract

Cholesterol, an essential membrane component, among others modifies membrane fluidity and regulates cell signaling. CNS cholesterol metabolism is separated from peripheral cholesterol by specific properties of the blood-brain-barrier. Therefore, cholesterol homeostasis within the lipid-rich brain is maintained by *ne novo* synthesis. In principle, every brain cell is capable of synthesizing cholesterol although astrocytes are generally considered to be the major producers that subsequently release and horizontally transfer cholesterol via lipoproteins to other brain cells. Intriguingly, disturbances in CNS cholesterol metabolism have been linked to Alzheimer´s disease (AD). Major genetic risk factors for sporadic AD are gene variants of apolipoprotein E (ApoE) and the apolipoprotein J (ApoJ). These lipoprotein variants have been considered to not only affect horizontal cholesterol transfer but also seeding, spreading and clearance of senile plaques. Most importantly, the primary neuropathological hallmark, extracellular senile plaques composed of amyloid β-peptides, is influenced by amyloid precursor protein (APP) metabolism which is predominantly situated in cholesterol-rich membrane lipid rafts in neurons. However, how exactly disturbances of CNS cholesterol homeostasis contributes to its pathogenesis is elusive.

This study is aimed at elucidating the role of *de novo* cholesterol synthesis in different cell types in mouse models of AD. The effect on amyloid burden by abolishing cholesterol synthesis in neurons, astrocytes, and microglia, respectively, was analyzed. This was achieved by cell-type specific genetically inactivated cholesterol synthesis gene *Fdft1*. The *Fdft1* gene encodes squalene synthase which catalyzes the first committed step of cholesterol synthesis. Surprisingly, lack of cholesterol synthesis in neurons did not alter APP processing or amyloid plaque burden. In contrast, glial cholesterol synthesis influenced the density of amyloid plaques. Whereas the disturbance of cholesterol in astrocytes resulted in a decrease in amyloid plaques, unexpectedly, mice lacking cholesterol synthesis in microglia showed an extensive increase. Using a transcriptomic approach, it could be shown that microglial cholesterol was required to mount the full DAM (disease associated microglia) signature upon amyloid exposure. In contrast, coverage of amyloid plaques by microglia was surprisingly increased. This work unraveled important cell- and glia-type- specific differences in the role of cholesterol synthesis on plaque metabolism. The here presented data suggest sterol synthesis in glia cells as an important disease modifier with intriguing opposite effects of astrocytic and microglial cholesterol synthesis inactivation. In addition, the findings highlight the need for cell-type specificity in the development of cholesterol-targeting drugs to combat AD.

1 Introduction

1.1 The central nervous system and its cells

The central nervous system (CNS) consists of two parts, the brain and spinal cord. Despite the fact that the brain is only 2% of the body weight, the brain uses 20% of the overall oxygen consumption to fulfil functions ranging from transmission of neuronal stimuli to immune defense mechanisms (Gallagher et al., 1998; Hyder et al., 2013). To fulfill this variety of functions, the brain is equipped with highly specialized cell types that can be roughly classified as neurons and glia cells. Via synapses, neurons form chemo-electrical circuits in which impulses can be conveyed between cells. Oligodendrocytes are derived from oligodendrocyte precursor cells (OPC); these comprise myelinating oligodendrocytes, which generate myelin to ensheath axons for faster signal propagation, and satellite cells that regulate the perineuronal microenvironment (Simons & Nave, 2015). Astrocytes, the most abundant cell type in the CNS provide structural support, are involved in formation of the blood brain barrier (BBB), and maintain synaptic transmission. Regulation of CNS homeostasis, repair following injury, and modulation of inflammatory events are other tasks performed by astrocytes (Sofroniew & Vinters, 2010). The main immunoregulating and immunosurveilling cells in the brain are microglia cells. Microglia can acquire phagocytotic activity to remove cellular debris and abnormal deposits (Li & Barres, 2018). Ependymal cells are located between nervous tissue and cerebrospinal fluid (CSF) with cilia protruding into the CSF to circulate the fluid. The exchange of molecules between the periphery and brain interstitial fluid is regulated by endothelial cells that form the BBB together with astrocyte end-feet and pericytes (Del Bigio, 2010). Pericytes partially cover endothelial cells and regulate tight junction (TJ) proteins, which regulates BBB permeability. Due to the BBB, lipid metabolism is largely separated from the peripheral circulation (Armulik et al., 2010).

1.1.1 CNS lipids and cholesterol

The brain is a highly lipid-rich organ and comprises roughly one quarter of the body cholesterol. Lipids are essential for forming cell membranes in general and for myelin in particular as a membrane protrusion by maintaining membrane fluidity, permeability and electrical characteristics and thereby facilitating transmembrane signal transduction and vesicular trafficking (Orth & Bellosta, 2012). Due to the BBB, lipoproteins and thereby cholesterol uptake into the brain is prevented therefore the synthesis of cholesterol, the key structural component of lipid membranes takes place endogenously (Bjorkhem & Meaney, 2004). Each cell type has its

individual need for sterols and therefore the capability to synthesize cholesterol. *In vitro* studies showed a 2-3 times higher production rate of cholesterol in astrocytes compared to neurons and an even higher synthesis activity in oligodendrocytes that could meet the needs for developmental myelination. Further studies suggest the capability of embryonic neurons to generate cholesterol and a redistribution of cholesterol production in the adult brain (Fünfschilling et al., 2007; Koper et al., 1984; Pfrieger, 2003; Saher et al., 2005; Saito et al., 1987). In the adult brain, when myelination is predominantly completed, stable but rather low levels of cholesterol synthesis ensure homeostasis. Cholesterol can be transferred between CNS cells depending on the cellular demands. Excess cholesterol can be exported from the CNS via two ways, in the shedding pathway surplus cholesterol is released into the CSF associated with apolipoprotein E (ApoE). In a second pathway cholesterol is exported via conversion to oxysterols that can pass the BBB due to their physical properties (Bjorkhem, 2006).

1.1.2 Cholesterol biosynthesis and metabolism

All mammalian nucleated cells have the ability to synthesize cholesterol. Cholesterol biosynthesis (Figure 1) is an energy consuming, complex multistep process that involves many enzymes (Bloch, 1965). Under physiological conditions cholesterol levels are quite stable only a small proportion is replenished on regular basis. The daily production rate of sterols in the brain is in the magnitude of 15-20mg/g bodyweight in several species, including mice (Dietschy & Turley, 2004). The counterparts of biosynthesis and excretion are tightly regulated to maintain homeostasis. De novo synthesis occurs predominantly in the endoplasmic reticulum (ER). The first part of cholesterol synthesis involves the isoprenoid biosynthesis pathway. Acetyl-CoA and acetoacetyl-CoA are converted to 3-hydroxy-3-methylglutaryl-CoA (HMG-CoA) by the enzyme HMG-CoA synthase (HMGCS) followed by the reduction to mevalonate by HMG-CoA reductase (HMGCR). HMGCR, one of the rate-limiting enzymes of the sterol synthesis is the target of statins, a widespread group of cholesterol lowering drugs. Mevalonate is activated by two subsequent phosphorylation steps to form mevalonate 5-phosphate and mevalonate 5-diphosphate. The activated isoprenoid molecule isopentenyl pyrophosphate (IPP) results from the decarboxylation of mevalonate 5-diphosphate. In equilibrium with IPP is its isomer dimethylallyl pyrophosphate (DMAPP), IPP and DMAPP combine to form geranyl pyrophosphate (GPP). By adding another IPP molecule farnesyl pyrophosphate (FPP) is generated, the condensation of FPP results in squalene. Squalene formation is the first committed step of the cholesterol synthesis and is catalyzed by farnesyl-diphosphate farnesyltransferase 1 (FDFT1). Squalene epoxidase (also called squalene monooxygenase, SQLE) catalyzes the second rate-limiting step to lanosterol.

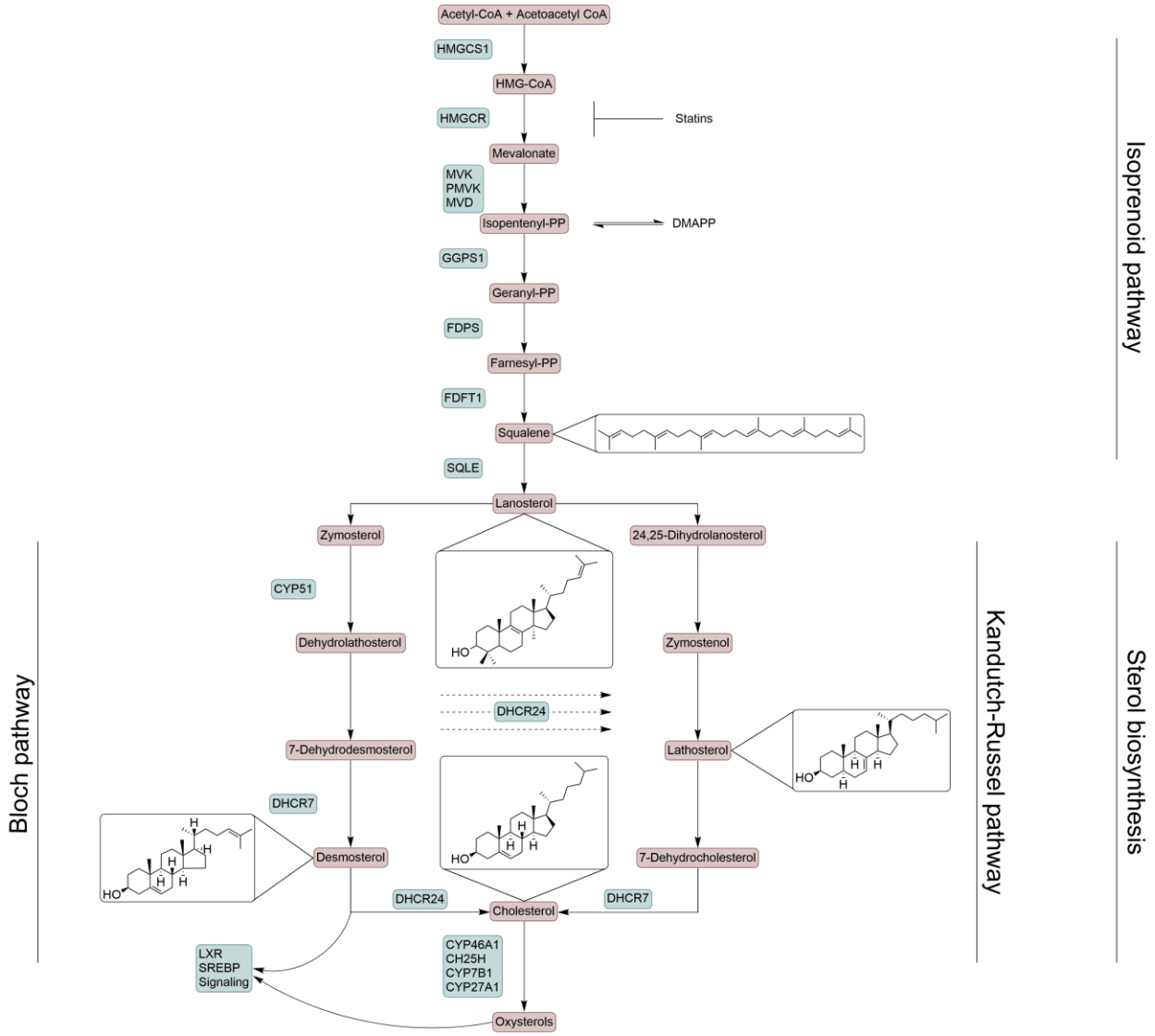

Figure 1 Cholesterol biosynthesis pathway. Synthesis is divided in the isopreonoid and sterol biosynthesis pathway that is separated in Bloch and Kandutsch-Russel pathway. The schematic illustration displays many intermediates and the most important enzymes involved in the formation of cholesterol. The regulation via SREBP and LXR signaling and the excretion of cholesterol as oxysterols is depicted at the end of the pathway.

Lanosterol is fed into two different pathways, the Bloch pathway and the Kandutsch-Russell pathway. These two pathways differ in the order of enzymatic steps. The conversion of lanosterol into desmosterol via the Bloch pathway starts with the reduction of the double bond catalyzed by the enzyme 14-alpha-demethylase (CYP51) and is followed by several reactions forming zymosterol, dehydrolathosterol, dehydrodesmosterol, and finally desmosterol. The intermediate desmosterol can be converted to cholesterol, catalyzed by the enzyme 24-dehydrocholesterol reductase (DHCR24) (Bloch, 1965). The post-lanosterol steps in the Kandutsch-Russell pathway

are dehydrolanosterol, zymostenol, lathosterol, and as terminal intermediate 7-dehydrocholesterol, which can be converted to cholesterol by 7-dehydrocholesterol reductase (DHCR7) (Kandutsch & Russell, 1960). Flux analysis studies suggested a third pathway that combines both pathways in a “modified Kandutsch-Russel” pathway. In this modified pathway, cholesterol is produced within the Bloch pathway and at later steps changing to Kandutsch-Russel pathway using DHCR24 (Mitsche et al., 2015).

1.1.3 Regulation of brain cholesterol

Cholesterol metabolism is differentially regulated in diverse brain areas. This includes differentially expressed cholesterol synthesis genes, cholesterol shuttle proteins, intracellular transporters and lipoprotein receptors are region specific, even the abundance of the sterol sensing protein SREBP cleavage-activating protein (SCAP) varies. Transcription of the rate-limiting enzyme *Hmgcr* and *Fdft1* is partially regulated by the transcription factor sterol regulatory element-binding protein 2 (*Srebp-2*) (Brown & Goldstein, 1997; Luo et al., 2020) (Figure 2). In high cholesterol circumstances the inactive SREBP-SCAP complex in anchored in the ER, the Insulin-induced gene 1 protein (INSIG) is bound to SCAP, which senses cholesterol in the ER membrane.

Low cholesterol conditions lead to unbound INSIG and thereby conformational changes of SCAP to transport the SREBP-SCAP complex to the Golgi apparatus via COPII vesicles. In the Golgi, SREBP undergoes proteolytic cleavage. The mature SREBP2 transcription factor binds sterol regulatory elements (SRE) in the nucleus to induce transcriptional regulation (Luo et al., 2020).

Another major regulator of cholesterol homeostasis are liver X receptors (LXRs) that serve to reduce cellular cholesterol levels. As SCAP, these nuclear receptors are cholesterol sensors and form heterodimers with retinoid X receptors (RXRs).

Endogenous ligands like oxysterols change the conformation of the heterodimer causing the dissociation of the corepressor complex and recruitment of the coactivator complex to initiate transcription of target genes like the apolipoprotein (*ApoE*) and the ABC-transporter *Abca1* and *Abcg1* (Bielska et al., 2012; Courtney & Landreth, 2016). The lipid transporters ABCA1/ABCG1 export cholesterol from the cells to lipidated APOE. APOE is the main component of the high density lipoproteins (HDL) like particles that are secrete into the intestinal fluid (Orth & Bellosta, 2012). LXR heterodimerization further leads to the suppression of cholesterol synthesis genes, such as *Fdft1* and *Cyp51*. Additionally, LXR signaling promotes the degradation of the low-density lipoprotein receptor (LDLR) leading to reduced cholesterol uptake. Other LXR agonist beside oxysterols are cholesterol intermediate like desmosterol and zymosterol, demonstrating the

diversity of regulatory adjustments (Kiss & Nagy, 2016; Muse et al., 2018; Wang et al., 2008; Zelcer et al., 2009).

To prevent accumulation of excess free cholesterol in the brain, cholesterol is hydroxylated to oxysterols to pass the BBB. Another way to reduce excess cholesterol is the esterification by acyl coenzyme-A cholesterol acyltransferase (ACAT1, also called SOAT1). SOAT1 can transform the free cholesterol into cholesterol esters (CE) for storage and transport via lipid droplets (Rogers et al., 2015).

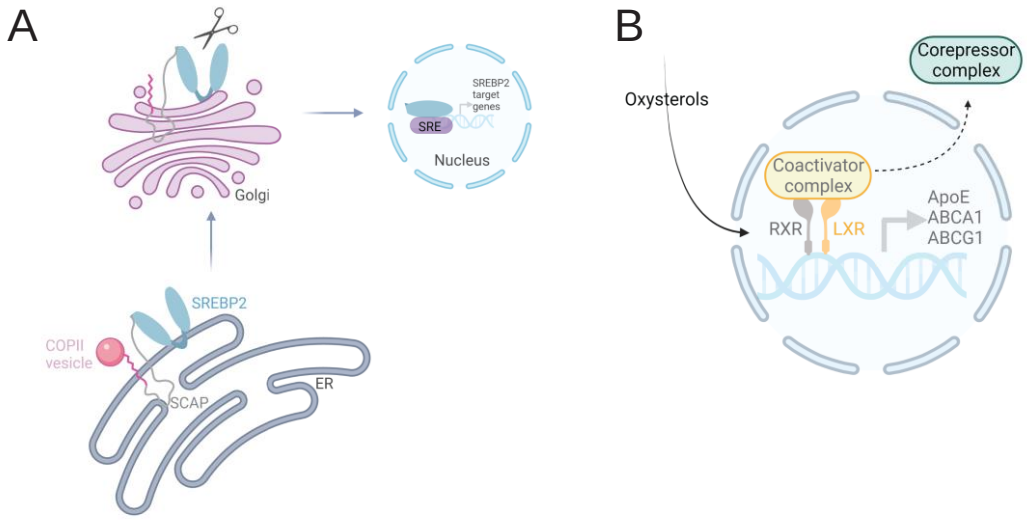

Figure 2 Regulation of cholesterol metabolism via SREBP and LXR signaling. (A) SREBP2 is the major transcriptional regulator of cholesterol synthesis. Under high-cholesterol conditions, the inactivate triple complex composed of SREBP2, SCAP and INSIG is localized in the ER. Low intracellular cholesterol concentrations lead to conformational changes and thereby the transport of SREBP2 to Golgi where proteolytic cleavage takes place. The binding to the sterol regulatory element (SRE) in the nucleus leads to transcriptional regulation to enhance cholesterol synthesis. (B) Liver X receptors (LXR) are cholesterol sensors and form heterodimers with RXRs. The confirmation of the heterodimers regulates the transcription of target genes like *ApoE, Abca1, Abcg1* and is regulated by oxysterols and cholesterol intermediates like desmosterol.

1.1.4 Cholesterol turnover and excretion from the CNS

CNS cholesterol is considerably stable, the sterol has a long half-life of four to six months and has a slow turnover with approximately 0,4% per day (Dietschy, 2009; Vance et al., 2005). About 99.5% of CNS sterols are unesterified cholesterol with a low quantity of desmosterol and cholesteryl esters. Around 70% of the brain cholesterol is stored in myelin sheaths and another considerable amount is located in plasma membranes. In plasma membranes, cholesterol is extensively enriched in membrane microdomains, these “lipid rafts” play a central role in

membrane organization and trafficking (Bjorkhem & Meaney, 2004; Silvius, 2003; Simons & Ehehalt, 2002).

The synthesis of cholesterol is an energy consuming process and therefore an efficient apolipoprotein-dependent recycling mechanism in the brain results in a low excretion rate into the periphery. In the case of excess cholesterol, shedding of cholesterol in association with ApoE into the CSF is limited to 1-2 mg per day; about 6-7 mg per day can be released into the circulation in the form of oxysterols. Oxysterols can pass the BBB due to their lipophilic properties faster than non-oxidized cholesterol (Bjorkhem & Meaney, 2004; Orth & Bellosta, 2012). The excretion through the BBB is sustained by cholesterol 24 hydroxylase (CYP46) a highly brain specific enzyme that is mainly expressed in neurons. CYP46 converts cholesterol to 24 hydroxycholesterol (24-OHC) to pass the BBB. The hydroxylated cholesterol 27-hydroxychoelsterol is mainly found in plasma but is imported into the CNS t of about 5mg daily (Vance et al., 2005). In the periphery the relation between cholesterol and oxysterols is more than 10.000-fold, in the brain the proportion of oxysterols is greater and varies between 1 to 500 and 1 to 1000. Oxysterols can be incorporated in lipoproteins and can be shuttled cells (Bjorkhem & Meaney, 2004; Orth & Bellosta, 2012).

1.1.5 Lipid transport between cells

Given the low rate of cholesterol synthesis in some CNS cells in the adult brain, sterols need to be transported between brain cells via CNS lipoproteins to maintain lipid homeostasis. Lipoprotein particles consist of a hydrophobic core and a hydrophilic surrounding. Within the lipophilic core polar lipids can be transported through aqueous environment like the blood circulation. A similar but less complex transport system is also present in the brain. Some components of lipoprotein-mediated transport exist in the periphery and in the brain whereas some apolipoproteins alternate. All brain cells express the mRNA to synthesize LDLR for the uptake of apolipoproteins. A second uptake route could be the LDL receptor-related protein (LRP) (Boyles et al., 1985; Bu et al., 1994; Danik et al., 1999). In addition to this, cholesterol efflux via ATP-binding cassette transporters (ABCA1) has a significant role in sterol flux between cells (Karasinska et al., 2009; Wellington et al., 2002). ABCA1 facilitates secretion and lipidation of ApoE and consequently the transport of cholesterol (Hirsch-Reinshagen et al., 2004; Wahrle et al., 2004) Apolipoprotein E is the most abundant apolipoprotein in the brain, other lipoproteins found in the brain are apolipoprotein A1 (ApoA1), apolipoprotein J (ApoJ) and apolipoprotein D (ApoD). ApoE is believed to be mainly produced by astrocytes and can be taken up by other brain cells. In humans, three different alleles of ApoE are distinguished, ApoE2, ApoE3, ApoE4. Carriers of the ApoE2 allele contain lower

blood cholesterol and low-density lipoprotein levels but higher high-density lipoprotein and triglyceride levels compared to Apoe4 carriers. In the human brain, ApoE4 leads to an altered lipidomic profile and the reduction in important lipid classes (Lefterov et al., 2019; Wolters et al., 2019). ApoE isoforms differ in the lipidation status, ApoE2 is highly lipidated whereas Apoe4 is poorly lipidated which has an effect on their functions like cholesterol and lipid transport (Lanfranco et al., 2020). Beside the central role of ApoE for cholesterol metabolism it is the leading risk factor for AD (Corder et al., 1993; Strittmatter et al., 1993).

1.1.6 Dysregulated lipid metabolism and CNS disorders

Deregulated lipid and cholesterol metabolism is a feature of various neurological disorders. Changes in lipid homeostasis are part of some disease even though the primary defect is unrelated to lipid metabolism. The determining role of lipids and cholesterol for cell physiology in CNS disorders is only partially elucidated. The hallmark of Parkinson´s disease is the accumulation of α-synuclein to form Lewy bodies. It was shown that lipids can interact with α-synuclein and thereby lead to accumulation. Biophysical properties of lipids and consequently the membrane fluidity affects aggregation in synaptic membranes (Galvagnion et al., 2016; O'Leary et al., 2018). The lysosomal storage disorder Niemann-Pick disease is caused by mutation of either of two genes involved in lysosomal storage of cholesterol and sphingolipids, *Npc1* and *Npc2*. (Porter et al., 2010; Winkler et al., 2019). Reduced expression of genes related to sterol synthesis were detected in post mortem cortex and striatum tissue of Huntington disease patients and animal models. Studies indicated positive effects on behavioral outcomes of HD mouse models when infusing cholesterol into the striatum (Birolini et al., 2020; Leoni et al., 2011). A further imbalance of cholesterol and lipoprotein levels in cerebrospinal fluid (CSF) and serum was detected in patients with Amyotrophic lateral sclerosis (ALS), a neurodegenerative disease that mainly affects motor neurons.

The role of circulating cholesterol levels is not well understood, elevated serum cholesterol levels showed a protective prognosis but contradicting to that a higher risk for developing ALS (Abdel-Khalik et al., 2017; Dodge et al., 2021; Ingre et al., 2020). Unprovoked recurrent seizures are the hallmark of epilepsy. Several studies investigate the impact of cholesterol on neuronal excitation and hereby the likelihood for seizures using an inhibitor of cholesterol 24-hydroxylase, to reduce the conversion of cholesterol to oxysterols (Aird & Gurchot, 1939; Hawkins et al., 2021; Warren et al., 2018). Experimental autoimmune encephalomyelitis (EAE) is a model for Multiple sclerosis, which represents the inflammatory and demyelinating aspects of the disease. In the human disease as well as in EAE phagocytes are recruited to the lesion area to remove myelin debris.

In the mouse model, repair fails when microglia lack intact sterol synthesis. Moreover, disrupted cholesterol export from phagocytes leads to reduced remyelination (Berghoff et al., 2021; Cantuti-Castelvetri et al., 2018; Spiteri et al., 2022). In Alzheimer´s disease the connection between lipid metabolism and different components of the disease are very complex and will be discussed in a separate section.

1.2 Alzheimer´s disease

1.2.1 Overview, history and epidemiology

In 1907 Alois Alzheimer, a German psychiatrist and neuropathologist published a clinical case report about a 50-year-old woman called Auguste Deter. In the paper “Über eine eigenartige Erkrankung der Hirnrinde”/“An Unusual Illness of the Cerebral Cortex“ he described symptoms ranging from paranoia and disorientation to progressive memory loss. In autopsy material he found neurofibrillary changes, small accumulations caused by a substance deposition, reactive glia cells, and brain atrophy. In 1908 Emil Kraepelin, the mentor of A. Alzheimer published the 8th edition of the textbook Psychiatrie and proposed the name Alzheimer´s disease to describe the characterized “unusual illness of the cerebral cortex” (Alzheimer, 1907; Hippius & Neundörfer, 2003; Kraepelin, 1913; Stelzmann et al., 1995).

Alzheimer´s disease, also called Morbus Alzheimer is the most common cause of dementia characterized by a progressive disease course, accelerating pathological accumulations of extracellular amyloid and intracellular tau, and decline of cognitive functions. Nowadays, approximately 50 million people suffer from dementia worldwide and AD accounts for 60-80% of these cases ("2020 Alzheimer's disease facts and figures," 2020; "World Alzheimer Report 2019,"). AD causes the decline of memory functions, language disabilities, and alterations of behavioral and social skills. Disease progression leads to a broad range of neuropsychiatric disorders such as sleep disturbances, mood change, depression, anxiety or aggressiveness. Together with irritability and delusions this can result in personality changes. These common symptoms are often summarized as behavioral and psychological symptoms of dementia. The first histopathological brain abnormalities establish themselves years before the diagnosis of dementia. Cognitive tests and neurological evaluation in addition to neuroimaging methods such as magnet resonance imaging (MRI) and computerized tomography (CT). In the CSF, a decrease in Aβ42 or increases in total tau and phosphorylated tau are reflecting the disease process. And are nowadays used as AD biomarkers. To a certain extent this is even reflected in the blood but the quality of AD blood biomarkers is currently controversially discussed (Janelidze et al., 2020; Khan et al., 2020). A confirmed diagnosis of AD can only be achieved post-mortem, by

histopathological evidence of the pathognomonic signs of AD. The histopathological hallmarks of AD are intraneuronal excess of hyperphosphorylated tau resulting in neurofibrillary tangles and extracellular aggregations of beta amyloid forming senile plaques (Hansson, 2021; Porsteinsson et al., 2021). Heiko and Eva Braak assessed these pathological characteristics in different stages of disease visualized by Bielschowsky silver staining and classified the disease progression in Braak stages I to VI (Braak & Braak, 1991). In the surrounding of senile plaques, activated microglia induce an inflammatory microenvironment. At a later disease stage astrocytes become reactive and also arrange around the plaques however more distant and fewer in numbers (DeTure & Dickson, 2019). In addition to the formation of amyloid plaques and neurofibrillary tangles, patients with Alzheimer´s dementia suffer from a drastic loss of synapses which correlates with the degree of cognitive impairment (Terry et al., 1991).

There are two subtypes of AD, the hereditary autosomal dominant familial AD (FAD) and sporadic AD (SAD). FAD generally has an early onset. Only about 1% of the AD cases develop before the age of 65 years. These cases are classified as Early-onset (EOAD) and are predominantly caused by surplus amyloid production (Blennow et al., 2006). FAD/EOAD is caused by mutations in the genes encoding APP, Presenilin-1 (PSEN1) or Presenilin-2 (PSEN2).

The majority (90-95%) of AD cases include a late-onset (LOAD) and unknown etiology (Harman, 2006). Aging is the primary risk factor for AD. Further risk factors include female sex and in respect to lipid metabolism the major genetic risk factor Apolipoprotein E ε4 allele (apoE4).

Relations to cardiovascular disease, obesity, diabetes, hypercholesterolemia and inflammation are discussed. Furthermore, environmental factors (reduced brain capacity and mental ability, low physical activity, sleep disturbances, late-life depression, and head injuries) may serve as risk factors for SAD (A. Armstrong, 2019). Beside ApoE4 as a metabolic risk factor, a genome wide study revealed clusterin (CLU), phosphatidylinositol-binding clathrin assembly protein (PICALM), complement C3b/C4b receptor 1 (CR1), bridging integrator 1 (BIN1), ATP-binding cassette subfamily A member 7 (ABCA7) and others (Kamboh et al., 2012). Some variants of the triggering receptor expressed on myeloid cells 2 (TREM2) gene have been associated with AD by altering the microglial interaction with the amyloid plaques and phagocytic activity. Due to the complexity of the disease, the underlying cause is not resolved yet.

1.2.2 Amyloid cascade hypothesis

The amyloid cascade hypothesis was first described in 1991 and has become the most widely accepted hypothesis ever since (Beyreuther & Masters, 1991; Hardy & Allsop, 1991; Selkoe, 1991). The amyloid cascade hypothesis states that the β-amyloid protein is central for developing

Alzheimer´s disease and triggers a detrimental cascade. The strongest indication for β-amyloid as the driving force of AD is the fact that the FAD genes APP, PSEN1 and PSEN2 are all involved in Aβ generation (Karran et al., 2011). Another genetic correlation referring to amyloid as starting point of AD is the elevated risk for developing the disease with the chromosomal anomaly trisomy 21. This genetic condition is caused by an extra copy of the chromosome 21, the chromosome where APP is localized. Most patients have significant increased levels of amyloid and tau by the age of 40 years (Masters et al., 1985). However, the amyloid cascade hypothesis does not consider the direct interaction between amyloid and tau as the two hallmarks of the disease. Mutations in the tau gene can lead to autosomal dominant dementia of the frontotemporal lobe but not to AD with additional amyloid pathology. Considering this fact, tau is more likely downstream of amyloid (Hutton et al., 1998). Further studies using APP transgenic mice show that reduced tau levels are beneficial for behavioral changes and amyloid-mediated deficits, which is in line with the amyloid hypothesis (Roberson et al., 2011; Roberson et al., 2007).

At present, there is no cure for AD and current therapies focus on symptomatic treatment. Several clinical trials that tested a broad range of drugs to target the processing and production of amyloid production, preventing amyloid aggregation or enhance its clearance, failed. Last year the anti-amyloid antibody, Aducanumab was approved by U.S. Food and Drug Administration (FDA) to treat AD. In clinical trials Aducanumab treatment reduced amyloid burden but was inefficient in alleviating the cognitive dysfunction and its approval has sparked controversy in the AD research field (Fillit & Green, 2021).

The lack of therapeutic achievements points in a direction of an intervention before clinical symptoms become apparent. Other approaches focus on targeting tau, inflammatory responses, and pathogenic infections among others (Liu et al., 2019). After many years of unsuccessful clinical trials focusing on amyloid reduction, the direction of AD therapy has expanded in numerous trajectories. One trajectory is “untangling” the tau protein, which is directly connected to cognitive decline. Another focus is on the role of neuroinflammation and the consequence of alternating the inflammatory surrounding. One possibility would be to rejuvenate exhausted immune cells for enhanced clearing and thereby more effective plaque reduction (Chee & Solito, 2021). As a common future perspective, the intervention at an early prodromal disease stage is the prevailing opinion for a successful treatment and therefore an early diagnosis involving valid biomarkers is an essential prerequisite (Porsteinsson et al., 2021).

1.2.3 Amyloid precursor protein processing

The amyloid precursor protein (APP) is the origin of the pathogenic amyloid-β protein. APP is located on the long arm of chromosome 21 and is ubiquitously expressed but highly abundant in neurons. Different isoforms of APP are generated by alternative splicing, ranging from 365 to 770 amino acid residues. APP695 is the most abundant in the brain followed by APP751 and APP770. (Sandbrink et al., 1996; Zhang et al., 2011). When newly synthesized APP passes through the secretory pathway, this single-pass transmembrane protein undergoes several posttranslational modifications including proteolytic processing, glycosylation, phosphorylation and sulfation, which is called APP maturation. In the maturation process APP relocates from the ER to the Golgi apparatus to the plasma membrane. Most of the APP protein remains associated to the Golgi apparatus. Some APP is localized in the plasma membrane, but a substantial part is internalized again and sorted into early endosomes and either recycled to the plasma membrane or degraded in lysosomes (Caporaso et al., 1994; Haass & Selkoe, 1993; Koo & Squazzo, 1994).

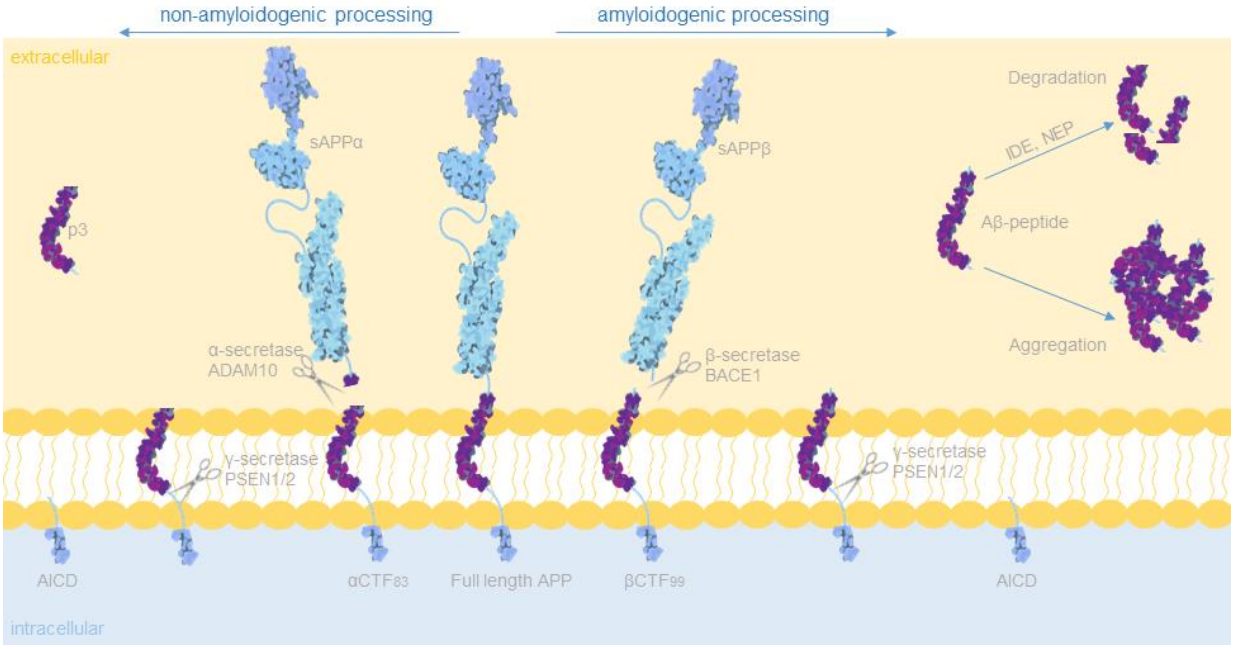

Figure 3 APP processing and Aβ generation. Schematic principle of amyloidogenic and non-amyloidogenic processing of APP. Full-length APP is cleaved by α-secretase and γ-secretase to generate the p3 fragment and C83. The pathogenic Aβ and the 99 amino acid c-terminal fragment peptide are produced by β-cleavage and subsequent γ-cleavage. Aβ can be removed by Aβ-degrading enzymes or accumulates to form extracellular deposits as senile plaques (adjusted from David Goodsell, (Berman et al., 2000)).

Proteolytic processing of APP involves consecutive cleavage, starting with α- or β-cleavage, followed by intramembrane γ-cleavage (Figure 3). The processing is distinguished in the

amyloidogenic pathway and the non-pathogenic pathway. In the non-amyloidogenic pathway, the α-secretase ADAM10, a disintegrin and metalloproteinase domain-containing protein 10 cleaves at the c-terminal side generating an 83 residue c-terminal fragment (C83) and the soluble APP α (sAPPα). C83 is then cleaved by the γ-secretases Presenilin-1 or Presenilin-2 to form P3, a 3 kDa non-amyloidogenic peptide. The non-amyloidogenic pathway takes place mainly in the plasma membrane where α-secretase is located. The amyloidogenic pathway includes beta-secretase 1 (BACE1) and subsequent cleavage by PSEN1/2 resulting in a 99 residue c-terminal fragment (C99) and as an end product the Aβ peptide. The β-secretase BACE1 is mainly located in the trans-Golgi network (TGN) and endosomes where APP is processed in the amyloidogenic pathway. This pathway was shown to be pH dependent, therefore, an acidic compartment is an important prerequisite for β-cleavage (Haass & Selkoe, 1993; Zhang & Song, 2013). γ-cleavage can result in different Aβ peptides depending on the cleavage site in the transmembrane domain. The primary amino acid sequence of amyloid-β was initially sequenced by Glenner and Wong in 1984 from purified fresh frozen autopsy material of CAA patients. The amino acid sequence comprises peptides from 37 to 49 residues, $Aβ_{40}$, a 40 amino acid long peptide is the major form but $Aβ_{42}$ plays a pivotal role in AD. (Glenner & Wong, 1984)

Mutations in APP can be classified into mutations in proximity to the Aβ locus, immediately before or directly after the Aβ sequence or within. The Swedish mutation (APPswe) is a double mutation at amino acid 670 and 671 just prior to the sequence of Aβ1-x. This mutation causes enhanced BACE1 cleavage and accelerated Aβ generation. Mutations carboxyterminally of the Aβ sequence affect the γ-secretase activity. The mutation at position 717 (APP717) increases the $Aβ_{42}$/ $Aβ_{40}$ ratio (Savonenko et al., 2015). APP mutations within the Aβ sequence can lead to conformational changes of the peptide that change aggregation kinetics. Most of the mutations within APP modify biochemical properties and thereby often creating highly pathological variants (Hatami et al., 2017). Most of the mutations either increase the Aβ production, the $Aβ_{42}$/ $Aβ_{40}$ ratio, or aggregation properties of Aβ. Beyond these mutations, there are some protective mutations, the best known is A673T also called Icelandic mutation. This mutation is located near the N-terminal end of Aβ and reduces amyloidogenic cleavage by interfering with BACE1 cleavage (Jonsson et al., 2012; Tambini et al., 2020).

1.2.4 Aβ aggregation and plaque seeding

In contrast to pathological levels, physiological levels of Aβ and other APP processing products support synaptic plasticity and memory (Lazarevic et al., 2017; Puzzo et al., 2011; Puzzo et al., 2008).

Pathological levels of $A\beta_{42}$ play a critical role in AD pathology. Aβ monomer to oligomer transition is the first step of the formation of insoluble Aβ fibrils and aggregation of plaques (Chen et al., 2017; Nag et al., 2011). Aβ oligomer levels are linked to neurotoxicity and the development of cognitive deficits. However, these correlations are weak because of the instable nature of Aß oligomers and their transition to form fibrils (Jongbloed et al., 2015; McLean et al., 1999; Ono et al., 2009). Primary murine neurons treated with stabilized $A\beta_{42}$ oligomers revealed the highly neurotoxic nature in comparison to Aβ fibrils. Amyloid fibrils harbor a secondary β-sheet structure which is a common biochemical property to form fibril and protein aggregations (Ahmed et al., 2010).

Senile plaques are composed of Aβ fibrils. Fibrillary aggregates originated from $A\beta_{42}$ are different compared to fibrils from $A\beta_{40}$. These peptides differ only in two amino acid residues, but $A\beta_{42}$ tend to form β-sheet like structures (Kim et al., 2007). Furthermore, $A\beta_{42}$ aggregates faster under artifact-free conditions when compared to $A\beta_{40}$ (Nirmalraj et al., 2020). Interestingly, the concentration of Aβ in CSF is lower than the concentration which is needed for spontaneous formation of fibrils (Seubert et al., 1992). Further conversion from fibrils to amyloid plaques is not well understood but some studies described intracellular Aβ accumulations in various cells after repetitive synthetic Aβ induction (Friedrich et al., 2010; Gellermann et al., 2006). Another study showed, neuroglia co-cultures treated with $A\beta_{42}$ protofibrils generates neurotoxic extracellular vesicles, inducing axonal swellings, neuronal cell body vacuolization, and pathological lysosomal cholesterol deposits (Beretta et al., 2020). Previously, intraneuronal amyloid accumulations has not been the focus of AD research because extracellular aggregates within plaques outnumber the intracellular accumulations. A number of reports, however showed aggregates with in neurons and a connection to synaptic pathology (Bayer & Wirths, 2010; Oddo et al., 2006; Takahashi et al., 2017). Present data suggest that amyloid plaques originate from intracellular Aβ accumulations that get released during degeneration of synapses or neurites and form the starting point for expansion into the extracellular parenchyma (Gouras et al., 2010) . Toxic oligomeric Aβ is deposited into developing amyloid plaques which could be a possible mechanism for reducing the circulating Aβ levels in brain tissue. With increased amyloid pathology inflammation exacerbates, leading to the formation of dystrophic neurons and the corralling of activated glia around senile plaques in later stages of the disease.

1.2.5 Aβ degradation and clearance

Increased Aβ levels enhance the likelihood for accumulation of the peptide, making non-enzymatic clearance and enzymatic degradation of Aβ important mechanism to maintain

homeostasis. Emerging evidence suggest impaired clearance as a crucial factor for the development of AD, especially in sporadic AD (Cheng et al., 2020; Weller et al., 2000). There are several ways to reduce the amount of Aβ in the CNS. The non-enzymatic clearance can be achieved by Aβ drainage via lymphatic pathways. The excretion can be accomplished via CSF drainage from the meningeal lymphatics or along the cranial nerves into the deep cervical lymph nodes (Ahn et al., 2019; Cheng et al., 2020). A further possibility is the perivascular pathway, Aβ can be diminished by interstitial fluid drainage through capillary walls into the internal carotid artery (Weller et al., 2009). Clearance based on the glymphatic pathway uses the paravascular space between vessels, glia endfeet and the leptomeninges to reduce CSF Aβ (Feng et al., 2020; Iliff et al., 2012). Additionally, to lymphatic efflux, receptor mediated transport into blood vessels via the BBB and subsequent transfer into the circulation exists. Excretion is orchestrated mainly by the endothelial cell receptors LDL Receptor Related Protein 1 (LRP1) in association with Phosphatidylinositol Binding Clathrin Assembly Protein (PICALM) (Hartz et al., 2018; Shibata et al., 2000). An abnormal clearance via the blood vessels can result in cerebral amyloid angiopathy (CAA) which is part of the pathological pattern of many AD patients (Love, 2004). Furthermore, via large vacuoles CSF can drain directly through the BBB into the circulation, known as the arachnoid granule-venous sinus pathway (Tripathi & Tripathi, 1974). Another clearance mechanism is the uptake of soluble Aβ and the fibrillary form by astrocytes and to a greater extent by microglia cells (Rogers et al., 2002). However, microglial Aβ clearance rate declines with age and disease progression (Flanary et al., 2007; Floden & Combs, 2011; Hickman et al., 2008; Wyss-Coray, 2006). Microglia degrade the incorporated Aβ by common degradation pathways involving lysosomes, endosomes and autophagosomes (Majumdar et al., 2008). Another possibility is the enzymatic degradation of Aβ by neurons, including various Aβ-degrading enzymes (ADE): insulysin (also called insulin-degrading enzyme, IDE), neprilysin (NEP), matrix metalloproteinase (MMP9) and glutamate carboxypeptidase II (GCPII) and others. Despite effective in animal studies, the beneficial effect of the Aβ cleavage from senile plaques is under debate, considering that smaller Aβ-derived peptides have toxic properties as well (Eckman et al., 2006; Farris et al., 2007; Iwata et al., 2004).

1.2.6 Mouse models of AD

Animal models are a widely used tool in AD research to model aspects of the complex disease pathogenesis *in vivo*. Murine models are the most common model due to the rather low husbandry costs, the convenience of a fast generation of descendants and the ease of genetic manipulation (Götz et al., 2018). An optimal model would harbor the histopathological hallmarks of AD, Aβ

plaques and neurofibrillary tangles of hyperphosphorylated tau accompanied by gliosis and synaptic and neuronal aggravations. Furthermore, the pathological changes should be comparable to the human disease, both in area and progression. To evaluate clinical relevance, cognitive decline should be a feature of such an animal model as well. For mimicking AD several mouse models are available, some of them present with amyloid plaques and others with tau tangles. The disease onset, the severity of gliosis, synaptic changes and cognitive impairment is very different. For example, the APP NL-G-F knock-in mouse builds senile plaques, the APP23 mouse model develops plaques and hyperphosphorylated tau but no tau tangles, the PS19 mouse displays tangles but lacks the amyloid burden.

A widely used mouse model of AD is the 5xFAD strain harboring 5 mutations linked to familial Alzheimer´s disease. This transgenic mouse line contains the Swedish (K670N/M671L), Florida (I176V), and London (V717I) mutation of the APP gene and two mutations in PSEN1, M146L and L286V driven by the neuronal Thy1 promotor (Oakley et al., 2006). These mutant mice present with an aggressive and early-onset AD-related pathology including severe amyloid pathology, gliosis, and synaptic degeneration and progressive cognitive deficits. The major disadvantage of this model is the lack of tau tangles, the second major hallmark of the human Alzheimer´s disease.

1.2.7 The role of microglia under physiological conditions and in neurodegenerative disease

Microglia were first visualized and described by Pio del Hortega in 1919 and originate from the yolk sac. During embryogenesis erythromyeloid progenitors migrate into the brain parenchyma and develop into immature microglia that start ramifying and populating the brain (Kierdorf et al., 2013). During CNS homeostasis, microglia are quite stable and nearly half of the microglia in a mouse brain can survive throughout the entire life of the animal (Fuger et al., 2017). Microglia fulfill an exceptionally broad variety of tasks in the healthy brain, ranging from innate immune system functions, trophic support, and angiogenesis to cell-cell communication to maintain the healthy brain microenvironment. However, as soon as the homeostasis is disturbed by infections, protein aggregations, cell death or another inflammatory stimulus, microglia start proliferating and change their homeostatic expression profile to a reactive signature.

Microglia cells take responsibilities for neuroprotection and produce growth factors for supporting neuronal survival, induce programmed cell death of surplus and defective neurons, eliminate malfunctioning synapses and clear the cellular debris (Badimon et al., 2020; Frade & Barde, 1998; Marín-Teva et al., 2004; Paolicelli et al., 2011; Wakselman et al., 2008). In the developing white matter, microglia contribute to physiological myelinogenesis by maintaining oligodendrocyte

progenitor maturation and maintenance (Hagemeyer et al., 2017). The interactions between astrocytes and microglia are bidirectional, as both cell types accomplish immune functions, has homeostatic responsibilities and micro-environmental balancing obligations. Astrocytes supply cholesterol loaded apoliporotein E and trophic support to microglia (Baxter et al., 2021; Bohlen et al., 2017; Saher & Stumpf, 2015).

In neurodegenerative diseases astrocytes and microglia transfer into reactive glia cells. Microglia participate in Aβ plaque clearing, contribute to the compaction of Aβ, and could thereby counteract the spreading (Clayton et al., 2021; Dionisio-Santos et al., 2019). Another remarkable study showed that microglia depletion before plaques arise, eliminates plaque deposition, suggesting a need of microglia for plaque deposition (Spangenberg et al., 2019). Further studies suggest an initial restriction of the disease progression by microglia and an age dependent transition closely associated with the exacerbation of amyloidosis. The gradual progression of the β-amyloid pathology leads to microglial production of proinflammatory cytokines and chemokines consequently reducing phagocytic activity (Heneka et al., 2010; vom Berg et al., 2012; Wang et al., 2015). Other studies showed phagocytes becoming more senescent with age, thereby limiting phagocytosing capacity and could lead to dysfunctional β-amyloid clearance (Flanary et al., 2007; Hickman et al., 2008).

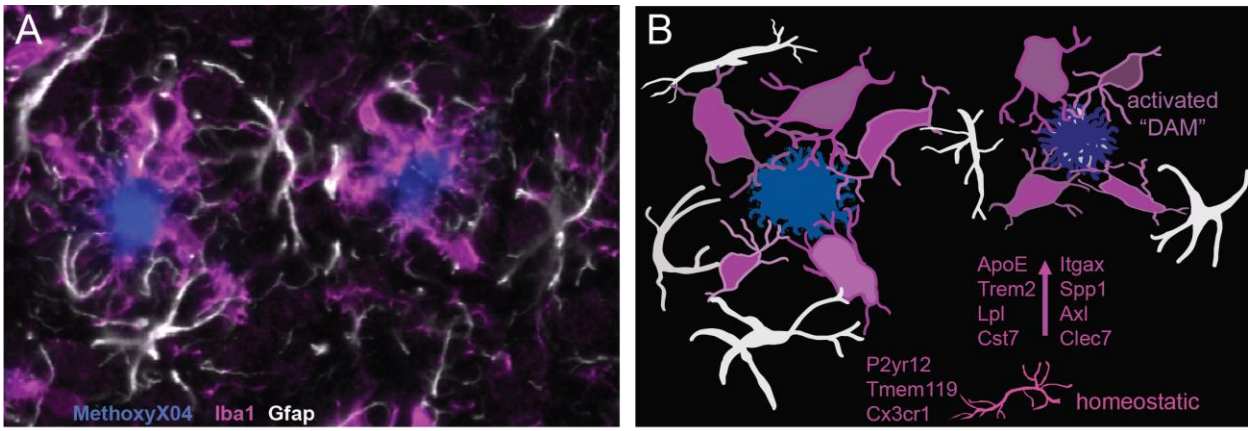

Figure 4 Microglia interaction with amyloid plaques. (A) Fluorescent microscopy of amyloid plaques (blue, stained with MethoxyX04), microglia (magenta, stained with Iba1) and astrocytes (white, stained with Gfap) of a 6-month-old AD mouse. Microglia localize around plaques and change morphology from homeostatic to activated. (B) Schematic modelling of microglia changing their morphology and expression under β-amyloid exposure. Homeostatic markers are downregulated and activation/DAM markers upregulated.

According to their expression profile, activated microglia have been classified as pro-inflammatory “M1” and an anti-inflammatory “M2” state (Tang & Le, 2016). Another microglia signature is associated with several neurodegenerative diseases, the so-called disease-associated microglia

(DAM). DAM microglia express reduced homeostatic marker genes like *P2ry12, Cx3Cr1* and *Tmem119* and upregulate specific genes in a *Trem2* dependent or independent fashion. (Keren-Shaul et al., 2017; Krasemann et al., 2017). The receptor tyrosine kinase *Axl*, C-type lectin domain containing 7A (*Clec7a*), and secreted phosphoprotein 1 (*Spp1*) are upregulated in a *Trem2* dependent whereas apolipoprotein E and TYRO protein tyrosine kinase-binding protein (*Tyrobp*) are regulated independent of *Trem2* (Sobue et al., 2021).

1.2.8 Lipids in Alzheimer´s disease

Multiple connections have been made between cholesterol and Alzheimer´s disease (AD). Several of the high-risk genes of AD like ApoE4 are associated with cholesterol metabolism. The ApoE4 allele has a population frequency of 13.7% and increases the risk of developing AD by 3-fold in heterozygous carriers and more than 10-fold in homozygous carriers (Liu et al., 2013). A protective effect has been shown for homozygous carriers of the APOE2 allele. In physiological conditions, ApoE is mainly produced by astrocytes whereas in neurodegenerative diseases neurons as well as activated microglia also produce ApoE. It has been proposed, that microglia-derived ApoE has smaller dimensions and can be deposited in amyloid plaques and thereby affecting the formation and morphology of plaques (Hemonnot-Girard et al., 2021). ApoE of activated microglia was shown to increase with the progression of amyloidosis whereas ApoE levels of astrocytes remain stable. Furthermore, the loss of *Trem2* reduced activation of microglia and plaque corralling and thereby ApoE deposits in plaques, suggesting a microglia dependent process (Liu et al., 2013; Parhizkar et al., 2019).

Additionally, cholesterol content affects β- and γ-secretase activity and low cholesterol levels shift the APP processing to the nonamyloidogenic processing in cell culture (Grimm et al., 2008; Kojro et al., 2001; Simons et al., 1998; Xiong et al., 2008). Decreased cholesterol levels and the adaption of the APP processing leads to reduced Aβ production (Ehehalt et al., 2003). APP can directly bind cholesterol and can localize to cholesterol-rich membrane rich lipid rafts. APP processing can be regulated by different lipid compositions which could explain the altered cholesterol and cholesterol ester levels of post mortem AD brains (Beel et al., 2008; Chan et al., 2012; Fabelo et al., 2014; Tajima et al., 2013). Furthermore, multiple genes that are highly upregulated in microglia during disease are connected to the regulation of lipid metabolism and microglia activation e.g. *Trem2*. In the DAM profile of activated microglia *Lpl* and *Cst7* are upregulated. These genes are involved in the process of lipid uptake and phagocytosis and lipid-rich debris (Hammond et al., 2019; Keren-Shaul et al., 2017). A study reported a correlation between increased expression of cholesterol 25 hydroxylase (*Ch25h*) with reduced phagocytic

activity in microglia (Ofengeim et al., 2017). The multitude of links between AD and lipid metabolism suggest a pivotal role of lipids in the amyloidosis and the etiology of AD. However, despite decades of research, the detrimental function of lipids in this devastating disease is still not fully elucidated. We hypothesize that the analysis of cell type-specific responsibilities will help understanding disease processes.

1.3 Aim of the study

In addition to aging as most prominent risk factor, there is growing evidence that CNS cholesterol and lipid metabolism is a fundamental player in AD. Already in 1907, Alois Alzheimer described lipid accumulations as a hallmark of AD, besides the well-known appearance of senile plaques and tau tangles. In AD, dysfunctional plaque associated microglia with lipid accumulations have been described that show reduced phagocytic capacity (Marschallinger et al., 2020). These lipid accumulations have been linked to lipid droplets that are observed in post-mortem human AD tissue (Farmer et al., 2020).

Aβ generation within the amyloidogenic pathway of APP processing includes β- and γ-secretase, both intensively expressed in neurons and located within the cholesterol-rich membrane. More than two decades ago studies showed the association between high cholesterol levels and Aβ accumulations as well as increased β-secretase activity resulting in more amyloidogenic processing (Marquer et al., 2011; Wolozin, 2004).

Despite this strong correlative data, it still remains enigmatic how cell-specific cholesterol synthesis contributes to the amyloid pathology.

In this study, I investigated the relationship between cell type-specific cholesterol metabolism and amyloidosis. Therefore, I generated conditional mutants of sterol synthesis using the Cre/LoxP system. I investigated the role of neuronal (CamKIIα-Cre), astrocytic (Aldh1l1-CreERT2) and microglial (Cx3c1-CreERT2) sterol synthesis. These mice were crossbred with the 5xFAD model of amyloidosis. First, I addressed the role of cellular cholesterol synthesis on amyloidosis by determining the load of senile plaques in the three complex mutants and their respective controls. The location and morphology of microglial cells around senile plaques have been postulated to reflect the activity of amyloid deposition and turnover. To investigate whether cellular cholesterol synthesis plays a role in this process, I determined the corralling phenotype of microglia in the complex mutants. Disturbances in CNS cholesterol homeostasis could affect APP metabolism. To get insight into the relevance of cell type-specific cholesterol on Aβ generation, I investigated APP processing and amyloid generation in the complex mutants. In addition to amyloid

generation, Aβ clearance could be influenced by the CNS cholesterol metabolism. To address the amyloid turnover independent of plaque formation, I performed ex vivo experiments by seeding isolated microglia on 5xFAD brain slices. It has been hypothesized that progressive plaque load is linked to increasingly inefficient microglial phagocytosis and turnover of Aβ. The explore the role of microglial cholesterol in this process, I determined phagocytosis rates in primary BMDM isolated from conditional mutants that were treated with Aβ. AD microglia show a specific signature of activated DAM genes. At present it is unclear whether these activation markers are required for amyloid deposition and clearance or are a marker of impaired turnover of amyloid.

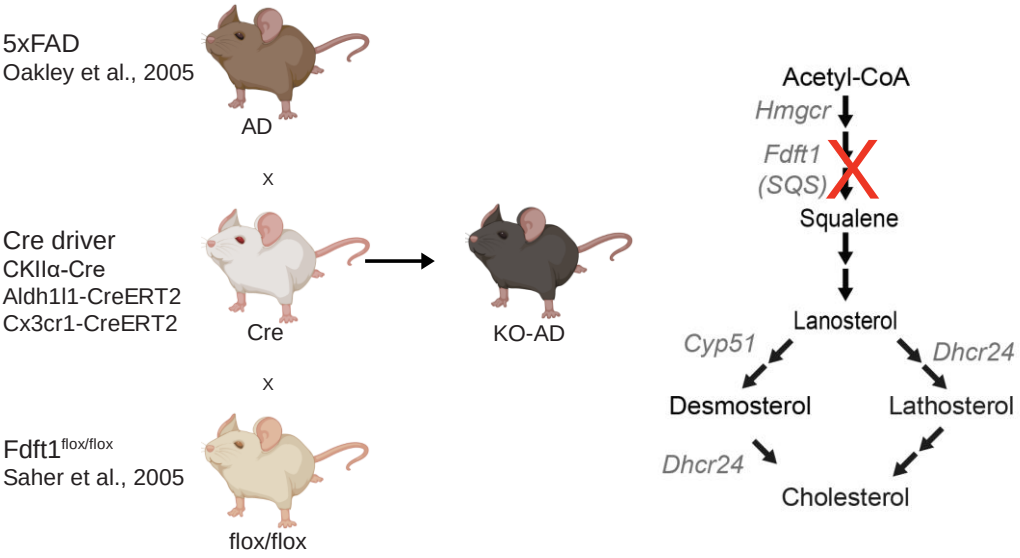

Figure 5 Experimental setup. Fdft1 is the first committed step within the cholesterol synthesis. Fdft1 floxed mice (Saher et al., 2005) were crossbred with cell-specific Cre drivers, CKIIα-Cre (Minichiello et al., 1999) for neurons, Aldh1l1-CreERT2 (Winchenbach et al., 2016) for astrocytes and Cx3cr1-CreERT2 (Parkhurst et al., 2013) for microglia. For analyzing the lipid metabolism in AD, cholesterol synthesis mutants were combined with 5xFAD mice (Oakley et al., 2005).

2 Material and methods

2.1 Materials

If not stated otherwise, the materials were purchased from Bio-Rad (Munich, Germany), BD Falcon (Heidelberg, Germany), Brand (Radebeul, Germany), Eppendorf (Hamburg, Germany), and chemicals were obtained from Sigma-Aldrich (Munich, Germany).

2.1.1 General laboratory devices

Table 1 List Devices for following methods

Device	Company	Application
STP 120	Leica	Paraffin embedding
HistoStar	Epredia	Paraffin embedding
Microm HMP110 tissue processor	Microm	IHC
AxioObserverZ1	Zeiss	Fluorescent IHC
UltramicroscopeII	LaVision Biotech	LSM
Precellys 24 tissue homogenizer	Bertin instruments	WB
Eon High Performance Microplate Spectrophotometer	BioTek	WB
SDS-PAGE gel casting unit	BioRad	WB
Mini Gel Tank	Thermo Fisher	WB
Wet Tank Blotting System	BioRad	WB
PowerPac 300 Power Supply	BioRad	WB
Odyssey infrared imager	Licor	WB
T3/Gradient Thermocycler	Biometra	Genotyping, qRT-PCR
Ultra Turrax T8 homogenizer	Kinematica	qRT-PCR
NanoDrop One	Thermo Fisher	qRT-PCR
Lightcycler 480 II	Roche	qRT-PCR
Sorvall WX+ Ultracentrifuge	Thermo Fisher	MACS
Ultra centrifuge rotor Th660	Thermo Fisher	MACS
Labofuge 400	Haraeus intruments	MACS
Octomacs magnet	Miltenyi Biotech	MACS

2.1.2 Buffers and solutions

Table 2 List of Buffers and Solutions

Solution	Composition	Application
Avertin	2% 2,2,2-Tribrome ethanol 99% 2% Amyl alcohol sterile filtered	Perfusion
Citrate buffer	1.8 mM Citric acid 8.2 mM Sodium citrate pH 6	IHC
Detergents	1 % Triton 2 % Lithium dodecyl sulfate 0,5 % sodiumdeoxycholate in PBS	WB
Diethylamine buffer (DEA)	0.25 % Diethylamine 50 mM NaCl pH 10	WB
DNA lysis buffer	50mM NaOH	Genotyping
DNA neutralizing buffer	1M Tris HCl pH8.0	Genotyping
Protein sample buffer	50mM DTT 1xTris Tricine loading buffer In RIPA buffer	WB
FastGreen destaining solution	50% Ethanol 50% TBS	WB
FastGreen staining solution	0.005 mg/ml Fast Green 30 % Methanol 6.7 % acetic acid 63.3 % ddH20	WB
FastGreen stock	0.05 mg/ml Fast Green 30 % Methanol 6.7 % acetic acid	WB

	63.3 % ddH20	
FastGreen wash solution	30% Methanol 6.7% Acetic acid 63.3% ddH20	WB
Formic acid buffer (FA)	70% formic acid 30% PBS	WB
PFA	25% PFA (16% stock solution) 50% 0.2 M phosphate buffer 0.8% NaCl	Perfusion
Phosphate buffer (0.2M)	40 mM NaH_2PO_4 160 mM Na_2HPO_4 pH 7.4	Perfusion
Phosphate-buffered saline (PBS)	137 mM NaCl 2.7 mM KCl 10 mM Na_2HPO_4 1.8 mM KH_2PO_4 pH 7.2	
PLL coating solution	0.1mg/ml borate buffer	
Radioimmunoprecipitation assay buffer (RIPA)	20 mM Tris-HCl (pH 7.5) 150 mM NaCl 1% NP-40 1% SDS 2.5 mM sodium pyrophosphate 1mM Na_2EDTA	WB
SDS loading dye 4x	40 % glycine 240 mM Tris/HCl (pH 6.8) 8% SDS 0.04 % bromphenole blue 6 % ddH20	WB
SDS running buffer	mM Tris base 190 mM Glycine	WB

	% SDS pH 8.3	
Sucrose buffer	320 mM Sucrose 10 mM Tris/HCL (pH7.4) 1 mM Na_2HCO_3 1 mM $MgCl_2$ Phosphatase inhibitor Protease inhibitor	WB
Tris tricine running buffer	100 mM Tris 100 mM Tricine 0.1 % SDS pH 8.3	WB
Transfer buffer	25 mM Tris base 190 mM Glycine 20% Methanol	WB
TE buffer	10 mM Tris base 1mM EDTA pH 9	IHC
Tris buffer	0.5 M Tris base 0.09% NaCl pH 7.6	IHC
Neutralizing Tris buffer	1 M Tris base pH 8.0	Genotyping
Tris-Milk (2%)	0.5 M Tris base 0.09% NaCl pH 7.6 2% milk powder	IHC
Tris-buffered saline TBS	20 mM Tris base 150 mM NaCl pH 7.5	WB
Tris-buffered saline with Tween (TBS-T)	20 mM Tris base 150 mM NaCl	WB

	0,1 % Tween 20 pH 7.5	
WB blocking buffer	TBS 5%BSA	WB

2.1.3 Consumables

Table 3 List of consumables

Consumable	Manufacturer	Application
Low fluorescent Immobilon PVDF membrane 0.45µm	Merck	WB
Tris-Tricine Novex 10-20% gradient gel	Thermo Fisher	WB
PageRuler 10-250kDa	Fermentas	WB
Protease Inhibitor mix (500x)	Sigma	WB
Cell strainer (40µm)	VWR	MACS
MS columns	Miltenyi Biotech	MACS
LS columns	Miltenyi Biotech	MACS
GeneRuler 100bp DNA ladder	Thermo	Genotyping
Aqua-Poly/Mount	Polysciences Inc.	IHC
Parablast	Leica	IHC
Qiazol	Qiagen	qRT-PCR
Tamoxifen	Sigma	
4-OH-Tamoxifen	Sigma	Cell culture
Glass bottom imaging chamber	Ibidi	Cell culture

2.1.4 Kits

Table 4 List of applied kits

Kit	Manufacturer	Application
DC Protein Assay (Lowry)	BioRad	WB
Precellys soft tissue lysis kit (P000933-LYSK0-A)	Bertin Instruments	WB
RNeasy Mini Kit	Qiagen	qRT-PCR
RNeasy Micro Kit	Qiagen	qRT-PCR
SuperScript III Reverse Transcriptase	Qiagen	qRT-PCR
Adult brain dissociation kit	Miltenyi Biotech	MACS
Anti-O4 MicroBead kit	Miltenyi Biotech	MACS
Anti-ACSA-2 MicroBead kit	Miltenyi Biotech	MACS

Anti-CD11b MicroBead kit	Miltenyi Biotech	MACS
Ovation PicoSL WTA System V2	Tekan	SPIA

2.1.5 qRT-PCR

Table 5 List of housekeeping gene primer sequences

House keeper	Primer sequence	Housekeeper	Primer sequence
18s	For 5'-AAATCAGTTATGGTTCCTTTGGTC-3' Rev 5'-GCTCTAGAATTACCACAGTTATCCAA-3'	Rplp0	For 5'-GATGCCCAGGGAAGACAG-3' Rev 5'-ACAATGAAGCATTTTGGATAATCA-3'
Hprt	For 5'-TCCTCCTCAGACCGCTTTT-3' Rev 5'-CCTGGTTCATCATCGCTAATC-3'	Rps13	For 5'-CGAAAGCACCTTGAGAGGAA-3' Rev 5'-TTCCAATTAGGTGGGAGCAC-3'

Table 6 List of qRT-PCR primer sequences

Gene	Primer sequence	Gene	Primer sequence
Abca1	For 5'- CTGTTTCCCCCAACTTCTG -3' Rev 5'- TCTGCTCCATCTCTGCTTTC -3	Abcg1	For 5'- TCTTTGATGAGCCCACCAGT -3' Rev 5'- GGGCCAGTCCTTTCATCA -3'
Abcg4	For 5'- TGATGTGCCCTTCCAGGT -3' Rev 5'-CAAGGCTGAGAAGAGCAGGA -3'	Aif1	For 5'-TGTTTTTCTCCTCATACATCAGAATC -3' Rev 5'- CCGAGGAGACGTTCAGCTAC -3'
ApoE	For 5'- GACCCTGGAGGCTAAGGACT -3' Rev 5'- AGAGCCTTCATCTTCGCAAT -3'	Aqp4	For 5'- TGGAGGATTGGGAGTCACC -3' Rev 5'- TGAACACCAACTGGAAAGTGA -3'
Bace1	For 5'- CCCTTTCCTGCATCGCTAC -3' Rev 5'- TACACACCCTTTCGGAGGTC -3'	Bace2	For 5'- CCTGAGAGATGAGAATGCCAGT -3' Rev 5'- ATCATGGGCTGAATGTAGAGC -3'
Car2	For 5'- CAAGCACAACGGACCAGA -3' Rev 5'- ATGAGCAGAGGCTGTAGG -3'	Ccl3	For 5'- TGCCCTTGCTGTTCTTCTCT -3' Rev 5'- GTGGAATCTTCCGGCTGTAG -3'
Ccl6	For 5'- TCTTTATCCTTGTGGCTGTCC -3' Rev 5'- TGGAGGGTTATAGCGACGAT -3'	Ch25h	For 5'- TGCTACAACGGTTCGGAGC -3' Rev 5'- AGAAGCCCACGTAAGTGATGAT -3'
Clu	For 5'-GCCATGGATGTCCAGCTC -3' Rev 5'-CACACAGTGCGGTCATCTTC -3'	Csf1	For 5'- ACACCCCCAATGCTAACG -3' Rev 5'- TGGAAAGTTCGGACACAGG -3'
Cst7	For 5'-ATGTGGCTGGCCATTCTG -3' Rev 5'-TGGAGATCAAATCTTTGGAACAA -3'	Cyp51	For 5'- TTAGAACAGAAAGCAGTGTGTGG -3' Rev 5'- TGCATCTATCAAGTAAATTCAGATCC -3'
Dhcr7	For 5'-TTGTAGCCTGGACCCTCATT -3' Rev 5'-GGTGGGTGAGCAGGATAGTC -3'	Dhcr24	For 5'- GGTCATGACGGACGACGTA -3' Rev 5'- AGGGCTTGTAGTAACTGCCAAT -3'
Ece1	For 5'- 5'-GTGCTGGTGACGCTTCTG -3' Rev 5'- ACATACCGGAGGCGTTCTT -3'	Ece2	For 5'-GCTTTGAGACTGCACAGGAGA -3' Rev 5'-CACCTCGGAGTGCAGGAC -3'
Fdft1	For 5'- CCAAACAGGACTGGGACAAG -3' Rev 5'- GACGAGAAAGGCCAATTCC -3'	Gfap	For 5'- TGCTCCTGCTTCGAGTCCTT -3' Rev 5'- CAAGAGGAACATCGTGGTAAAGA -3'
Hmgcs1	For 5'- GGACCGCTGCTATTCTGTCT -3' Rev 5'- AGCCAAAATCATTCAGGGTAAA -3'	Hmgcr	For 5'- TGATTGGAGTTGGCACCAT -3' Rev 5'- TGGCCAACACTGACATGC -3'
Ide	For 5'- TTCGATGTTTCCCATGAACA-3' Rev 5'- AGGGGCACAGGAAAAACTG-3'	Igf1	For 5'- AGCAGCCTTCCAACTCAATTAT -3' Rev 5'- GAAGACGACATGATGTGTATCTTTATC -3'
Itgax	For 5'-GAGCCAGAACTTCCCAACTG -3' Rev 5'-TCAGGAACACGATGTCTTGG -3'	Lamp2	For 5'- AAGGTGCAACCTTTTAATGTGAC -3' Rev 5'- TGTCATCATCCAGCGAACAC -3'
Ldlr	For 5'- GATGGCTATACCTACCCCTCAA -3' Rev 5'- TGCTCATGCCACATCGTC -3'	Lpl	For 5'- CTCGCTCTCAGATGCCCTAC -3' Rev 5'- AGGCCTGGTTGTGTTGCTT -3'
Lrp1	For 5'-ACCACCATCGTGGAAAATG -3' Rev 5'- GTCCCAGCCACGGTGATA -3'	Lrp2	For 5'- TGGAGGATGCAGCCATATCT -3' Rev 5'- GTGTGGACACTGGCACTCAG -3'
Mertk	For 5'-GATGGTTCTGGCCCCACT -3' Rev 5'-CTGATCTAGCTCGGTCTCTTCC -3'	Nceh1	For 5'-AAGGTCGACCCTGGAAGAG -3' Rev 5'-CAGGCTGGCAACGTAGGTA -3'

Npc1	For 5'-CCTTCGGGCCTCCATTG -3' Rev 5'-TGTCACGGTTTCATTGTTGTAAGA -3'	Npc2	For 5'-CCGGTGAAGAATGAATACCC -3' Rev 5'-TTCTTTTTGTCATCTTCAAGTTTCC -3'
Olig2	For 5'- AGACCGAGCCAACACCAG -3' Rev 5'- AAGCTCTCGAATGATCCTTCTTT -3'	Picalm	For 5'-GATGTTCACCTGCCCATTGCTTC -3' Rev 5'-TGGCTGTGCAACTGGAGAAGGA -3'
Plp1	For 5'- TCAGTCTATTGCCTTCCCTAGC -3' Rev 5'- AGCATTCCATGGGAGAACAC -3'	S100b	For 5'- AACAACGAGCTCTCTCACTTCC -3' Rev 5'- CTCCATCACTTTGTCCACCA -3'
Soat1	For 5'- CGCTATGCAGTTTTTACAGGTG-3' Rev 5'- GGGCACAGAGTCTCTCAAAGAT-3'	Srebp2	For 5'- ACCTAGACCTCGCCAAAGGT -3' Rev 5'- GCACGGATAAGCAGGTTTGT -3'
Trem2	For 5'- GACCTCTCCACCAGTTTCTCC -3' Rev 5'- TACATGACACCCTCAAGGACTG -3'	Tyrobp	For 5'-TGGTGTTGACTCTGCTGATTG -3' Rev 5'-GTCTCAGCAATGTGTTGTTTCC -3'
Vldlr	For 5'- AAGTCAGTGTTCCCCCAAAA -3' Rev 5'- TGCTGCCATCACTAAGAGCA -3'		

2.1.6 Antibodies and staining reagents

Table 7 List of primary antibodies

Target	Species	Company	Dilution	Application
APP A8717	Rabbit	Abcam	1:1000	WB
Aβ (6E10)	mouse	Biolegend	1:500	IHC
Aβ (D3E10)	rabbit	Cell signaling	1:500	IHC
GAPDH	mouse	Enzo	1:500	WB
GFAP	mouse	Leica	1:200	IHC
Iba1	rabbit	Wako	1:500	IHC
Lamp1	rat	BD Biosciences	1:500	IHC

Table 8 List of secondary antibodies

Target	Fluorophor	Species	Company	Dilution	Application
Mouse IgG	Alexa 555	Donkey	Thermo	1:1000	IHC
Rabbit IgG	Alexa 488	Donkey	Thermo	1:1000	IHC
Rabbit IgG	DyLight 633	Donkey	Thermo	1:500	IHC
Rabbit IgG	IRDye 800	Goat	Licor	1:5000	WB
Rat IgG	Alexa 555	Donkey	Thermo	1:1000	IHC

Table 9 List of Dyes

Target	Name	Company	Dilution	Application
DNA	DAPI	Thermo Fisher	300nM in PBS	IHC
DNA	GelRed	BioTrend	1:4000	Genotyping
β-sheets	Congo red	Tocris	0.01% in PTwH	LSM
β-sheets	Methoxy-X04	Tocris	4µg/ml in 50% EtOH	IHC, FACS
Protein	Fastgreen	Serva	0.0005% in FG wash buffer	WB

2.1.7 Cell culture

Table 10 List of cell culture materials

Reagent	Company/Composition
DMEM	Sigma
DMEM-F12	Gibco
LPDS	Alfa Aesar
FCS	Gibco
P/S	Lonza
GM-CSF	Sigma
L929 medium	DMEM
	10% FCS
	1% P/S
	1 week cultivation of L929 fibroblasts
Complete microglia medium	DMEM-F12
	10% FCS or LPDS
	1% P/S
	10ng/ml GM-CSF
L929 conditioned medium	DMEM
	10% FCS
	1% P/S
	15% L929 medium
BMDM reduced medium	DMEM
	10% LPDS
	1% P/S
Aβ42 peptide	Peptide Specialty Laboratories
Fluorescent Aβ42 peptide	Bachem

2.1.8 Mouse lines

Table 11 List of mouse Lines and genetic modifications

Name	Reference
5xFAD	Oakley et al. 2006
Aldh1l1-CreERT2	Winchenbach et al., 2016
CaMKIIα-Cre	Minichiello et al., 1999
Cx3cr1-CreERT2	Parkhurst et al., 2013
Fdft1 flox/flox	Saher et al., 2005

Table 12 List of generated mice and Acronym

Mutant name	Genotype
AcKO-AD	Aldh1l1-CreERT2 $Fdft1^{flox/flox}$ $5xFAD^{tg}$
ACtrl-AD	$Fdft1^{flox/flox}$ $5xFAD^{tg}$
McKO	$Cx3cr1\text{-}CreERT2^{+/-}$ $Fdft1^{flox/flox}$
Cre	$Cx3cr1\text{-}CreERT2^{+/-}$
McKO-AD	$Cx3cr1\text{-}CreERT2^{+/-}$ $Fdft1^{flox/flox}$ $5xFAD^{tg}$
Cre-AD	$Cx3cr1\text{-}CreERT2^{+/-}$ $5xFAD^{tg}$
NcKO-AD	CamKIIα-Cre $Fdft1^{flox/flox}$ $5xFAD^{tg}$
NCtrl-AD	$Fdft1^{flox/flox}$ $5xFAD^{tg}$

2.1.9 Genotyping

Table 13 List of genotyping primer and protocols

Mutant	Genotyping primer	Protocol		
5xFAD	5'-CGGGCCTCTTCGCTATTAC -3'	94°C	3 min	
	5'-ACCCCCATGTCAGAGTTCCT -3'	94°C	20 s	
	5'-TATACAACCTTGGGGGATGG -3'	65°C	15 s	5 cycles
		86°C	10 s	
		94°C	20 s	
		62°C	15 s	5 cycles
		68°C	10 s	
		94°C	15 s	

		60°C	15 s	28 cycles
		72°C	10 s	
		72°C	2 min	
		4°C	pause	
Aldh1l1	5'-CAACTCAGTCACCCTGTGCTC -3'	95°C	3 min	
	5'-TTCTTGCGAACCTCATCACTCG -3'	58°C	30 s	
		72°C	60 s	36 cycles
		95°C	30 s	
		58°C	1 min	
		72°C	10 min	
		4°C	Pause	
CaMKIIα	5'-GGGAGGTAGGAAGAGCGATG -3'	95°C	3 min	
	5'-CCATGAGTGAACGAACCTGG -3'	58°C	30 s	
		72°C	80 s	30 cycles
		95°C	30 s	
		58°C	1 min	
		72°C	10 min	
		4°C	pause	
Cx3cr1	5'-GAACTACAATCCTTTAAGGCTCACG -3'	95°C	3 min	
	5'-GCAGGACCTCGGGGTAGTCAC -3'	58°C	30 s	
	5'-CACCAGAGACGGAAATCCATCG -3'	72°C	45 s	35 cycles
		95°C	30 s	
		58°C	1 min	
		72°C	10 min	
		4°C	pause	
Fdft1	5'-CAGTCATAGGTGGCGAAAAAGGTGTT -3'	95°C	3 min	
	5'-ACTTGTGGAAGGAAGTTCCAACCAGA -3'	58°C	30 s	
	5'-GAGGAAATCCTGGCATGAACACAGT -3'	72°C	45 s	36 cycles
		95°C	45 s	
		58°C	1 min	
		72°C	5 min	
		4°C	pause	

2.1.10 Software

Table 14 List of software

Software	Company
Fiji	Fiji: an open-source platform for biological-image analysis (Schindelin et al., 2012)
Prism	Graphpad
Illustrator	Adobe
ChemSketch	Advanced Chemistry Development
Biorender	Biorender
Zen	Zeiss
LASX	Leica

2.2 Methods

2.2.1 Animals

All animal experiments were performed according to German animal welfare policies, confirmed with the Max Planck Institute of Experimental Medicine and approved by the German Federal State of Lower Saxony. With regards to the animal husbandry, in addition to the *ad-libitum* supply of food, water and cleaning of housing, mice were kept and bred under the care of animal caretakers, veterinarians and trained scientists. Mice were generally kept in groups with a 12h dark and 12h light cycle. All mice used for this study (Table 12 List of generated mice) were facilitated at a C57BL/6 background and compared to sex and age matched controls, either as littermate controls or closely related controls. Genotyping of the mice used for experiments were performed from ear punches after weaning and confirmed with a second biopsy after sacrificing. DNA isolation of ear biopsies was achieved by lysis with 50mM NaOH under boiling alkaline conditions and subsequent neutralization with 1M Tris/HCl pH8.0. Performing mutation specific polymerase chain reactions (Table 13 List of genotyping) and following gel electrophoresis for visualizing the amplified DNA fragments completes the determination of the diverse genotypes. This method was performed mainly by Annika Schmidke and Vanessa Schlotzig (both student assistants).

Table 15 Genotyping protocol

Reagent	Volume	Company
Go-Taq 5x buffer	4µl	Promega
Nucleotides (2mM)	2µl	Promega
Primermix	0.5µl per primer	Custom made, AGCT Lab MPI-MNAT
GoTaq	0.1µl	Promega
Magnesiumchloride (25mM)	1µl	BioLabs
dH20	Add to 19 µl	
DNA	1µl	

2.2.2 Tissue preparation for immunohistochemistry and microscopy

For microscopy, erythrocytes had to be removed from tissue to remove background signals, therefore mice were anesthetized with Avertin followed by transcardial flushing with Hank´s buffered salt solution until blood was removed and liver was decolorized. Subsequently perfusion with the fixative paraformaldehyde (4% PFA) was performed and the tissue for microscopy was removed and postfixed with 4%PFA and stored at 4°C in PBS until further processing.

2.2.3 Light sheet microscopy of whole tissue

Whole brain imaging was performed on the perfused tissue following the iDisco protocol (Liebmann et al., 2016; Renier et al., 2014) displayed in (Table 16 Dehydration and staining for light sheet microscopy). Protocol was applied by Dr. Constanze Depp and Andrew Sasmita (Depp et al., 2021). Following the clearing and staining protocol samples were imaged with the UltraMicroscope II (LaVision Biotec) in an Eci filled sample holder. The red fluorescence of congo red as acquired 80% laser power and a 585/40 emission filter in the mosaic acquisition mode (settings: 5µm thickness, 20% sheet width, 0.154 sheet numerical aperture, 4µm z-step size, 1000x1600 px, 4x4 tiling, dual light sheet illumination, 100ms camera exposure). Acquired and stitched whole brain images were annotated based on Allen brain atlas to analyze regions of interest separately (Depp et al., 2021).

Table 16 Dehydration and staining for light sheet microscopy (LSM)

Step	Solution	Time	Temperature
Dehydration	50% MeOH/ 50% PBS	1h	RT
	80% MeOH/20% PBS	1h	RT
	100% MeOH	1h	RT
	100% MeOH	1h	RT
Bleaching	1:1:4 H2O2:DMSO:MeOH	O/N	4°C
Delipidation	100% MeOH	30min	4°C
	100% MeOH	3h	-20°C
	100% MeOH	O/N	4°C
	80% MeOH/20% PBS	2h	RT
Rehydration	80% MeOH/20% PBS	2h	RT
	50% MeOH/ 50% PBS	1h	RT
	100% PBS	1h	RT
	0.2% Triton X-100/PBS	1h	RT
	0.2% Triton X-100/PBS	1h	RT
Permeabilisation	PBS/0.2% Triton X-100/ 20% DMSO/0.3 M glycine	O/N	37°C
	PBS/0.2% Tween-20/10 mg/ml heparin/5mM sodium azide (PTwH)	1h	RT
	PTWH	1h	RT
Labelling	PBS/0.2% Triton X-100/ 20% DMSO/0.3 M glycine	3d	37°C
Washing	6x PTwH	1d	RT
Dehydration	20% MeOH/ 80% PBS	1h	RT
	40% MeOH/ 60% PBS	1h	RT
	60% MeOH/ 40% PBS	1h	RT
	100% MeOH	1h	RT
Delipidation	1:2 MeOH:dichloromethane	O/N	RT
	Dichloromethane	40min	RT
Clearing	Ethylcinnamate	1h	RT
Storage	Ethylcinnamate		RT

2.2.4 Immunolabeling and epifluorescent microscopy

For fluorescent labeling of tissue sections, fixed brains were embedded in paraffin (Table 17 Paraffin embedding) using the STP 120 tissue processing machine (Leica) and HistoStar embedding station (Epredia) and cut into 5µm sections to mount and store on glass slides. Paraffin sections were stained according to a well-established staining protocol (Table 18 Staining protocol for fluorescent labeling) and the listed antibodies (Table 7 List of Primary antibodies,

Table 8 List of Secondary Antibodies, Table 9 List of Dyes) and finally mounted with Aqua Poly/Mount.

Table 17 Paraffin embedding

Step	Solution	Time
Dehydration	50% EtOH	1h
	70% EtOH	2h
	70% EtOH	2h
	80% EtOH	1h
	100% EtOH	1h
	100% EtOH	1h
	100% Isoproponal	1h
	50% Isoproponal/ 50% Xylol	2h
	100% Xylol	2h
	100% Xylol	2h
Embedding	Paraffin	2h
	Paraffin	2h

Table 18 Staining protocol for fluorescent labeling

Step	**Solution**	**Time**
Deparaffination	60°C oven	10min
	100% Xylol	10min
	100% Xylol	10min
	50% Isoproponal/ 50% Xylol	10min
Rehydration	100% EtOH	5min
	90% EtOH	5min
	70% EtOH	5min
	50% EtOH	5min
	Aqua dest	5min
Antigen retrieval	Tris/EDTA buffer pH9.0 or	
	Citrate buffer pH6.0	
	Boiling at 600W	10min
	Cooling down	20min
Washing	PBS	5min
	PBS	5min
Blocking	10% Goat serum/PBS	1h
1st antibody	5% Goat serum/PBS	O/N
	+1st antibody at 4°C	
Washing	PBS	5min

	PBS	5min
2nd antibody	5% Goat serum/PBS +2nd antibody	2h
Amyloid dye	Methoxy-X04 in 50% EtOH	30min
Contrasting	50%EtOH	5min
Washing	PBS	5min
	PBS	5min
	PBS	5min
Mounting	Aqua Poly/Mount	Storage dark and at 4°C

2.2.5 RNA expression analysis

RNA was isolated from fresh frozen material of microdissected cortical tissue, extraction of RNA was implemented using Qiazol and the RNeasy Mini Prep Kit (Qiagen). To extract the tissue, mice were sacrificed and brain was removed and meninges were removed from brain surface through rolling on whatman paper. Brain was sliced using a 1mm brain matrix to cut coronar sections and separate specific brain areas and immediately frozen on dry ice.

RNA was extracting as stated in following (Table 19 Tissue RNA extraction with Qiazol). After RNA isolation, concentration was measured and the calculated amount used for cDNA synthesis (Table 20 cDNA synthesis). Quantitative Real-time PCR was performed in 384 well plates using the SybrGreen mix (Promega), therefore 10ng cDNA was used for each of the triplicates. Gene specific intron spanning primes (Table 6 List of qRT-PCR primer sequences) were provided from the in-house AGCT lab and polymerase chain reaction was executed using a 45-cycle heating protocol (Table 21 qRT-PCR procedure) in the LightCycler 480 II. The corresponfing LightCycler 480 software was used for background substraction and thresholding and afterwards CT values (cycle thresholds) were exported to excel for further normalization to housekeeping genes (Table 5 List of housekeeping gene primer sequences). Results were analyzed using the ΔΔCT method and displayed significance was calculated using the Student´s t-test.

Table 19 Tissue RNA extraction with Qiazol

Step	Solution	Process
Lysis	Qiazol	Homogenate
Separation of cellular components	Chloroform	Incubate
		Centrifuge
		Separate aqueous phase
RNA precipitation	70% EtOH	Transfer on columns
		Centrifuge
Column washing	RW1 buffer	Apply on column, centrifuge
	RPE buffer	Apply on column, centrifuge
	RPE buffer	Apply on column, centrifuge
Dry silica membrane		Centrifuge with open lid
Elution of RNA	Nuclease free water	Apply on column, centrifuge

Table 20 cDNA synthesis

Step	Solution	Protocol
Primer annealing	4µl RNA	70°C 2 min
	1µl dT primer mix (0.6pmol/µl)	
	1µl N9 primer (120pmol/µl)	
cDNA synthesis	2µl 5x first strand buffer	25°C 10 min
	0.5µl dNTP (10 mM)	50°C 45 min
	1µl DTT (100 mM)	55°C 45 min
	1µl SuperScript III reverse transcriptase (200 U/µl)	
Dilution	Nuclease free water	Final concentration 5ngµl

Table 21 qRT-PCR protocol

Solution	Protocol		
2µl cDNA	50°C	2 min	
5µl SybrGreen	95°C	10 min	
0.4µl forward primer (10pM)	95°C	15 s	
0.4µl reverse primer (10pM)	60°C	1 min	45 cycles
2.2µl ddH_20			

2.2.6 Cell isolation

For cell specific analysis cells were isolated according to the manufacturer's protocol of the Adult brain dissociation kit (Miltenyi Biotec) displayed in short (Table 22 Cell isolation via magnetic-activated cell sorting). Magnetic-activated cell sorting (MACS) separates cell fractions using antibody covered beads for surface protein detection. The cell fraction was used for analysis of gene expression changes and therefore RNA was extracted using the RNeasy micro Kit (Table 23 RNA isolation of cells in RLT buffer), established for small amounts of mRNA and either send for transcriptomic analysis or precipitated and amplified using the Ovation PicoSL WTA System V2 (Tacan, Switzerland) Table 24 RNA precipitation with glycogen, Table 25 Single primer isothermal amplification).

Table 22 Cell isolation via magnetic-activated cell sorting (MACS)

Step	Solution	Process
Tissue preparation		Extract brain
		Remove meninges
	DPBS	Separate cortex
		Dissect tissue
Cell suspension	Enzyme mix	Incubate at 37°C
		Triturate gently
Debri removal	DPBS	Gradient
	Debri removal solution	Remove myelin and debris
Red blood cell removal	Red blood cell removal solution	Erythrocyte lysis
Magnetic labeling	O4 beads	Oligodendrocyte isolation
	AcsaII beads	Astrocyte isolation
	CD11b beads	Microglia isolation
Elution	MS columns	Magnetic coupled cells stay
	RLT buffer	Remove for RNA

Table 23 RNA isolation of cells in RLT buffer

Step	Solution	Process
RNA precipitation	70% EtOH	Transfer on columns
		Centrifuge
Column washing	RW1 buffer	Apply on column, centrifuge
	RPE buffer	Apply on column, centrifuge
	80% EtOH	Apply on column, centrifuge
Dry silica membrane		Centrifuge with open lid
Elution of RNA	Nuclease free water	Apply on column, centrifuge

2.2.7 Transcriptomic analysis

Extracted total RNA from acutely isolated microglia was subjected to 50bp single-end mRNA sequencing using Illumina RNA library preparation system under manufacturer instructions. Constructed libraries were sequenced using HiSeq4000 (Illumina). Raw data was recovered into FASTQ format and its quality was primarily evaluated by FASTQC v0.72, low quality sequencing data profiles (n=2) were excluded from further analysis. The remaining data was aligned towards reference genome GRCm38 (mm10) using STAR v2.5.2b-2 with default parameters, and raw counts of genes for each sample were extracted by featureCount v1.6.3. The raw count profiles were firstly used for calculating transcript per million (TPM) in order to perform further sample distances evaluations, and were used for differential gene expression (DGE) analysis for each pair of genotypes using DESeq2 v1.26.0. For all DESeq2 comparisons, genes with adjP<0.05 were considered to be significantly regulated. Lastly, differentially regulated genes from all statistics comparisons were summarized, and their TPM values across all samples were scaled and clustered using kmeans clustering (k=10). (Sequencing was performed by the NGS-facility, University Medical Center Göttingen, Analysis was performed by Dr. Ting Sun)

2.2.8 Isolation of Methoxy-X04 stained microglia

For separating microglia for their Methoxy fluorescence or the absence, brain tissue was extracted and dissected, incubation with 0.4mg/ml Methoxy-X04 in buffer at 37°C for 30 minutes and subsequent cell suspension with enzymes (according to the MACS protocol, Table 22). The single cell suspension was labeled with the CD11b microglia kit (Table 4 List of applied kits) and sorted in LS columns (Miltenyi Biotec). The CD11b+ cell fraction was sorted for Methoxy+ and Methoxy- cells using flow cytometry (FACS sorting was performed by Dr. Leon Hosang). Equal numbers of

cells were separated and RNA was extracted (Table 23 RNA isolation of cells in RLT buffer) for expression analysis with the intermediate steps of RNA precipitation (Table 24 RNA precipitation with glycogen) and SPIA (Table 25 Single primer isothermal amplification).

Table 24 RNA precipitation with glycogen

Step	Solution	Process
RNA binding and precipitation	100µl RNA	
	1µl Glycogen (20µg/µl)	
	50µl NH4Ac	
	375µl 100% EtOH	Mix and incubate on ice
Pelleting		Centrifuge
Washing	1ml 100% EtOH	Mix, centrifuge
Drying		Remove supernatant and let dry
Elution	5µl nuclease free water	Resuspend for amplification

Table 25 Single primer isothermal amplification (SPIA)

Step	Solutions	Protocol
First Strand cDNA Synthesis	4µl precipitated RNA 2µl First Strand Primer Mix	65°C 2 min
	2.5µl First Strand Buffer 0.5µl First Strand Enzyme Mix	4°C 2 min 25°C 30 min 42°C 15 min 70°C 15 min
Second Strand cDNA Synthesis	9.7µl Second Strand Buffer 0.3µl Second Strand Enzyme Mix	4°C 1 min 25°C 10 min 50°C 30 min 80°C 20 min
Purification of double-stranded cDNA	32µl RNAClean XP beads Place on magnet 70% EtOH 70% EtOH 70% EtOH	Incubate 10 min Separation 5 min Wash Wash Wash Dry beads

SPIA amplification	10µl SPIA Primer mix 10µl SPIA Enzyme mix 20µl SPIA buffer	4°C 1 min 47°C 75 min 95°C 5 min
Purification of amplified cDNA	Place on magnet Separate liquid phase wit cDNA	Separation 5 min

2.2.9 Protein biochemistry

Immunoblots from dissected and frozen material, tissue was homogenized in the Precellys and the special soft tissue lysing kit (Table 4 List of applied kits). The tissue lysate was fractioned to separate membrane-bound proteins, soluble proteins and removing proteins out if the fibrillary structure of amyloid plaques (Table 26 Fractioning of protein samples). Protocols were established in the lab in collaboration with Dr. Constanze Depp from protocols that were kindly provided by Dr. Michael Willem and Prof. Christian Haas. The protein concentration of the membrane-bound and soluble fraction was determined by a Lowry protein assay (Biorad) and calculated using detergent comparable BSA standards. 20µg per sample was mixed with DTT and Laemmli loading dye and loaded into separate lanes of gradient Tris-Tricine SDS PAGE gels (10-20%, Thermo Fisher). Gels were run at 120V for approximately 1 hour in Tricine running buffer and stopped when low molecular weight proteins are at the end of the gel for better resolution of c-terminal fragments. Proteins were transferred onto low fluorescent membrane (Immobilon-FL membrane, 0.45µm pore size, Merck) in a wet blot system for 1 hour at 500mA in blotting buffer. Determination of the protein content was given by FastGreen total protein staining solution, the protein concentration was used for normalizing the concentration of the proteins of interest. After the FastGreen staining the dye was removed with FastGreen washing buffer, ethanol and water washes and blocked afterwards with 5% BSA for 1 hour. The blocked membrane was incubated overnight in the APP antibody in 5% BSA at 4°C (Table 7 List of primary antibodies). After incubation membrane was washed 3 times with TBS-T and incubated in the fluorescent secondary antibody in 5% BSA for 1 hour at room temperature (Table 8 List of secondary antibodies). After several washes with TBS-T and subsequent washes with TBS fluorescent labeled proteins were visualized at the Odyssey scanner (Licor). Quantification of the protein of interest including background subtraction was performed using Fiji. The integrated density of the bands of the c-terminal fragments were normalized to full length protein and the whole protein staining.

Table 26 Fractioning of protein samples

Step	Solution	Settings
Soluble fraction	Homogenization in DEA buffer	Precellys: 6500rpm, 30s, 4°C
	Centrifugation	5000g, 10min, 4°C
	Supernatant: ultracentrifugation	130000g, 1h, 4°C
	Neutralization	pH adjustment with 10% with 0.5M Tris pH6.8
	DEA fraction	store at -80°C
Membrane-bound fraction	Pellet from first step	
	Homogenization in RIPA buffer	Precellys: 5000rpm, 12s, 4°C
	Centrifugation	5000g, 10min, 4°C
	Supernatant: ultracentrifugation	130000g, 1h, 4°C
	RIPA fraction	store at -80°C
Amyloid fraction	Pellet from second step	
	Homogenization in 70% formic acid	Sonication, 7min
	Ultracentrifugation	130000g, 1h, 4°C
	Supernatant: **FA fraction**	store at -80°C
	Neutralization	pH adjustment with 1:20 with 1M Tris pH9.5

2.2.10 In vitro characterization of amyloid handling

Microglia cells were obtained by magnetic-activated cell sorting in a fast protocol in accordance with the cell isolation protocol. The protocol was adjusted by gentler trituration with BSA coated pipettes, removing the debris removal and erythrocyte lysate step and the cell separation on LS columns. The cell isolation was performed under sterile conditions following incubation of CD11b positive cells in complete microglia medium (Table 10 List of cell culture materials). Isolated microglia cells were used for two approaches, for the ex vivo phagocytosis assay and for treating cells with Aβ. For evaluating the plaque clearance efficiency microglia (from McKO and Cre) were seeded on 10µm thick fresh frozen 5xFAD sections that were pre-treated with anti-amyloid antibody to prime microglia. Microglia were kept in culture for 5 days for clearing plaques from amyloid burdened brain and efficiency was evaluated by fluorescent staining and microscopy of microglia and plaques. The reduction of plaques comparing to the consecutive slide that was incubated without microglia displays the clearance efficiency (Protocol was kindly provided by Dr. Sabina Tahirovic).

A second experiment using the primary microglia isolated from McKO and Cre is the in vitro treatment with synthetic Aβ. The Aβ was diluted to 100µM and incubated at 37°C for 2 days to build pre-fibrils and treat microglia with 10pM. After 3 incubation cells were lysed for mRNA isolation and expression analysis (Table 23 RNA isolation of cells in RLT buffer, Table 21 qRT-PCR procedure).

Bone marrow derived macrophages (BMDM) from McKO and Cre were isolated from femoral bones and resuspended in L929 conditioned medium for plating and incubation. 4-hydroxy-tamoxifen was added for 10 days for in vitro recombination. For experiments cultivated cells were plated on PLL coated cover slips for imaging and on glass bottom imaging chambers. BMDMs were treated with pre-aggregated fluorescent Aβ in reduced medium for 24 hours. The cells within the imaging chambers were imaged every 5 minutes to track the phagocytosis. The macrophages on the cover slips were fixed with 4%PFA and stained for IBA1 and LAMP1 (Table 27 In vitro staining). Cells from McKO mice were compared with Cre cells for assessing changes of the phagocytosis efficiency.

Table 27 *In vitro* staining

Step	Solution	Time
Permeabilization	0.3% Triton in PBS	10min
Wash	PBS	3x5min
Block	10% goat serum	1h
	0.03% Triton in PBS	
Primary antibody	1.5% goat serum in PBS	2h
Wash	PBS	3x5min
Secondary antibody	10% goat serum in PBS	30min
Wash	PBS	5min
Cell nucleus dye	Dapi	5min
Wash	PBS	2x5min

3 Results

3.1 Neuronal cholesterol synthesis does not alter Aβ generation and deposition

In vitro reduced neuronal cholesterol levels inhibited amyloidogenic APP processing (Ehehalt et al., 2003) and decreased generation of Aβ (Simons et al., 1998). For evaluating the role of

neuronal cholesterol synthesis on amyloidosis in vivo we generated mice lacking *Fdft1* in neurons driven by the *CamKIIα*-Cre line (Funfschilling et al., 2012; Minichiello et al., 1999). Recombination of projections neurons in the cortex and hippocampus starts postnatally (Dragatsis & Zeitlin, 2000). Mutants used for this study harbored the genotype *CamKIIα*-Cre *Fdft1*$^{fl/fl}$ 5xFAD^{tg} (called NcKO-AD) and were compared to age and sex matched controls with the genotype *Fdft1*$^{fl/fl}$ 5xFAD^{tg} (NCtrl-AD). Surprisingly, the loss of cholesterol synthesis in neurons did not change plaque load at 3.5 months of age as quantified in 2D slices and fluorescent labeling of plaques in the subiculum and in 3D light-sheet microscopic analysis of the cortex and hippocampus (Figure 6a-c). Due to the Thy1 promotor of the 5xFAD model hAPP is restricted to neurons. *In vivo* neuronal cholesterol synthesis did not affect neuronal APP processing. Immunoblot analysis using the anti-APP antibody A8717 binding to the carboxyterminal fragment of APP uncovered no alterations of full-length APP and C-terminal fragments (Figure 6 d-e). In addition to the steady-state APP processing and amyloid deposition, the glial response to plaques was similar in mutants and control. Summarizing the observations in NcKO-AD mice, ablation of neuronal cholesterol synthesis had no effect on amyloid plaque density with the applied methods.

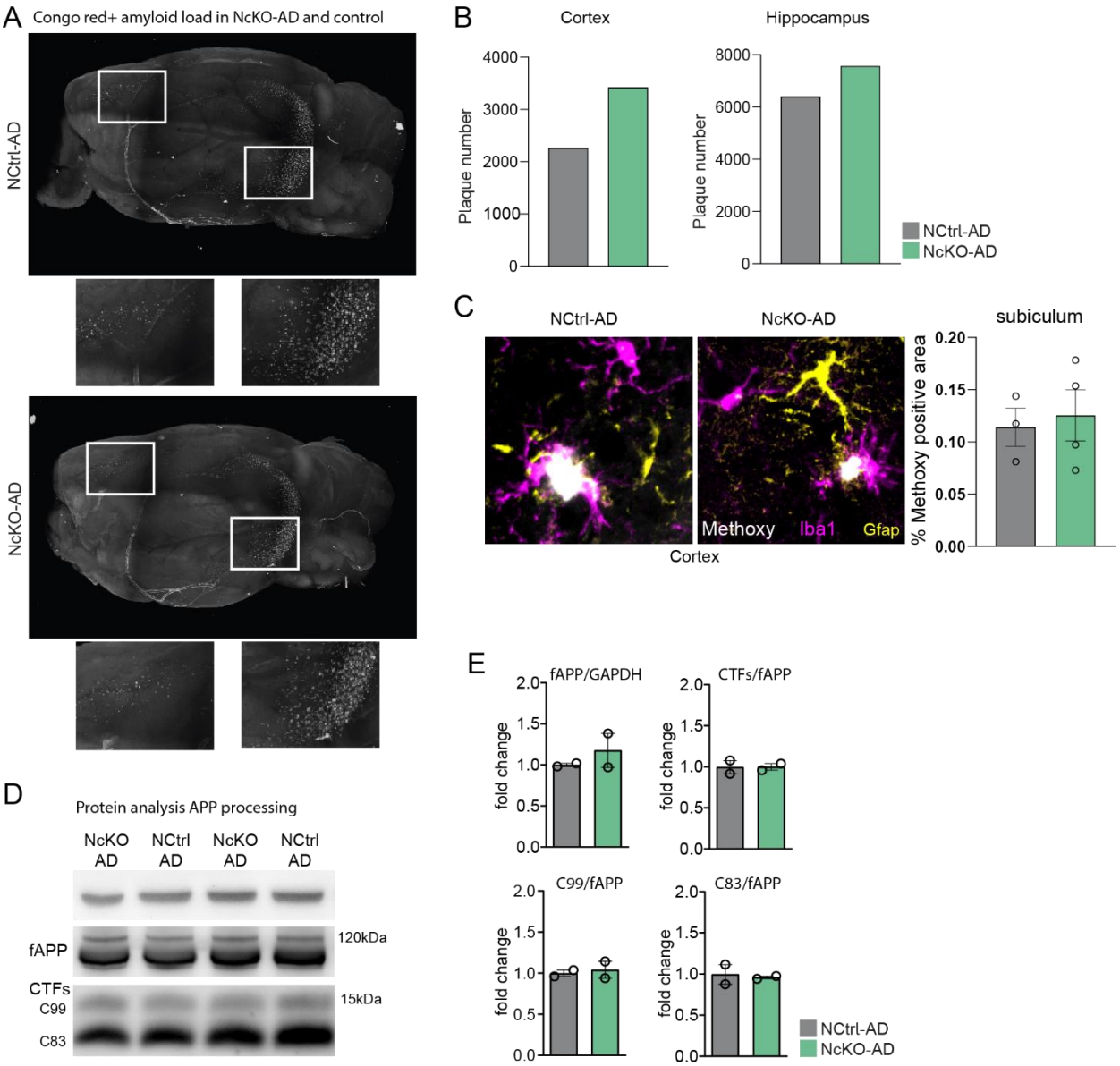

Figure 6 Neuronal sterol synthesis ablation is not involved in plaque pathology. (A) Light sheet microscopy displays similar congo red stained plaque burden in NcKO-AD mice and the corresponding controls at 3.5 month of age. (B) Quantification of plaques in cortex and hippocampus from whole tissue imaging. (C) Quantification of Methoxy-X04 positive area in the subiculum from 2 months old mice is comparable. Further in the cortex of mutants and control microglia and astrocytes surrounding the plaques (D+E). Immunoblot of APP processing is comparable in both groups. Full-length protein and C-terminal fragments of APP are visualized by A8717 APP antibody and normalized to the housekeeper GAPDH (Blot was performed by Jan Winchenbach). Analysis of full-length APP and c-terminal fragments normalized to the housekeeping protein GAPDH confirms the unchanged processing of APP.

3.2 Amyloid burden is reduced when astrocytes lack sterol synthesis

In response to pathological conditions astrocytes undergo morphological changes and become reactive. The astrogliosis is detectable in post-mortem brains as well as in mouse models of AD and can be correlated to dementia (Rodríguez et al., 2009). Astrocytes are a central player of brain cholesterol homeostasis, because astrocytes are the main producers of cholesterol in the brain and supply other brain cells via ApoE. To evaluate the impact of the astrocyte-specific cholesterol synthesis on APP processing, Aβ generation and glial response, mice lacking FDFT1 in astrocytes using *Aldh1l1*-CreERT2 (Winchenbach et al., 2016) were created and combined with the 5xFAD mouse model, here referred to AcKO-AD. The generated AcKO-AD (*Aldh1l1*-CreERT2 *Fdft1*$^{fl/fl}$ 5xFAD^{tg}) were compared to age- and sex-matched controls further called ACtrl-AD (*Fdft1*$^{fl/fl}$ 5xFAD^{tg}). The recombination of astrocytes was induced by applying tamoxifen at the age of 5 weeks. The plaque burden was investigated by in toto brain imaging of congo red+ stained plaques (Figure 7a). Reduced plaque numbers were found in the hippocampus and a tendency of reduction as well in the cortex at the age of 3.5 month (Figure 7b). Next the effect of the astrocyte specific loss of sterol production on tissue level was analyzed by quantitative RT-PCR (Figure 7c-e). Ablated cholesterol synthesis in astrocytes upregulated *Gfap* and the expression of *Trem2* and *Tyrobp* was significantly enhanced. *Trem2* and *Tyrobp* are part of the inflammatory response to amyloid and were widely discussed to be part of the microglia transition to form disease associated microglia (DAM). The significant upregulation of low density *Ldlr* and *Abca1* in AcKO-AD mice showed enhanced lipid trafficking. *Abca1* on the one hand is an important exporter of lipids and on the other hand *Ldlr* mediates the import of cholesterol into cells. Another gene that is highly regulated is the Aβ degrading enzyme endothelin-converting enzyme 1 (*Ece1*), which among others is known as Aβ- degrading enzyme. Changes in plaque load can be either due to modified clearance or higher production. The β-site cleaving enzyme *Bace1* is essential to generate Aβ. Even if the expression level of the main amyloidogenic APP cleaving enzyme *Bace1* was not modified on tissue level the processing of APP could be altered. APP processing was investigated on protein level performing immunoblots. The immunoblots showed neither a regulation of full-length APP nor the carboxterminal fragments C99 and C83 (Figure 7f-g), which indicated that APP processing was unaffected by astrocytic cholesterol synthesis. Despite unaltered APP processing, plaque load was changed. The induction of activated microglia markers and the increased levels of the amyloid-degrading enzyme Ece1 could indicate an alteration of elevated microglia plaque interaction and enhanced phagocytosis.

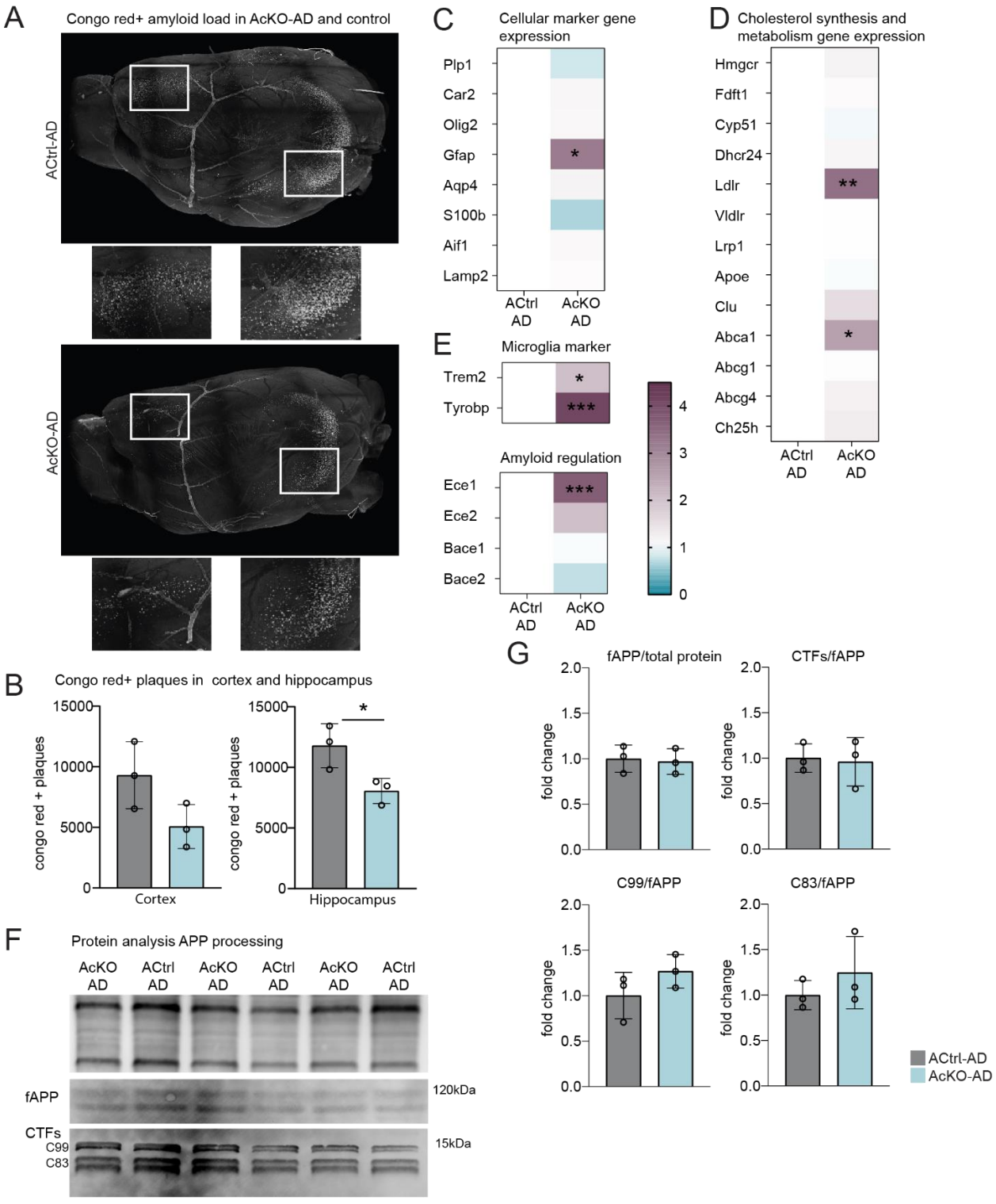

Figure 7 Lack of cholesterol in astrocytes reduces plaque burden. (A) Light sheet microscopy of congo red+ plaques in hemispheres of AcKO-AD and ACtrl-AD with detailed magnification of cortical plaque load and hippocampus. (B) Quantification of 3D plaque number in the cortical and hippocampal area of one hemisphere at 3.5 months. Circles represent single animals (n=3). Asterisks represent significant differences with *p < 0.05, **p < 0.01, ****p < 0.0001 (unpaired Student´s t-test). (C-E) Expression analysis of cortical tissue of 3.5-month-old mice (n=5) depicting glial

changes, adaptions of the cholesterol synthesis and lipid transport, alterations of the amyloid regulation to the lack of sterol synthesis in astrocytes. Heatmap represents fold changes normalized the mean of to ACtrl-AD expression levels. Asterisks represent significant differences with *p < 0.05, **p < 0.01, ****p < 0.0001 (unpaired Student´s t-test). (F) Immunoblots of full-length APP and the carboxyterminal fragments in cortical tissue from 3.5-month-old mice is presented (Immunoblot was performed together with Hoang Duy Nguyen, BA student). The protein levels are normalized to total protein levels stained with FastGreen. (G) APP cleavage analysis were normalized to the total protein content and each dot represents one animal. Every animal is represented in a single lane (F) and dot of the bar graphs (G). (n=3)

3.3 Cholesterol synthesis ablation in microglia cells drives amyloid plaque deposition

In Alzheimer´s disease and the 5xFAD mouse model microglia play a pivotal role in disease progression, especially via their interaction with senile plaques. To study the role of microglia-specific cholesterol synthesis in AD, 5xFAD mice were crossbred with *Fdft1* floxed mice to generate 5xFAD *Fdft1*$^{fl/fl}$ and further bred with *Cx3cr1*-CreERT2^{+} (Parkhurst et al., 2013), a microglia-specific Cre driver. The resulting offspring harboring the microglia specific ablation of squalene synthase on an amyloidosis background (*Cx3Cr1*-CreERT2$^{+/-}$ *Fdft1*$^{fl/fl}$ 5xFAD^{tg}, further called McKO-AD) were analyzed. These mutants were compared to the age- and sex-matched controls (*Cx3Cr1*-CreERT2$^{+/-}$ 5xFAD^{tg}, named Cre-AD). Cre driver controls were used to control for the effect of the CX3CR1 effect on the AD progression and microglia activation. Recombination was achieved by applying tamoxifen at the age of 5 weeks. Light sheet microscopy was used to study amyloid plaque load in 3.5 months old mice in 3D (Figure 8a). Quantification of the most affected brain areas in the 5xFAD mouse model unrevealed a significantly enhanced plaque burden in McKO-AD in both, cortex and hippocampus when compared to controls. The plaque number in the hippocampus of mutants was approximately 2-fold and in the cortex and about three-times as many plaques were found (Figure 8b). Consequences of inactivated microglial sterol synthesis on tissue expression levels of cell type specific markers were evaluated in the cortex. The expression of cellular marker genes for oligodendrocytes, astrocytes and microglia did not differ from animals with functional sterol synthesis in microglia except a minor upregulation of the oligodendrocyte lineage marker *Olig2* (Figure 8c). Expression of genes related to cholesterol synthesis were unaffected suggesting only a minor contribution of microglia cholesterol synthesis to the brain cholesterol homeostasis or an involvement of other brain cells to compensate for the abolished microglia synthesis to maintain cholesterol requirements (Figure 8d). A significant upregulation of *Ece1*, the Aβ-degrading enzyme could hint towards

counteracting elevated plaque levels (Figure 8e). The signature marker of fully activated microglia, *Trem2* that enables the development of the disease associated microglia state (DAM) was downregulated in the mutant cortex. Additional to that, *Trem2* was shown to modulate lipid metabolism in microglia (Nugent et al., 2020) (Figure 8f). This alteration can affect the microglia amyloid response and thereby the plaque burden. One cause of the elevated plaque burden can be higher Aβ production. The full-length APP and the processed c-terminal APP fragments can be depicted by the protein abundance in the membrane-bound fractions. The fAPP and CTFs were visualized using the c-terminal APP antibody A8717 and were normalized to the total protein content stained with FastGreen solution (Figure 8g). CTFs and fAPP of the microglia specific cholesterol synthesis depleted mice were comparable to the controls suggesting no changes in the processing of the amyloid precursor protein (Figure 8h). To conclude, highly elevated plaque density in 5xFAD mice lacking sterol synthesis in microglia were independent of APP processing changes but are likely the result of altered glial activity, plaque clearance or plaque building.

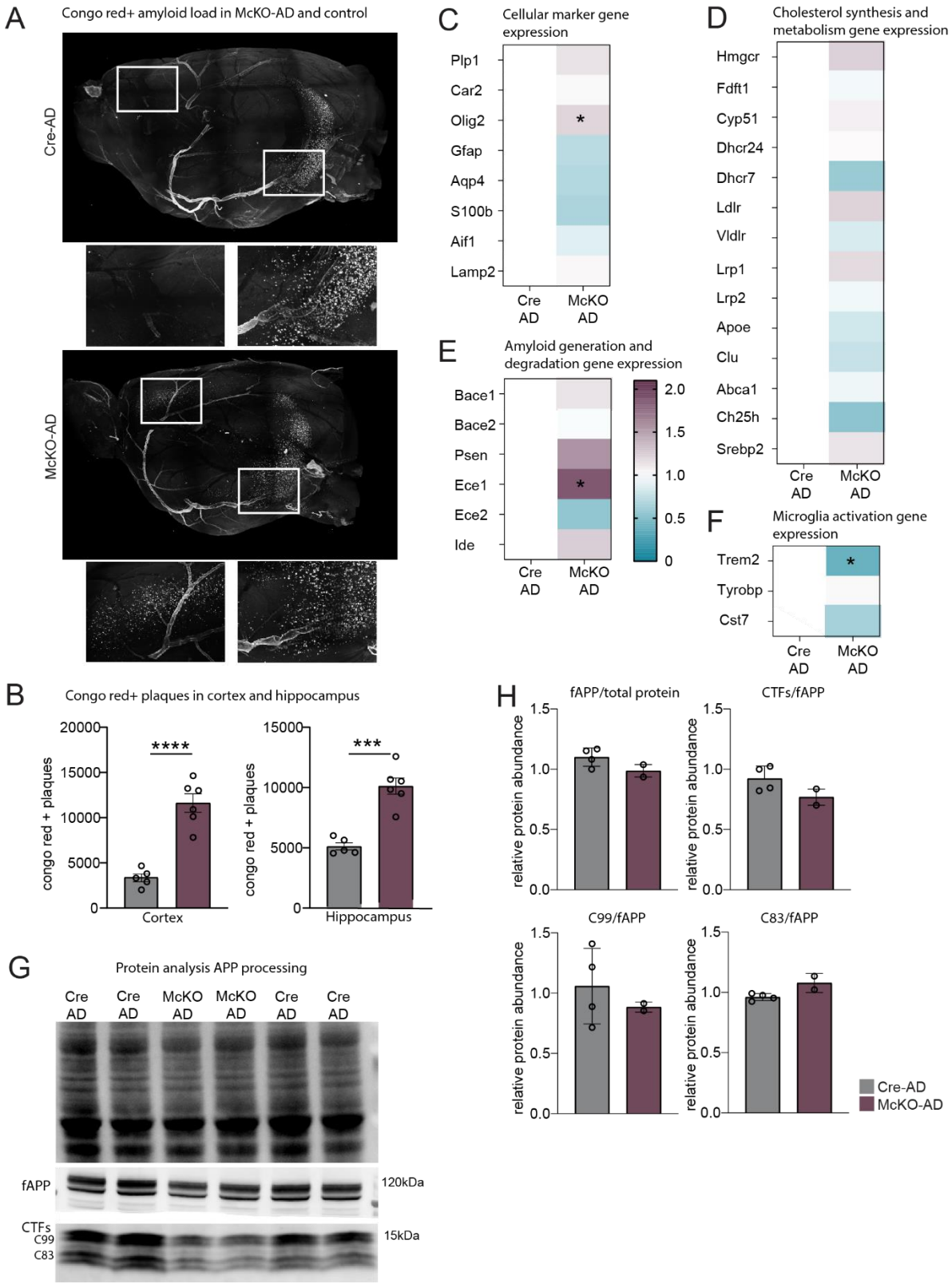
A
Congo red+ amyloid load in McKO-AD and control
Cre-AD
McKO-AD
B
Congo red+ plaques in cortex and hippocampus
congo red + plaques
20000
15000
10000
5000
0
****
Cortex
15000
10000
5000
0
***
Hippocampus
C
Cellular marker gene expression
Plp1
Car2
Olig2
Gfap
Aqp4
S100b
Aif1
Lamp2
*
Cre AD
McKO AD
D
Cholesterol synthesis and metabolism gene expression
Hmgcr
Fdft1
Cyp51
Dhcr24
Dhcr7
Ldlr
Vldlr
Lrp1
Lrp2
Apoe
Clu
Abca1
Ch25h
Srebp2
Cre AD
McKO AD
E
Amyloid generation and degradation gene expression
Bace1
Bace2
Psen
Ece1
Ece2
Ide
*
2.0
1.5
1.0
0.5
0
Cre AD
McKO AD
F
Microglia activation gene expression
Trem2
Tyrobp
Cst7
*
Cre AD
McKO AD
G
Protein analysis APP processing
Cre AD
Cre AD
McKO AD
McKO AD
Cre AD
Cre AD
fAPP
120kDa
CTFs
C99
C83
15kDa
H
fAPP/total protein
CTFs/fAPP
C99/fAPP
C83/fAPP
relative protein abundance
1.5
1.0
0.5
0.0
Cre-AD
McKO-AD

Figure 8 Lack of cholesterol synthesis in microglia enhances plaque load. (A) Plaque load in 3D reconstructed hemispheres of 3.5-month-old McKO-AD and Cre-AD with congo red + plaques with enlargement of marked areas in cortex and hippocampus. (B) Quantification of plaques in cortex and hippocampus in McKO-AD and Cre-AD controls in indicated brain areas. Circles represent single animals (n= 5-6). Asterisks represent significant differences with *p < 0.05, **p < 0.01, ****p < 0.0001 (unpaired Student´s t-test). (C) Gene expression analysis of cortical tissue in McKO-AD in comparison to Cre-AD. Gene expression profile of cellular marker (C) genes related to sterol synthesis and metabolism (D) APP processing and amyloid degradation (E) and microglia activation (F) were analyzed via quantitive RT-PCR and presented as heatmaps. Heatmap represents fold changes normalized to the mean of Cre-AD samples. (n=5-6) Asterisks represent significant differences with *p < 0.05, **p < 0.01, ****p < 0.0001 (unpaired Student´s t-test). (G) Western blot analysis of APP processing of McKO-AD and control. Immunoblots show total protein content stained with fast green, full-length APP and c-terminal fragments of the RIPA fraction of brain lysates. (H) Quantification of fAPP normalized on total protein, CTFs normalized on fAPP, C99 and C83 normalized on fAPP. Every animal is represented in a single lane (G) and dot of the bar graphs (H). (n=2-4).

3.4 Morphological alterations of plaque associated microglia

Microglia morphology changes with activation of the phagocytosing cells. A ramified morphology is linked to a homeostatic state. Reactive microglia are part of the healthy brain during the whole life to control debris removal, pathogen clearance, maintenance and immune surveillance functions, while an imbalance towards activated microglia is described in pathological conditions. Switches in microglia morphology, especially in the microglia cells surrounding plaques have been observed in human Alzheimer´s patients and mouse models of AD and have been referred to “corralling” microglia (Hammond et al., 2019; Keren-Shaul et al., 2017; Krasemann et al., 2017). The microglial activation state of the plaque-corralling microglia was shown to facilitate plaque modulation and Aβ removal (Huang et al., 2021; Kulkarni et al., 2022). Analysis of the microglia number and corralling phenotype around plaques in the cortex was implemented using two separate approaches. Using concentric circles around plaques to analyze the area covered by surrounding microglia pointed towards a higher coverage of plaques by sterol synthesis-deficient microglia (Figure 9a). The IBA1- positive area around plaques was enhanced in all sizes of plaques therefore suggesting a size independent but genotype-based alteration (Figure 9b). Using a microglia and plaque co-staining microglia numbers with cellular contact to a plaque were analyzed (Figure 9c). Sterol-synthesis deficient microglia clustered more extensively around the plaques (Figure 9d). The enhanced plaque load and elevated number of microglia surrounding the plaques suggests a higher ratio of plaque-associated microglia to parenchymal microglia. For uncovering the transcriptional signal of the “hypercorralling” microglia in comparison to microglia of control mice and if the activation profile is altered, isolated microglia were analyzed by bulk seq transcriptional analysis.

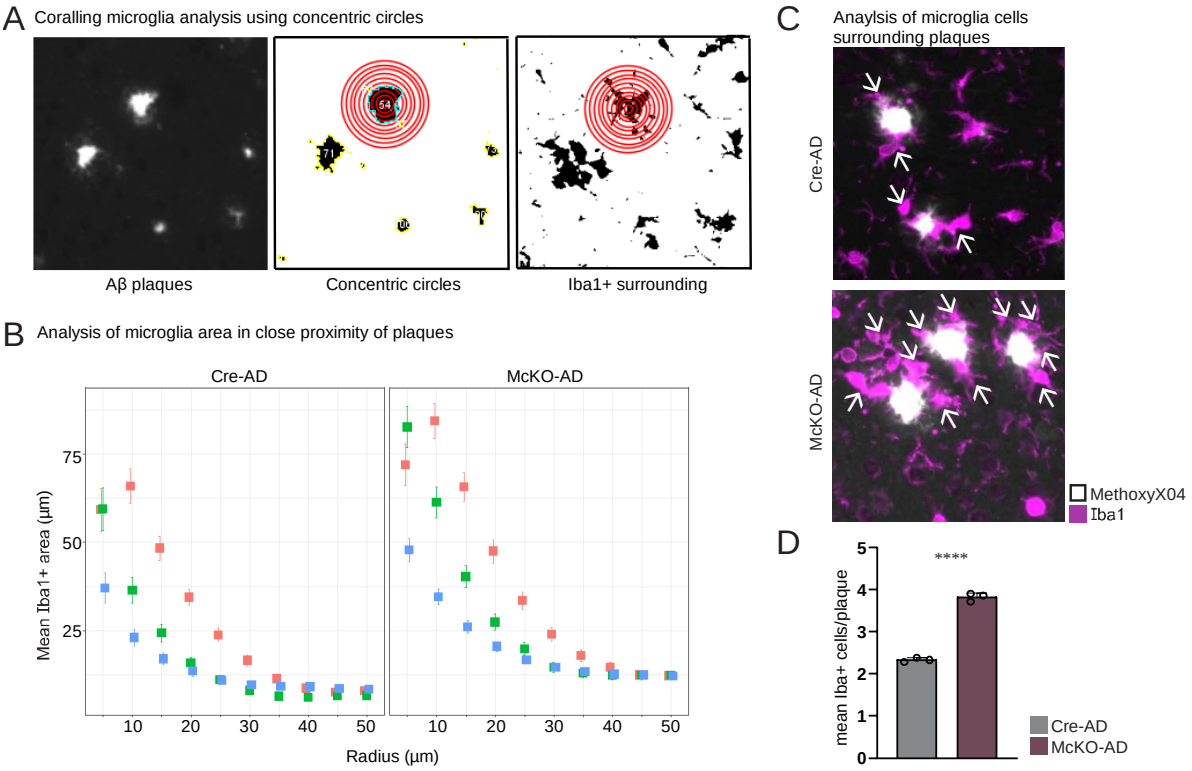

Figure 3 Microglia plaque corralling is affected by the lack of cholesterol synthesis. (A) Concentric circles around amyloid plaques show the distance of microglia from the border of plaque (analyzed together with Henrike Jungeblut, rotation student). (B) Analysis of Iba1+ area around and distance from plaques in McKO-AD and Cre-AD. Intensity and distance of microglia from large (red), medium (green) and small (blue) radius plaques are plotted separately. (C) Fluorescent image of Iba1+ (magenta) microglia corralling MethoxyX04 (white) stained plaques. (D) Analysis of mean number of microglia surrounding plaques. n= 3 mice per group.

3.5 Transcriptional regulation of microglia lacking sterol synthesis

To analyze if the altered plaque load and the modified distribution of microglia towards the plaque side is expressed by their transcriptional signature. The analysis was done in MACS isolated CD11b+ cells from four groups of mice at the age of 3.5 months. Mice deficient in cholesterol synthesis in the 5xFAD model (McKO-AD), control microglia from 5xFAD mice (Cre-AD) and cholesterol mutant microglia (*Cx3Cr1*$^{+/-}$ *Fdft1*$^{fl/fl}$), further referred to McKO and cells that just contain the Cre driver (*Cx3Cr1*$^{+/-}$), from herein called Cre, were analyzed in parallel. Transcriptional analysis using the DESeq2 analysis work flow classified the expression changes in 10 differentially regulated gene clusters (Figure 10a). Interestingly the microglial cholesterol mutants showed only minor transcriptional changes compared to Cre controls. Only few genes were significantly regulated, 56 downregulated, 30 upregulated. The comparison of Cre-AD mice

to Cre controls revealed enhanced inflammatory response gene expression, as expected. The upregulation of inflammation genes was the most prominent change in AD. In contrast, this inflammatory gene cluster was comparably low expressed in the McKO-AD microglia. In the line plots the expression trend of a gene cluster within the four groups is depicted. Mean expression levels of clusters were displayed in line plots for easier visualization of the diversity of microglial transcriptional changes between the groups (Figure 10b). In the volcano plots the distribution of up- and downregulated genes was visualized. In the ten most upregulated genes of Cre-AD and McKO-AD, shown in the first volcano plot, five genes were similar in both conditions, lipoprotein lipase (*Lpl*), brain-specific angiogenesis inhibitor 1-associated protein 2-like protein 1 (*Baiap2l2*), cholesterol 25-hydroxylase (*Ch25h*), cystatin F (*Cst7*) and glycoprotein Nmb (*Gnmb*). *Lpl, Cst7* and *Ch25h* have been associated with the DAM signature that is common in AD (Figure 10c). The second volcano plot is depicting the differentially regulated genes between McKO-AD vs Cre. Surprisingly, the overall significance of upregulation was way higher in Cre-AD than McKO-AD and the previously mentioned DAM genes were stronger regulated in Cre-AD microglia. In the right volcano plot the significantly regulated genes comparing McKO-AD with Cre-AD were clearly reduced. In summary, microglia lacking cholesterol synthesis detect senile plaques and react to the amyloid burden through an upregulation of activation markers known for their disease association. On the other hand, the upregulation is considerably lower than in control microglia, suggesting only a partially activated status of all microglia or might propose that a lower number of microglia initiate the DAM signature.

A RNA sequencing microglia cluster of Cre, McKO, Cre-AD and McKO-AD

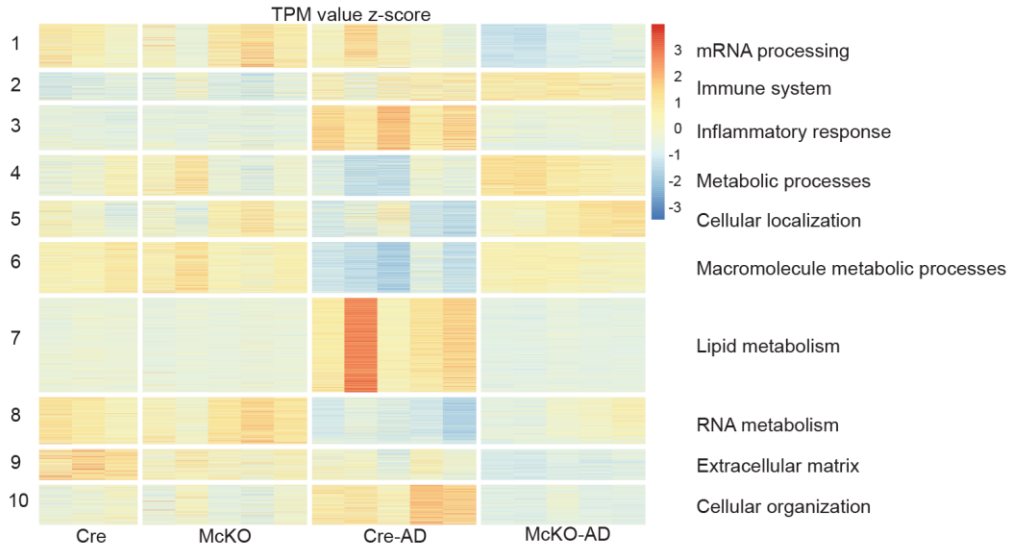

B Line plots of all microglia cluster

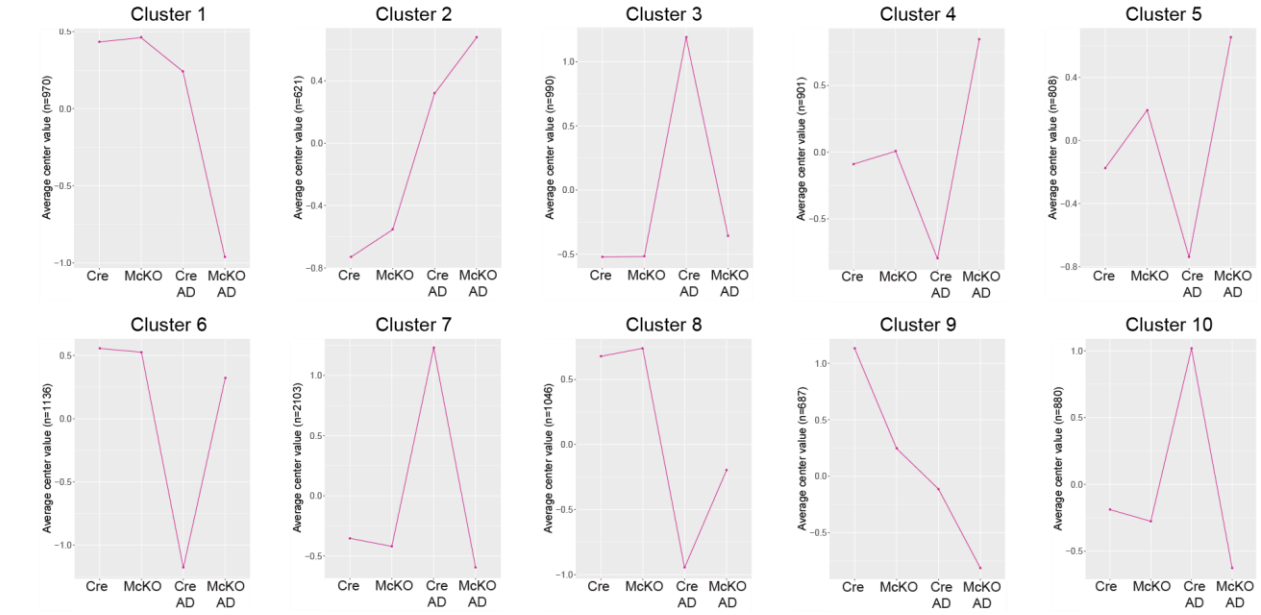

C Vulcano plots comparing the different genotypes

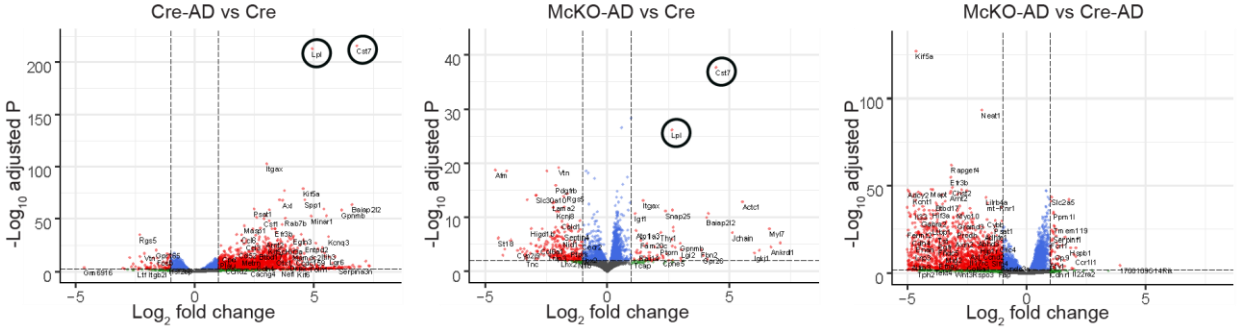

Figure 10 RNA-seq analysis of microglia in Cre, McKO, Cre-AD, McKO-AD. (A) Heatmap of microglia cluster of acutely isolated microglia cells isolated from cortex of four genotypes. Cluster were classified using k-means clustering and named after most obviously regulated pathways (B) Line plots showing differences in gene expression between genotypes and regulation of the cluster. (C) Volcano plots display significantly regulated genes (red) between different groups and most upregulated DAM genes marked with black circles. (n=3-5)

3.6 DAM signature is reduced in sterol synthesis deficient microglia

The RNA-seq analysis gave profound insights into the importance of microglial cholesterol synthesis in the presence of amyloid. Selected pathways of the transcriptomic analysis were displayed and examined in more detail. Effects on cholesterol synthesis and lipid handling were analyzed as well as extensive effect on microglia activation. The basal knockout of *Fdft1* in microglia only slightly affected the cholesterol homeostasis and the lipid transport. This was expected due to the fact that in the healthy brain microglia barely contribute to the cholesterol production (Figure 11 a-b). Furthermore, the microglia signature was neither changed in homeostatic genes nor in activation genes. In the isolated microglia bulk sequencing data set from pure AD mice, cholesterol synthesis genes were upregulated and the lipid transport was enhanced as well. This suggested enhanced cholesterol turnover in microglia. These gene sets were not upregulated any longer in McKO-AD mice. Furthermore, in ordinary 5xFAD microglia homeostatic markers were downregulated and the widely studied activation genes of microglia in amyloid pathology were significantly upregulated. This transition from homeostatic microglia to the activated DAM signature was less prominent in microglia lacking sterol synthesis (Figure 11c). This finding indicated that lack of microglial sterol synthesis affected the inflammatory response to amyloidosis. Microglia with altered activation and inflammatory response could suggest a change in phagocytosis and thereby plaque clearance.

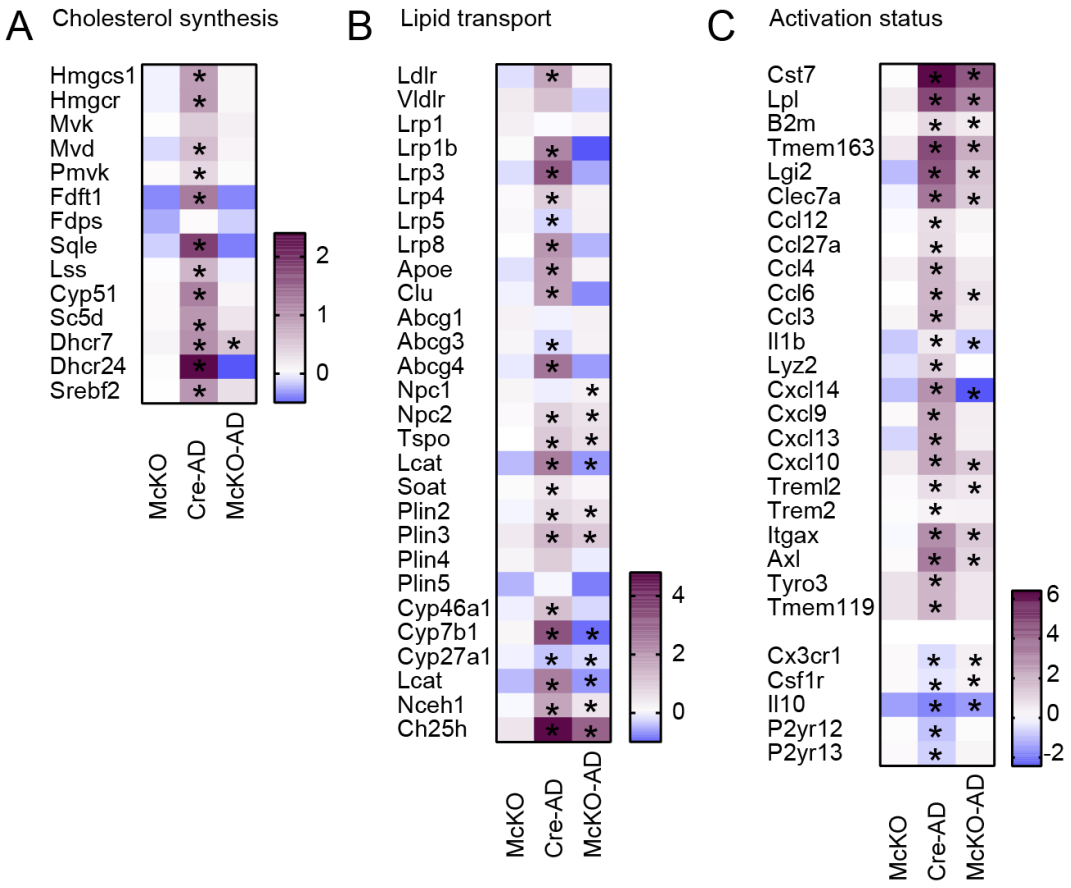

Figure 11 Depicted heatmaps from RNA-seq illustrate log2 fold change of selceted genes in cortical microglia. McKO, Cre-AD, and McKO-AD were normailzed to Cre controls. (A) Expression of genes involved in colesterol synthesis. (B) Lipid transport, lipid storage and excretion of cholesterol is depicted. (C) Gene expression changes of microglia activation status was categorized in activated and homeostatic marker genes. (n=3-5) Asterisks represent significant differences with *p < 0.05, **p < 0.01, ****p < 0.0001 (unpaired Student´s t-test).

3.7 The role of microglia on plaque clearance

Amyloid plaque removal is highly dependent on the functional detection of plaques by microglia, their motility, and clearance efficiency. It has been suggested that with disease progression microglia cells become less efficient in amyloid phagocytosis and thereby plaque clearance (Streit et al., 2004). To investigate whether microglia plaque clearance depend on cholesterol synthesis, an *ex vivo* phagocytosis assay was performed. Brain sections from a one-year old plaque loaded 5xFAD brain were incubated with an anti-Aβ-antibody to prime microglia for amyloid and transferred into medium. CD11b+ cells were acutely isolated from mutant (McKO) and control (Cre) mice, and seeded on the brain slices (Figure 12a). After 5 days in culture slices were fixed and stained for plaques and microglia and plaque load was analyzed compared to the untreated

consecutive slice (Figure 12b). Microglia displayed a partially ramified morphology and enriched around the plaques in both conditions (Figure 12c). The density of plaques was reduced in both conditions, to a similar extent (Figure 12d). These data suggest that, both microglia genotypes can clear amyloid plaques under *ex vivo* conditions. It is possible that the clearance is comparable because the microglia cells were purified from healthy brains and were only exposed to amyloid for the time of the assay. How amyloid was ingested and how it is processed cannot be answered by this assay. The visualization within cells is difficult due to the background signal originating from the brain tissue.

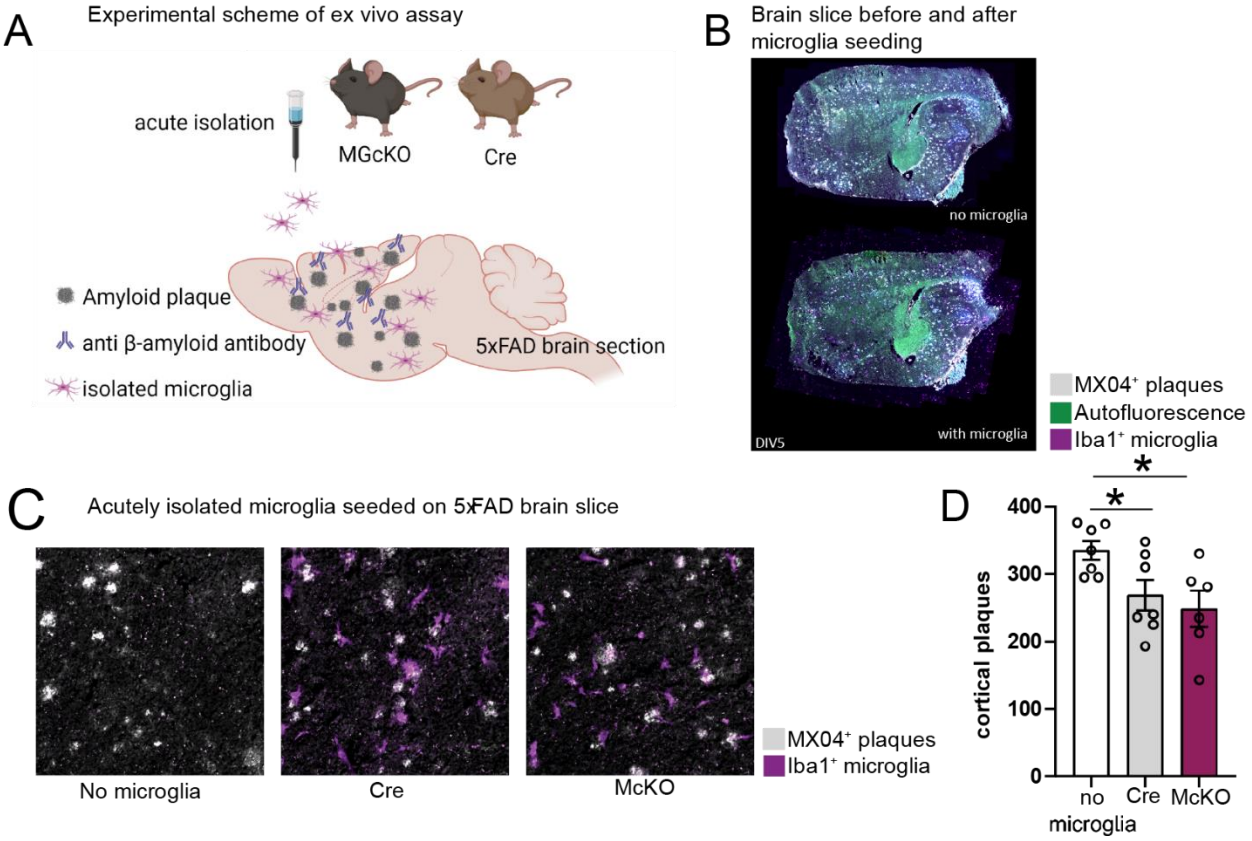

Figure 12 Ex vivo amyloid plaque phagocytosis assay. (A) Schematic illustration of an amyloid plaque ex vivo phagocytosis assay to analyze plaque clearance by microglia. Acutely isolated microglia from Cre and McKO were seeded on fresh frozen 5xFAD brain sections of a 1-year old mouse. The ability of seeded microglia to clear amyloid plaques was analyzed by the staining of plaques and their reduction after 5 days in culture by comparison with the untreated consecutive slice. (B) Representation of fluorescent microscopy of consecutive brain slices without and with seeded microglia. (C) Enlarged microscopy images of cortical plaques (white, MethoxyX04) without microglia (left), microglia (magenta, Iba1) from Cre mice (middle) and microglia from McKO mice. (D) Analysis of plaque reduction after 5 days incubation. Each circle is a separate assay with microglia isolated from 2 different mice per group. Asterisks represent significant differences with *p < 0.05, **p < 0.01, ****p < 0.0001 (unpaired Student´s t-test).

3.8 Aβ accumulation is altered in cholesterol synthesis deficient macrophages

To evaluate the ingestion of amyloid and its processing the amount of intracellular fluorescently labeled Aβ (fluoro Aβ) after 24 hours was depicted. Therefore, primary bone marrow derived macrophages (BMDMs) from McKO and Cre mice taken in culture and the knockout was induced by *in vitro* tamoxifen for 10 days. Afterwards, fluorescently labeled Aβ (fluoro Aβ) was added for 24 hours to assess the ingestion and the intracellular handling. The cells were seeded on cover slips and treated with fluoro Aβ for 24 hours, fixed, stained and analyzed using fluorescent imaging (Figure 13a-b). Surprisingly, the treatment with fluoro Aβ after 24 hours resulted in different appearances of ingested amyloid. These appearances of amyloid were categorized by the fluorescent signals into 1) dense aggregated protein further referred to “accumulated” and 2) more evenly distributed in the cell soma and smaller in spot size further called “spotty” (Figure 13c). For evaluation of the Aβ intake the total amount of internalized Aβ was normalized to Iba1+ macrophages, the intake was similar in both genotypes. However, the fraction with accumulated appearance was increased in the control group compared to McKO, whereas the spotty particles were more frequent in mutant macrophages. The lysosome-associated membrane protein 1 (LAMP1) intensity normalized to the Iba1+ cell area was increased in sterol synthesis deficient cells (Figure 13d). Lamp1 is a transmembrane protein mainly localized to lysosomal membranes. Lysosomes serve as hubs for degrading components by autophagy or endocytosis. The change of LAMP1 signal after Aβ internalization could either suggest a processing in different cellular compartments or different stages of digestion.

To assess the viability of the cells after amyloid treatment, BMDMs were seeded into chambers for live imaging and treated with amyloid for 24 hours. The survival of macrophages lacking cholesterol was reduced when treated with synthetic amyloid, indicating a less competent handling (Figure 13e). For further details on Aβ handling, expression analysis via qRT-PCR of microglia treated with pre-fibrillary amyloid confirmed the knockout of *Fdft1.* Interestingly, *ApoE* was contrarily regulated: controls upregulated the expression upon Aβ treatment and mutant microglia responded with downregulating when compared to the respective control (Figure 13f). A significant downregulation of *Trem2* expression was found in McKO microglia in response to amyloid. Alterations in LAMP1 intensity in mutant macrophages could be a response to changes in intracellular Aβ handling without endogenously produced cholesterol or changes in the degradation system. Furthermore, the opposing regulation of *ApoE* could be an indication for changes in lipid transport.

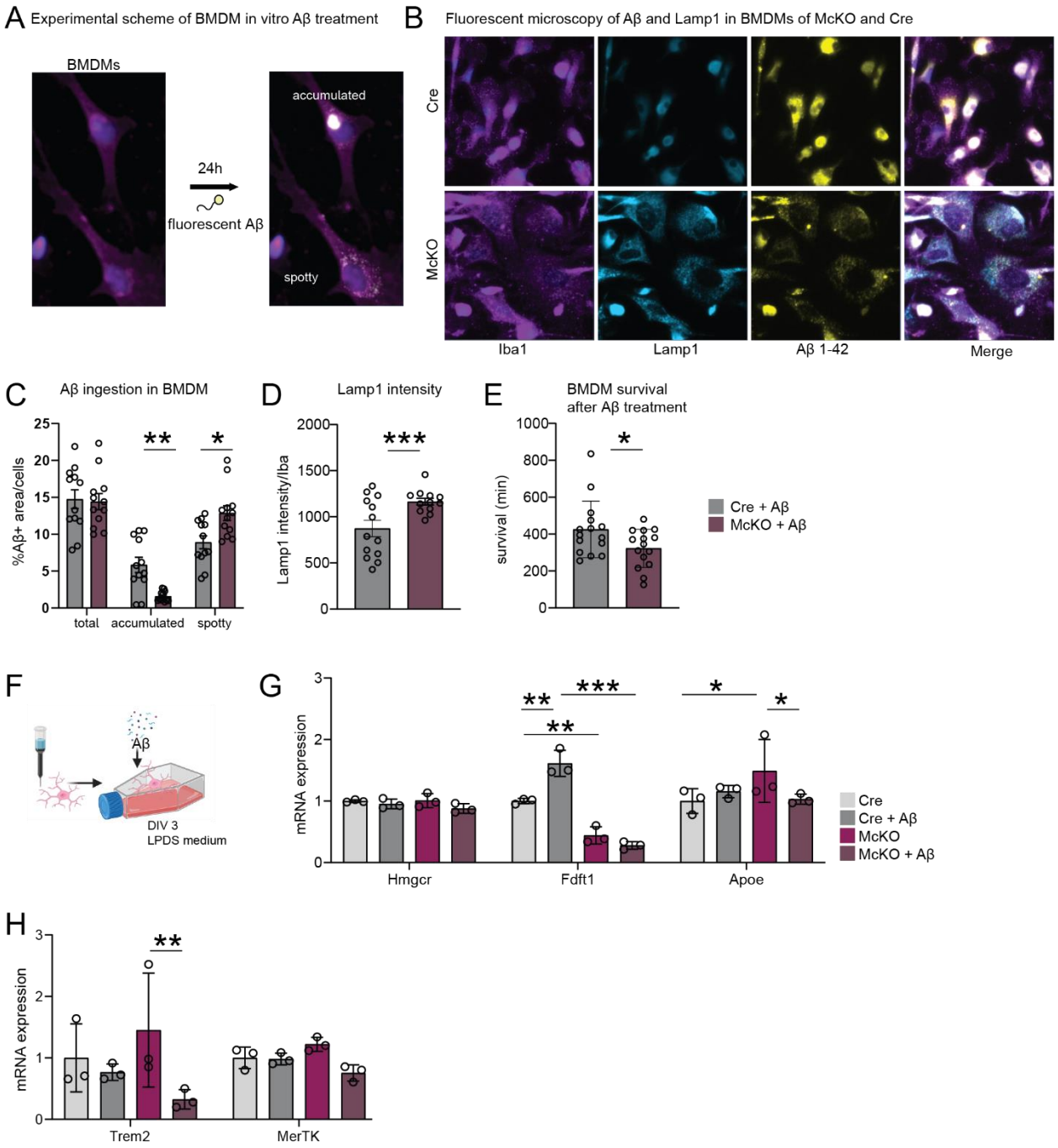

Figure 13 Phagocytosis of synthetic Aβ by primary macrophages and microglia. (A) Schematic representation of bone-marrow derived macrophages (BMDMs, magenta) treated with fluorescent Aβ for 24 hours (yellow). (B) Representative fluorescent images of BMDMs from Cre and McKO mice stained for microglia (magenta, Iba1), lysosomal membranes (cyan, Lamp1) and visualization of the fluorescent coupled Aβ (yellow, Tide Fluor™ 5WS-Amyloid β-Protein$_{1-42}$). (Lamp1 staining was done by Sophie Siems) (C) Bar graph visualized the analysis of ingested Aβ, separated by total Aβ (left), accumulated (middle) and spotty (right). (D) Representation of Lamp1 intensity normalized to Iba1+ area. (E) BMDM survival after Aβ addition was analyzed via live imaging (Analysis was performed together with Taisiia Nazarenko, rotation student). (F) Scheme of acutely isolated microglia cultured in LPDS medium for 3 days with 1µM

Aβ. (G-H) Fold mRNA expression of microglia from McKO and Cre with and without 3 days of Aβ (n=3) Asterisks represent significant differences with *p < 0.05, **p < 0.01, ****p < 0.0001 (unpaired Student´s t-test).

3.9 Amyloid phagocytosis changes microglial expression profile

Investigating microglial in vivo phagocytosis of Aβ and the differentiation between phagocytosing and non-phagocytosing microglia could unravel a modification in amyloid handling. Altered proportions of phagocytosing and non-phagocytosing or different expressional regulations between these groups could expose an adaptation of microglia lacking sterol synthesis. A variety of studies showed different properties of microglia with amyloid inclusions and non-laden microglia. More specifically, morphological alterations, inflammatory and phagocytic properties as well as alterations in channel activity are some changes between these distinct microglia populations (Grubman et al., 2021; Hemonnot-Girard et al., 2021).

To distinguish microglia with amyloid inclusions from microglia that had not taken up and handled amyloid, an experimental setup to label microglia involved in plaque phagocytosis *ex vivo* was established. Here, microglia were first isolated by MACS and stained for amyloid inclusions by virtue of the β-sheet dye Methoxy-04. Methoxy levels were subsequently analyzed by flow cytometry. An added bonus of this method is the analysis of cell numbers extracted per brain as well as the subdivision in phagocytosing and non-phagocytosing cells to compare the proportion in the microglia lacking sterol synthesis and controls.

Brains from Cre, Cre-AD and McKO-AD mice were dissected, the single cell suspension was stained for ingested amyloid using Methoxy-X04. The MACS sorted CD11b+ microglia cells were subsequently sorted by fluorescent intensity using flow cytometry (Figure 14a). Cre controls were proceeded in parallel to AD brains to control for unspecific staining of the β-sheet dye. The cells were sorted by their genetic modification, the fluorescent reporter labeling which induced an endogenous YFP signal, followed by the separation of Methoxy high and low fluorescent signal. Cre microglia clustered in a single population low in intensity, microglia from Cre-AD (and McKO-AD, data not shown) distributed in two separate populations showing that a fraction of microglia internalized X04, likely reflecting Aβ phagocytosing cells (Figure 14b-c). Comparing microglia densities from Cre mice, Cre-AD and McKO-AD animals revealed increased numbers in both AD groups showing apparent microgliosis in brains with amyloidosis (Figure 14d). Differentiating the proportions of phagocytosing versus non-phagocytosing microglia populations in Cre-AD and McKO-Cre resulted in similar numbers. Given the increased density of amyloid plaques and associated microglia corralling around plaques in McKO-AD mice, this finding was unexpected

Figure 14e). These findings suggest that either not all corralling microglia phagocytose or that the change in corralling is due to less effective amyloid ingestion.

Sorted cells were additionally analyzed for gene expression changes to depict differences between microglia with ingested X04 material and microglia supposedly not involved in the phagocytosing process. Gene expression in X04-positive microglia and microglia negative for X04 differed especially in cholesterol synthesis and lipid transport/storage genes (Figure 14f). MethoxyX04- cells elevated genes involved in cholesterol synthesis and lipid transport whereas X04 positive cells do not. Furthermore, the two populations differed in the expression levels related to activation state of microglia. The X04-negative fraction showed highly elevated expression of DAM-signature genes, whereas the X04-positive population expressed these genes only partly or to a lesser extent.

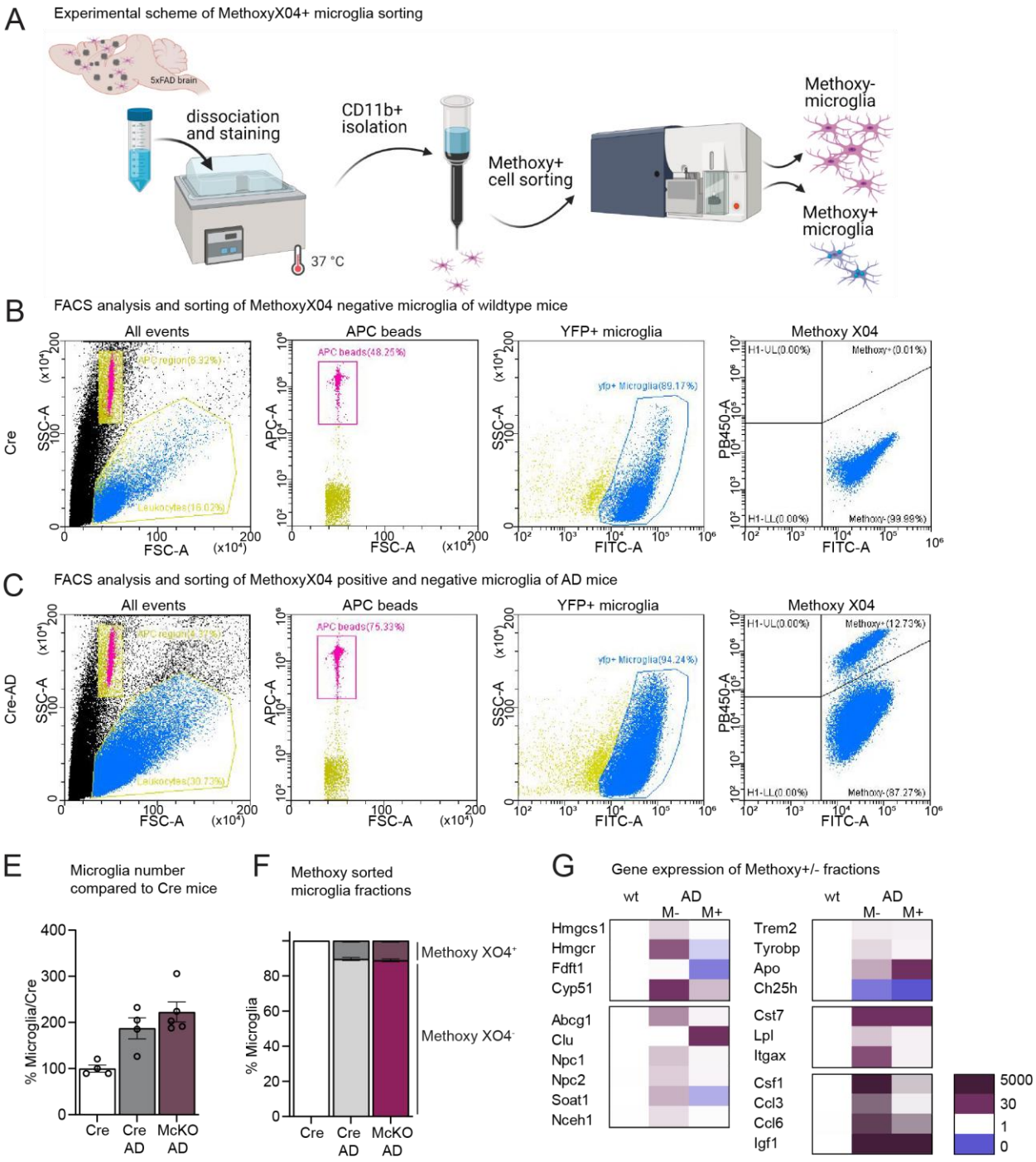

Figure 14 In vivo phagocytosis of Aβ was examined by MethoxyX04 staining of freshly isolated cells. (A) Experimental setup of microglia isolation and separation between MethoxyX04 positive and negative. Tissue was dissociated and stained for MethoxyX04, CD11b positive fraction was MACS isolated and separated by fluorescent signal. (B) Illustration of gating and sorting in flow cytometry of Cre microglia and (C) Cre-AD microglia. (D) Microglia numbers of Cre, Cre-AD and McKO Cre brains (E) Proportion of microglia with and without internalized XO4 fluorescence displaying high fluorescent signal and undyed microglia without internalized XO4 low fluorescence signal (G) Expression pattern

of microglia isolated from Cre mice versus Cre-AD mice divided in MethoxyX04 positive and negative fraction. (n= 4). Asterisks represent significant differences with *p < 0.05, **p < 0.01, ****p < 0.0001 (unpaired Student´s t-test).

4 Discussion

4.1 Glial cholesterol synthesis is a prominent modifier of plaque burden *in vivo*

Combining genetic approaches with different imaging modalities, biochemical analyses, bulk RNA sequencing and in vitro experiments, this study sheds new light on the interaction of cholesterol metabolism and the pathophysiology of Alzheimer´s disease. The core of this project was the investigation of amyloid density by ablation of cholesterol synthesis in neurons, astrocytes and microglia in an AD mouse model. Surprisingly, depletion of neuronal cholesterol synthesis did not affect amyloid plaque burden, whereas alterations in glial sterol synthesis modifies the plaque load.

Previously, cholesterol-rich membrane microdomains of neurons were associated with Aβ generation due to the subcellular location of the β- and γ-secretase and APP to these domains. Several *in vitro* studies utilizing neuronal cultures established a link between cholesterol metabolism and APP processing. More specifically, a shift of APP processing towards the amyloidogenic direction and Aβ secretion was connected to enhanced cholesterol levels (Bodovitz & Klein, 1996; Marquer et al., 2011). Conversely, a recent study revealed reduced interactions between BACE1 and APP in human iPSC- derived neurons under low cholesterol levels, achieved by statin treatment, in vivo versus ex vivo studies (Langness et al., 2021). However, they modified cholesterol by applying statins, these drugs inhibit sterol synthesis at the level of HMG CoA reductase. My approach of genetically targeting *Fdft1*, cholesterol synthesis is diminished at a later step and thereby no other pathways regulated by intermediates of the synthesis pathway are affected. Surprisingly, my data presented in this thesis shows that the lack of cholesterol synthesis in neurons did not affect the plaque burden in the 5xFAD mouse model. In the disease establishing phase, amyloidosis is progressing in the hippocampus and first plaques establish in the cortex layer 5. Aβ generation is dependent on APP processing which occurs primarily in neurons in this AD mouse model. In mutant brain lysates neither full length APP nor c-terminal fragments were modified. This is in agreement with unaltered plaque burden in these animals. How can these findings be explained in comparison to earlier studies? First, previous studies were restricted to investigating the effect of changes in cholesterol metabolism *in vitro*. Second, neuronal cholesterol levels might not be depleted by ablation of cholesterol

synthesis in neurons in our *in vivo* approach, as other brain cells could potentially supply sufficient amount of cholesterol to neurons via horizontal transfer. The latter possibility has to be further investigated in the future.

An alternative source of cholesterol for neurons could be astrocytes that have been previously shown to be the main producers of cholesterol and shuttle lipids via lipoproteins (Fünfschilling et al., 2007; Quan et al., 2003). Likewise, ApoE is the most frequent carrier of lipids and cholesterol in the cerebrospinal fluid and is almost exclusively produced by astrocytes. The strongest genetic risk factor for LOAD is the ApoE4 allele, indicating a connection between astrocytes, ApoE and the generation of Aβ by determining the cholesterol content of neurons. Corresponding to this possible interaction, plaque quantity was significantly reduced in 5xFAD mice with astrocytes unable to generate cholesterol (Mahan et al., 2022). However, APP processing in cortical tissue seemed unaffected, suggesting an effect on amyloidosis independent of Aβ generation. Tissue expression analysis of mice with deactivated cholesterol synthesis in astrocytes revealed enhanced levels of *Abca1,* a protein relevant for cholesterol export and lipidation of APOE. The robustly upregulated *Ldlr* is a receptor for APOE and mediates cholesterol uptake. *Ldlr* also mediates Aβ clearance in astrocytes (Kim et al., 2009) suggesting astrocytic cholesterol synthesis affects APOE mediated or direct effects on Aβ drainage. Additionally, *Ece1*, an Aβ-degrading enzyme, is highly enriched in the cortex of mice deficient in astrocyte sterol synthesis. In addition to the upregulation of microglia activation genes e.g. *Trem2* and *Tyrobp*, these findings suggest an effect on Aβ clearance rather than Aβ generation in animals with astrocytes deficient in cholesterol synthesis. Taken together, cholesterol deficient astrocytes do not affect APP processing but rather could affect plaque clearance and could thereby alter disease progression.

The most prominent effect on the plaque burden was observed when microglia cells lacked the ability to synthesize cholesterol. Here, plaque burden was massively exacerbated. Many risk genes for LOAD, such as *Trem2*, *CD33*, and *Ms4a* are expressed by microglia and are associated with microgliosis. While microglia sustain brain homeostasis in health, in AD the homeostatic gene signature shifts to an activated condition and may reflect a highly phagocytic state. In the early disease stage, the activation of microglia could be part of a beneficial attempt to resolve the inflammation causing agent, with disease progression microglia might detrimentally fail in handling amyloid deposits. Considering the extremely elevated plaque density in microglia deficient in sterol synthesis, the expression pattern was only minimally changed. These mainly physiologic expression levels could be assigned to the low specificity of whole tissue analysis. Intriguingly in animals with microglia deficient in cholesterol synthesis, *Trem 2* expression, was slightly downregulated. TREM2 is known to enhance phagocytosis and microglia activation

(Kleinberger et al., 2014). In addition to these functions the receptor affects inflammatory signaling (Jay et al., 2015). The reduced expression could contribute to less Aβ handling by microglia cells. For further conclusions cell specific expression analysis of microglia is needed. As in the other cell-specific sterol synthesis mutants, APP processing was not dependent on cholesterol production in microglia.

Altogether, glial cholesterol production but not neuronal production seems to be highly involved in controlling amyloid plaque burden with astrocytic synthesis favoring and microglial synthesis diminishing plaque deposition. Importantly, both effects seem not be mediated by direct changes to APP metabolism in neurons. This suggests a mechanism of action that involves variations in plaque deposition or Aβ clearance.

4.2 “Hypercorralling” – microglia lacking sterol synthesis organize around senile plaques

Plaque clearance is dependent on microglial detection and phagocytosis of amyloid fibrils (Huang et al., 2021). Plaque-associated microglia present with morphological changes that resemble a classical activated phenotype. The cells surrounding senile amyloid plaques are thought to limit the plaque expansion by forming a barrier for brain protection (Condello et al., 2015). On the other hand, some studies suggest that microglia cells are involved in initial plaque seeding. Cholesterol synthesis affected the interaction between microglia and plaques: more amoeboid microglia surrounded the plaques. Supposing that microglia shield the brain parenchyma to protect unaffected brain areas from the senile plaques, why should more microglia be detrimental? The efficacy of plaque clearance could be diminished by lack of sterol synthesis, by possibly altering the phagocytosis efficiency or the handling of ingested amyloid. Eventually this could lead to an increased recruitment of microglia to plaques, explaining the hypercorraling.

4.3 Microglia DAM signature is attenuated through sterol deficiency

Corresponding to the different tasks of microglia during development and the entire life of a mouse, microglia are a heterogeneous population of cells with their transcriptomic profile depending on their function. Similarities between populations arising in the early development and microglia in neurodegenerative disease were reported (Hammond et al., 2019). Microglia in neurodegenerative diseases and development, present with an inflammatory signature which in the development could relate to the phagocytosis of synapses and cell debris and in disease the activation through pathological protein accumulations (Salter & Stevens, 2017; Zia et al., 2020).

Microglia from AD mice are characterized by downregulating of homeostatic markers and the upregulation of activation profiles. (Keren-Shaul et al., 2017; Wang et al., 2015). However, the role of the activated disease associated microglia is not completely understood. For instance, in Trem2 KO mice plaque recognition and corralling by microglia is reduced along with the expression of DAM markers is diminished (Ulland & Colonna, 2018). This raises the question whether some microglia activation patterns are beneficial for the disease, by actively clearing amyloid from senile plaques (Butovsky & Weiner, 2018).

The RNA sequencing data of isolated microglia from AD mice (Cre-AD) displayed the expected signature of microglia in amyloid disease. *Lpl*, *Cst7* and the Integrin Subunit Alpha X (*Itgax*) were highly upregulated compared to microglia from healthy controls. The overall inflammatory response is elevated compared to microglia from mice without 5xFAD, this displayed the activated status of microglia. In contrast to the extensive transcriptional changes of pure AD microglia, microglia lacking the ability to synthesize sterol failed to upregulate these genes to the same extent. The deeper analysis uncovered several pathways that depend on cholesterol synthesis during amyloidosis. Expression levels of cholesterol synthesis depleted microglia in AD a rather low level more comparable to the profile of microglia in a healthy microenvironment. Genes implicated in lipid transport were highly enriched in Cre-AD microglia, ranging from lipid export genes and lipid receptors to enzymes converting cholesterol to oxysterols. This indicates not just an accelerated sterol synthesis but an enhanced lipid handling and transfer in 5xFAD mice. In the McKO-AD expression profile, lipid transport transcripts were at normal levels compared to the microglia with functional sterol synthesis. Genes involved in making cholesterol more accessible were regulated, oxysterol conversion (*Cyp46a1, Cyp7b1, Cyp27a1*) and ester formation (*Lcat*) genes were reduced and in addition to that neutral cholesterol ester hydrolase 1 (*Nceh1*) was upregulated. Not all lipid related genes were regulated in a contrary manner, as genes contributing to lipid droplet stabilization (*Plin2, Plin3*) were enhanced similar to Cre-AD thereby suggesting a certain degree of preservation of lipid droplet formation capability independent of sterol synthesis. Lipid droplets are storage organelles enhanced in neurodegenerative disease and have been shown to be upregulated by DAM genes in AD (Hamilton et al., 2015; Moulton et al., 2021; Ralhan et al., 2021). DAM genes were only partially induced in McKO-AD mice. The classical marker genes were highly expressed in the control microglia as it has been shown in other studies of AD mouse models and human AD (Deczkowska et al., 2018; Sobue et al., 2021; Wang, 2021). While in AD microglia homeostatic markers were downregulated, in the sterol synthesis deficient expression levels were comparable with non-AD microglia. These changes in the classical induction of microglia activation in response to amyloid plaques could imply a lower number of

microglia upregulating DAM genes. Furthermore, it could be a consequence of a blocked transition of microglia and thereby only a partially activated status.
Importantly, the sterol synthesis mutants without amyloid pathology were similar compared to Cre control microglia. Only minor changes in healthy conditions could hint towards the importance of microglial cholesterol synthesis only in pathology. This was expected because microglia contribute to cholesterol metabolism only to a low level.
In summary, sterol synthesis deficiency in microglia altered the induction of lipid transport in AD and modified the activation status of microglia. In conjunction with the fact that microglia lacking sterol synthesis were able to recognize and migrate to the plaque, the question is if the mutant microglia are able to phagocytose and digest Aβ?

4.4 Sterol deficient microglia phagocytose plaques but the Aβ digestion is altered

Activated microglia are linked to amyloid clearance (Bacskai et al., 2001; Wyss-Coray et al., 2001). With disease progression and increasing plaque load and thereby prolonged activation, microglia slow down their phagocytic activity (Hu et al., 2021). Exhausted or poorly functioning microglia give rise to amyloid plaques (Flanary et al., 2007; Flanary & Streit, 2004). As a consequence, the question arises whether microglia with reduced DAM signature show phagocytosis defects. I addressed this question in three different experimental paradigms.
In the functional assessment of plaque clearance in the *ex vivo* phagocytosis assay control microglia as well as mutant microglia reduced the plaque number to a similar degree. This result can be a confirmation of the ability of the sterol synthesis deficient microglia to phagocytose plaques or these microglia have never encountered amyloid-β *in vivo*. Although this finding shows the capability of McKO microglia to reduce plaques at a similar rate like Cre controls, this might not translate well to the *in vivo* situation. Within the AD brain parenchyma microglia could be fatigued by longer exposure to Aβ *in vivo*, overloaded with fibrils, or gathering problems regarding the processing of the internalized amyloid-β.
Considering the fact, that imaging approaches to unravel the internalization of amyloid into the cells is difficult when seeded on a brain slice, *in vitro* experiments were performed. The uptake of synthetic Aβ was investigated using bone marrow derived macrophages. Despite an overall similar uptake of amyloid-β in Cre and McKO cells, the internalization pattern was different. In Cre controls internalized Aβ accumulated into dense amyloid aggregations whereas in the sterol synthesis deficient macrophages a spotty signal distributed over the entire cell body was

observed. In addition, the enhanced LAMP1 intensity in the mutant cells suggests an ongoing digestion or an internalization in different compartments. It was shown that LAMPs sustain essential function in the endocytic pathway, especially the successful phagosome-lysosome fusion (Huynh et al., 2007). In AD, LAMP1 positive microglia predominantly localized around senile plaques and may either indicate Aβ removal or deposition (Barrachina et al., 2006). *Ex vivo* and *in vitro* experiments suggest that microglia without functional cholesterol synthesis are capable to phagocytose Aβ and clear plaques. Acute isolation of microglia cells from McKO-AD and Cre-AD mice and subsequent sorting of plaques with stained ingested amyloid fibrils revealed similar proportions in both groups. Microglia stained with Methoxy-X04 were sorted as a proxy for Aβ-phagocytosing cells and the unstained microglia as non-phagocytosing cells. Comparable numbers suggest the ability to take up amyloid-β by microglia independent of cholesterol synthesis. The sorted populations were analyzed for changes in expression patterns in the context of phagocytosis. Only the non-phagocytosing population upregulated cholesterol synthesis genes implying a difference in cholesterol metabolism in plaque-interacting microglia and microglia without ingested amyloid. The characteristic DAM signature genes like *Cst7*, *Lpl* and *Itgax* were surprisingly also highly upregulated in the Methoxy negative fraction. Of note is, this experimental paradigm has its limitations in differentiating the distinct populations. Even if it was validated that microglia from Cre control mice only have one population with low levels of internalized X04 fluorescent microglia, there is still a chance that the fluorescently labeled amyloid (or a percentage) was only ingested *ex vivo* due to an activation within the process. Inflammation markers were strongly expressed by the Methoxy negative population as well, leading to the suggestion that the non-phagocytosing cells dominate the characteristic signature of disease associated microglia. This could mean, that plaque phagocytosis microglia, here separated by X04 positivity are not necessarily the plaque corralling microglia.

4.5 Cholesterol metabolism regulates microglia activation and thereby amyloid pathology

Summarizing the effects of cholesterol synthesis on the amyloid pathology, this study demonstrates the manifold influence of glial sterol synthesis on plaque burden. A positive effect on the plaque load was shown in cholesterol synthesis deficient astrocytes. In contrast, as a consequence of diminished sterol synthesis in microglia amyloidosis was exacerbated. The moderate induction of DAM signature genes is in line with studies showing increased amyloidosis when microglial activation is impaired (Dani et al., 2018; Sobue et al., 2021). Further studies could

correlate anti-inflammatory treatment and thereby more homeostatic microglia and elevated plaque levels (Jantzen et al., 2002; Wyss-Coray et al., 2001). Taking together all these findings indicates a prominent role of microglial activation for amyloid plaque control which in turn seems to be highly dependent on functional cholesterol synthesis. In addition, the disease associated microglia signature is regulated by sterol metabolism in microglia. Interestingly, this signature can be traced back to the substantial non-phagocytosing microglia population. Due to the fact that mutant microglia are capable of phagocytosing amyloid, the disturbance of sterol homeostasis might affect the intracellular handling of amyloid. Considering the evidence that depleting microglia before plaque seeding, eradicates plaque formation, microglia are essential for plaque deposition. Could cholesterol synthesis control the plaque deposition by modifying amyloid processing in the different compartments within microglia and thereby seeding of new plaques?

5.5 Translation into human AD

Uncovering the relevance of sterol metabolism in human Alzheimer´s disease is more complex. In comparison to the 5xFAD model, including an assured disease onset due to the inserted mutations most of the human AD cases originate spontaneous.

Additionally, the complexity of the cholesterol metabolism is even higher considering that the horizontal transfer of cholesterol between cells is mainly achieved by ApoE, which is polymorphic in humans. The different alleles are structurally different and harbor their individual lipid binding affinities. Surprisingly, the residues responsible for lipid binding are not conserved between species suggesting distinguished lipid binding properties in various species (Frieden et al., 2017). To perform normal functions, ApoE has to be adequately lipidated. The AD risk gene ApoE4 is less lipidated compared to ApoE2, whereas ApoE2 is more capable of supporting cholesterol efflux. (Lanfranco et al., 2020). Could the alteration of cholesterol synthesis affect the lipidation status of ApoE and thereby be a possible intervention to reduce plaque burden? In human AD a further complication can be expected by the appearance of hyperphosphorylated tau tangles. The translation of effects from mice to human is always uncertain but regarding the simplified pathology in mouse models compared to the complex pathology in humans the impact on phosphorylated tau as further disease aspect is even more difficult to assess.

Targeting cholesterol synthesis specific in a certain cell type in humans is another challenge. The common way of lowering cholesterol synthesis, is the application of statins that block sterol synthesis at the level of HMG CoA reductase. The overall intervention in cholesterol metabolism is not advisable given the fact that alterations in the cholesterol synthesis of each cell type has different consequences.

5 References

2020 Alzheimer's disease facts and figures. (2020). *Alzheimers Dement*. https://doi.org/10.1002/alz.12068

A. Armstrong, R. (2019). Risk factors for Alzheimer's disease [journal article]. *Folia Neuropathologica*, *57*(2), 87-105. https://doi.org/10.5114/fn.2019.85929

Abdel-Khalik, J., Yutuc, E., Crick, P. J., Gustafsson, J. A., Warner, M., Roman, G., Talbot, K., Gray, E., Griffiths, W. J., Turner, M. R., & Wang, Y. (2017). Defective cholesterol metabolism in amyotrophic lateral sclerosis. *J Lipid Res*, *58*(1), 267-278. https://doi.org/10.1194/jlr.P071639

Ahmed, M., Davis, J., Aucoin, D., Sato, T., Ahuja, S., Aimoto, S., Elliott, J. I., Van Nostrand, W. E., & Smith, S. O. (2010). Structural conversion of neurotoxic amyloid-beta(1-42) oligomers to fibrils. *Nat Struct Mol Biol*, *17*(5), 561-567. https://doi.org/10.1038/nsmb.1799

Ahn, J. H., Cho, H., Kim, J. H., Kim, S. H., Ham, J. S., Park, I., Suh, S. H., Hong, S. P., Song, J. H., Hong, Y. K., Jeong, Y., Park, S. H., & Koh, G. Y. (2019). Meningeal lymphatic vessels at the skull base drain cerebrospinal fluid. *Nature*, *572*(7767), 62-66. https://doi.org/10.1038/s41586-019-1419-5

Aird, R. B., & Gurchot, C. (1939). PROTECTIVE EFFECT OF CHOLESTEROL IN EXPERIMENTAL EPILEPSY. *Archives of Neurology & Psychiatry*, *42*(3), 491-506. https://doi.org/10.1001/archneurpsyc.1939.02270210129006

Alzheimer, A. (1907). Über eine eigenartige Erkrankung der Hirnrinde [article in German]. *Allg Z Psych Psych-gerich Med*, *64*, 146-148.

Armulik, A., Genové, G., Mäe, M., Nisancioglu, M. H., Wallgard, E., Niaudet, C., He, L., Norlin, J., Lindblom, P., Strittmatter, K., Johansson, B. R., & Betsholtz, C. (2010). Pericytes regulate the blood–brain barrier. *Nature*, *468*(7323), 557-561. https://doi.org/10.1038/nature09522

Bacskai, B. J., Kajdasz, S. T., Christie, R. H., Carter, C., Games, D., Seubert, P., Schenk, D., & Hyman, B. T. (2001). Imaging of amyloid-β deposits in brains of living mice permits direct observation of clearance of plaques with immunotherapy. *Nature Medicine*, *7*(3), 369-372. https://doi.org/10.1038/85525

Badimon, A., Strasburger, H. J., Ayata, P., Chen, X., Nair, A., Ikegami, A., Hwang, P., Chan, A. T., Graves, S. M., Uweru, J. O., Ledderose, C., Kutlu, M. G., Wheeler, M. A., Kahan, A., Ishikawa, M., Wang, Y. C., Loh, Y. E., Jiang, J. X., Surmeier, D. J., . . . Schaefer, A. (2020). Negative feedback control of neuronal activity by microglia. *Nature*, *586*(7829), 417-423. https://doi.org/10.1038/s41586-020-2777-8

Barrachina, M., Maes, T., Buesa, C., & Ferrer, I. (2006). Lysosome-associated membrane protein 1 (LAMP-1) in Alzheimer's disease. *Neuropathology and Applied Neurobiology*, *32*(5), 505-516. https://doi.org/https://doi.org/10.1111/j.1365-2990.2006.00756.x

Baxter, P. S., Dando, O., Emelianova, K., He, X., McKay, S., Hardingham, G. E., & Qiu, J. (2021). Microglial identity and inflammatory responses are controlled by the combined effects of neurons and astrocytes. *Cell Rep*, *34*(12), 108882. https://doi.org/10.1016/j.celrep.2021.108882

Bayer, T., & Wirths, O. (2010). Intracellular accumulation of amyloid-beta - a predictor for synaptic dysfunction and neuron loss in Alzheimer's disease [Review]. *Frontiers in Aging Neuroscience*, *2*. https://doi.org/10.3389/fnagi.2010.00008

Beel, A. J., Mobley, C. K., Kim, H. J., Tian, F., Hadziselimovic, A., Jap, B., Prestegard, J. H., & Sanders, C. R. (2008). Structural Studies of the Transmembrane C-Terminal Domain of the Amyloid Precursor Protein (APP): Does APP Function as a Cholesterol Sensor? *Biochemistry*, *47*(36), 9428-9446. https://doi.org/10.1021/bi800993c

Beretta, C., Nikitidou, E., Streubel-Gallasch, L., Ingelsson, M., Sehlin, D., & Erlandsson, A. (2020). Extracellular vesicles from amyloid-β exposed cell cultures induce severe dysfunction in cortical neurons. *Scientific Reports*, *10*(1), 19656. https://doi.org/10.1038/s41598-020-72355-2

Berghoff, S. A., Spieth, L., Sun, T., Hosang, L., Schlaphoff, L., Depp, C., Duking, T., Winchenbach, J., Neuber, J., Ewers, D., Scholz, P., van der Meer, F., Cantuti-Castelvetri, L., Sasmita, A. O., Meschkat, M., Ruhwedel, T., Mobius, W., Sankowski, R., Prinz, M., . . . Saher, G. (2021). Microglia facilitate repair of demyelinated lesions via post-squalene sterol synthesis. *Nat Neurosci*, *24*(1), 47-60. https://doi.org/10.1038/s41593-020-00757-6

Berman, H. M., Westbrook, J., Feng, Z., Gilliland, G., Bhat, T. N., Weissig, H., Shindyalov, I. N., & Bourne, P. E. (2000). The Protein Data Bank. *Nucleic Acids Research*, *28*(1), 235-242. https://doi.org/10.1093/nar/28.1.235

Beyreuther, K., & Masters, C. L. (1991). Amyloid precursor protein (APP) and beta A4 amyloid in the etiology of Alzheimer's disease: precursor-product relationships in the derangement of neuronal function. *Brain Pathol*, *1*(4), 241-251. https://doi.org/10.1111/j.1750-3639.1991.tb00667.x

Bielska, A. A., Schlesinger, P., Covey, D. F., & Ory, D. S. (2012). Oxysterols as non-genomic regulators of cholesterol homeostasis. *Trends in endocrinology and metabolism: TEM*, *23*(3), 99-106. https://doi.org/10.1016/j.tem.2011.12.002

Birolini, G., Valenza, M., Di Paolo, E., Vezzoli, E., Talpo, F., Maniezzi, C., Caccia, C., Leoni, V., Taroni, F., Bocchi, V. D., Conforti, P., Sogne, E., Petricca, L., Cariulo, C., Verani, M., Caricasole, A., Falqui, A., Biella, G., & Cattaneo, E. (2020). Striatal infusion of cholesterol promotes dose-dependent behavioral benefits and exerts disease-modifying effects in Huntington's disease mice. *EMBO Mol Med*, *12*(10), e12519. https://doi.org/10.15252/emmm.202012519

Bjorkhem, I. (2006). Crossing the barrier: oxysterols as cholesterol transporters and metabolic modulators in the brain. *J Intern Med*, *260*(6), 493-508. https://doi.org/10.1111/j.1365-2796.2006.01725.x

Bjorkhem, I., & Meaney, S. (2004). Brain cholesterol: long secret life behind a barrier. *Arterioscler Thromb Vasc Biol*, *24*(5), 806-815. https://doi.org/10.1161/01.ATV.0000120374.59826.1b

Blennow, K., de Leon, M. J., & Zetterberg, H. (2006). Alzheimer's disease. *The Lancet*, *368*(9533), 387-403. https://doi.org/10.1016/S0140-6736(06)69113-7

Bloch, K. (1965). The Biological Synthesis of Cholesterol. *Science*, *150*(3692), 19-28. https://doi.org/doi:10.1126/science.150.3692.19

Bodovitz, S., & Klein, W. L. (1996). Cholesterol modulates alpha-secretase cleavage of amyloid precursor protein. *J Biol Chem*, *271*(8), 4436-4440. https://doi.org/10.1074/jbc.271.8.4436

Bohlen, C. J., Bennett, F. C., Tucker, A. F., Collins, H. Y., Mulinyawe, S. B., & Barres, B. A. (2017). Diverse Requirements for Microglial Survival, Specification, and Function Revealed by Defined-Medium Cultures. *Neuron*, *94*(4), 759-773 e758. https://doi.org/10.1016/j.neuron.2017.04.043

Boyles, J. K., Pitas, R. E., Wilson, E., Mahley, R. W., & Taylor, J. M. (1985). Apolipoprotein E associated with astrocytic glia of the central nervous system and with nonmyelinating glia of the peripheral nervous system. *J Clin Invest*, *76*(4), 1501-1513. https://doi.org/10.1172/jci112130

Braak, H., & Braak, E. (1991). Neuropathological stageing of Alzheimer-related changes. *Acta Neuropathol*, *82*(4), 239-259. https://doi.org/10.1007/bf00308809

Brown, M. S., & Goldstein, J. L. (1997). The SREBP Pathway: Regulation of Cholesterol Metabolism by Proteolysis of a Membrane-Bound Transcription Factor. *Cell*, *89*(3), 331-340. https://doi.org/https://doi.org/10.1016/S0092-8674(00)80213-5

Bu, G., Maksymovitch, E. A., Nerbonne, J. M., & Schwartz, A. L. (1994). Expression and function of the low density lipoprotein receptor-related protein (LRP) in mammalian central neurons. *J Biol Chem*, *269*(28), 18521-18528.

Butovsky, O., & Weiner, H. L. (2018). Microglial signatures and their role in health and disease. *Nature reviews. Neuroscience*, *19*(10), 622-635. https://doi.org/10.1038/s41583-018-0057-5

Cantuti-Castelvetri, L., Fitzner, D., Bosch-Queralt, M., Weil, M.-T., Su, M., Sen, P., Ruhwedel, T., Mitkovski, M., Trendelenburg, G., Lütjohann, D., Möbius, W., & Simons, M. (2018). Defective cholesterol clearance limits remyelination in the aged central nervous system. *Science*, *359*(6376), 684-688. https://doi.org/doi:10.1126/science.aan4183

Caporaso, G. L., Takei, K., Gandy, S. E., Matteoli, M., Mundigl, O., Greengard, P., & De Camilli, P. (1994). Morphologic and biochemical analysis of the intracellular trafficking of the Alzheimer beta/A4 amyloid precursor protein. *J Neurosci*, *14*(5 Pt 2), 3122-3138. https://doi.org/10.1523/jneurosci.14-05-03122.1994

Chan, R. B., Oliveira, T. G., Cortes, E. P., Honig, L. S., Duff, K. E., Small, S. A., Wenk, M. R., Shui, G., & Di Paolo, G. (2012). Comparative Lipidomic Analysis of Mouse and Human Brain with Alzheimer Disease*. *Journal of Biological Chemistry*, *287*(4), 2678-2688. https://doi.org/https://doi.org/10.1074/jbc.M111.274142

Chee, S. E. J., & Solito, E. (2021). The Impact of Ageing on the CNS Immune Response in Alzheimer's Disease [Review]. *Frontiers in Immunology*, *12*. https://doi.org/10.3389/fimmu.2021.738511

Chen, G.-f., Xu, T.-h., Yan, Y., Zhou, Y.-r., Jiang, Y., Melcher, K., & Xu, H. E. (2017). Amyloid beta: structure, biology and structure-based therapeutic development. *Acta Pharmacologica Sinica*, *38*(9), 1205-1235. https://doi.org/10.1038/aps.2017.28

Cheng, Y., Tian, D.-Y., & Wang, Y.-J. (2020). Peripheral clearance of brain-derived Aβ in Alzheimer's disease: pathophysiology and therapeutic perspectives. *Translational Neurodegeneration*, *9*(1), 16. https://doi.org/10.1186/s40035-020-00195-1

Clayton, K., Delpech, J. C., Herron, S., Iwahara, N., Ericsson, M., Saito, T., Saido, T. C., Ikezu, S., & Ikezu, T. (2021). Plaque associated microglia hyper-secrete extracellular vesicles and accelerate tau propagation in a humanized APP mouse model. *Mol Neurodegener*, *16*(1), 18. https://doi.org/10.1186/s13024-021-00440-9

Condello, C., Yuan, P., Schain, A., & Grutzendler, J. (2015). Microglia constitute a barrier that prevents neurotoxic protofibrillar Aβ42 hotspots around plaques. *Nature Communications*, *6*(1), 6176. https://doi.org/10.1038/ncomms7176

Corder, E. H., Saunders, A. M., Strittmatter, W. J., Schmechel, D. E., Gaskell, P. C., Small, G. W., Roses, A. D., Haines, J. L., & Pericak-Vance, M. A. (1993). Gene Dose of Apolipoprotein E Type 4 Allele and the Risk of Alzheimer's Disease in Late Onset Families. *Science*, *261*(5123), 921-923. https://doi.org/doi:10.1126/science.8346443

Courtney, R., & Landreth, G. E. (2016). LXR Regulation of Brain Cholesterol: From Development to Disease. *Trends Endocrinol Metab*, *27*(6), 404-414. https://doi.org/10.1016/j.tem.2016.03.018

Dani, M., Wood, M., Mizoguchi, R., Fan, Z., Walker, Z., Morgan, R., Hinz, R., Biju, M., Kuruvilla, T., Brooks, D. J., & Edison, P. (2018). Microglial activation correlates in vivo with both tau and amyloid in Alzheimer's disease. *Brain*, *141*(9), 2740-2754. https://doi.org/10.1093/brain/awy188

Danik, M., Champagne, D., Petit-Turcotte, C., Beffert, U., & Poirier, J. (1999). Brain lipoprotein metabolism and its relation to neurodegenerative disease. *Crit Rev Neurobiol*, *13*(4), 357-407. https://doi.org/10.1615/critrevneurobiol.v13.i4.20

Deczkowska, A., Keren-Shaul, H., Weiner, A., Colonna, M., Schwartz, M., & Amit, I. (2018). Disease-Associated Microglia: A Universal Immune Sensor of Neurodegeneration. *Cell*, *173*(5), 1073-1081. https://doi.org/https://doi.org/10.1016/j.cell.2018.05.003

Del Bigio, M. R. (2010). Ependymal cells: biology and pathology. *Acta Neuropathologica*, *119*(1), 55-73. https://doi.org/10.1007/s00401-009-0624-y

Depp, C., Sun, T., Sasmita, A. O., Spieth, L., Berghoff, S. A., Steixner-Kumar, A. A., Subramanian, S., Möbius, W., Göbbels, S., Saher, G., Zampar, S., Wirths, O., Thalmann, M., Saito, T., Saido, T., Krueger-Burg, D., Kawaguchi, R., Willem, M., Haass, C., . . . Nave, K.-A. (2021). Ageing-associated myelin dysfunction drives amyloid deposition in mouse models of Alzheimer's disease. *bioRxiv*, 2021.2007.2031.454562. https://doi.org/10.1101/2021.07.31.454562

DeTure, M. A., & Dickson, D. W. (2019). The neuropathological diagnosis of Alzheimer's disease. *Molecular Neurodegeneration*, *14*(1), 32. https://doi.org/10.1186/s13024-019-0333-5

Dietschy, J. M. (2009). Central nervous system: cholesterol turnover, brain development and neurodegeneration. *Biol Chem*, *390*(4), 287-293. https://doi.org/10.1515/BC.2009.035

Dietschy, J. M., & Turley, S. D. (2004). Thematic review series: brain Lipids. Cholesterol metabolism in the central nervous system during early development and in the mature animal. *J Lipid Res*, *45*(8), 1375-1397. https://doi.org/10.1194/jlr.R400004-JLR200

Dionisio-Santos, D. A., Olschowka, J. A., & O'Banion, M. K. (2019). Exploiting microglial and peripheral immune cell crosstalk to treat Alzheimer's disease. *J Neuroinflammation*, *16*(1), 74. https://doi.org/10.1186/s12974-019-1453-0

Dodge, J. C., Yu, J., Sardi, S. P., & Shihabuddin, L. S. (2021). Sterol auto-oxidation adversely affects human motor neuron viability and is a neuropathological feature of amyotrophic lateral sclerosis. *Sci Rep*, *11*(1), 803. https://doi.org/10.1038/s41598-020-80378-y

Dragatsis, I., & Zeitlin, S. (2000). CaMKIIalpha-Cre transgene expression and recombination patterns in the mouse brain. *Genesis*, *26*(2), 133-135. https://doi.org/10.1002/(sici)1526-968x(200002)26:2<133::aid-gene10>3.0.co;2-v

Eckman, E. A., Adams, S. K., Troendle, F. J., Stodola, B. A., Kahn, M. A., Fauq, A. H., Xiao, H. D., Bernstein, K. E., & Eckman, C. B. (2006). Regulation of steady-state beta-amyloid levels in the brain by neprilysin and endothelin-converting enzyme but not angiotensin-converting enzyme. *J Biol Chem*, *281*(41), 30471-30478. https://doi.org/10.1074/jbc.M605827200

Ehehalt, R., Keller, P., Haass, C., Thiele, C., & Simons, K. (2003). Amyloidogenic processing of the Alzheimer beta-amyloid precursor protein depends on lipid rafts. *J Cell Biol*, *160*(1), 113-123. https://doi.org/10.1083/jcb.200207113

Fabelo, N., Martín, V., Marín, R., Moreno, D., Ferrer, I., & Díaz, M. (2014). Altered lipid composition in cortical lipid rafts occurs at early stages of sporadic Alzheimer's disease and facilitates APP/BACE1 interactions. *Neurobiology of Aging*, *35*(8), 1801-1812. https://doi.org/https://doi.org/10.1016/j.neurobiolaging.2014.02.005

Farmer, B. C., Walsh, A. E., Kluemper, J. C., & Johnson, L. A. (2020). Lipid Droplets in Neurodegenerative Disorders [Review]. *Frontiers in Neuroscience*, *14*. https://doi.org/10.3389/fnins.2020.00742

Farris, W., Schütz, S. G., Cirrito, J. R., Shankar, G. M., Sun, X., George, A., Leissring, M. A., Walsh, D. M., Qiu, W. Q., Holtzman, D. M., & Selkoe, D. J. (2007). Loss of neprilysin function promotes amyloid plaque formation and causes cerebral amyloid angiopathy. *Am J Pathol*, *171*(1), 241-251. https://doi.org/10.2353/ajpath.2007.070105

Feng, W., Zhang, Y., Wang, Z., Xu, H., Wu, T., Marshall, C., Gao, J., & Xiao, M. (2020). Microglia prevent beta-amyloid plaque formation in the early stage of an Alzheimer's disease mouse model with suppression of glymphatic clearance. *Alzheimer's Research & Therapy*, *12*(1), 125. https://doi.org/10.1186/s13195-020-00688-1

Fillit, H., & Green, A. (2021). Aducanumab and the FDA — where are we now? *Nature Reviews Neurology*, *17*(3), 129-130. https://doi.org/10.1038/s41582-020-00454-9

Flanary, B. E., Sammons, N. W., Nguyen, C., Walker, D., & Streit, W. J. (2007). Evidence that aging and amyloid promote microglial cell senescence. *Rejuvenation Res*, *10*(1), 61-74. https://doi.org/10.1089/rej.2006.9096

Flanary, B. E., & Streit, W. J. (2004). Progressive telomere shortening occurs in cultured rat microglia, but not astrocytes. *Glia*, *45*(1), 75-88. https://doi.org/10.1002/glia.10301

Floden, A. M., & Combs, C. K. (2011). Microglia demonstrate age-dependent interaction with amyloid-β fibrils. *J Alzheimers Dis*, *25*(2), 279-293. https://doi.org/10.3233/jad-2011-101014

Frade, J. M., & Barde, Y.-A. (1998). Microglia-Derived Nerve Growth Factor Causes Cell Death in the Developing Retina. *Neuron*, *20*(1), 35-41. https://doi.org/https://doi.org/10.1016/S0896-6273(00)80432-8

Frieden, C., Wang, H., & Ho, C. M. W. (2017). A mechanism for lipid binding to apoE and the role of intrinsically disordered regions coupled to domain–domain interactions. *Proceedings of the National Academy of Sciences*, *114*(24), 6292-6297. https://doi.org/doi:10.1073/pnas.1705080114

Friedrich, R. P., Tepper, K., Rönicke, R., Soom, M., Westermann, M., Reymann, K., Kaether, C., & Fändrich, M. (2010). Mechanism of amyloid plaque formation suggests an intracellular basis of Abeta pathogenicity. *Proc Natl Acad Sci U S A*, *107*(5), 1942-1947. https://doi.org/10.1073/pnas.0904532106

Fuger, P., Hefendehl, J. K., Veeraraghavalu, K., Wendeln, A. C., Schlosser, C., Obermuller, U., Wegenast-Braun, B. M., Neher, J. J., Martus, P., Kohsaka, S., Thunemann, M., Feil, R., Sisodia, S. S., Skodras, A., & Jucker, M. (2017). Microglia turnover with aging and in an Alzheimer's model via long-term in vivo single-cell imaging. *Nat Neurosci*, *20*(10), 1371-1376. https://doi.org/10.1038/nn.4631

Funfschilling, U., Jockusch, W. J., Sivakumar, N., Mobius, W., Corthals, K., Li, S., Quintes, S., Kim, Y., Schaap, I. A., Rhee, J. S., Nave, K. A., & Saher, G. (2012). Critical time window of neuronal cholesterol synthesis during neurite outgrowth. *J Neurosci*, *32*(22), 7632-7645. https://doi.org/10.1523/JNEUROSCI.1352-11.2012

Fünfschilling, U., Saher, G., Xiao, L., Möbius, W., & Nave, K. A. (2007). Survival of adult neurons lacking cholesterol synthesis in vivo. *BMC Neurosci*, *8*, 1. https://doi.org/10.1186/1471-2202-8-1

Gallagher, D., Belmonte, D., Deurenberg, P., Wang, Z., Krasnow, N., Pi-Sunyer, F. X., & Heymsfield, S. B. (1998). Organ-tissue mass measurement allows modeling of REE and metabolically active tissue mass. *Am J Physiol*, *275*(2), E249-258. https://doi.org/10.1152/ajpendo.1998.275.2.E249

Galvagnion, C., Brown, J. W., Ouberai, M. M., Flagmeier, P., Vendruscolo, M., Buell, A. K., Sparr, E., & Dobson, C. M. (2016). Chemical properties of lipids strongly affect the kinetics of the membrane-induced aggregation of alpha-synuclein. *Proc Natl Acad Sci U S A*, *113*(26), 7065-7070. https://doi.org/10.1073/pnas.1601899113

Gellermann, G. P., Ullrich, K., Tannert, A., Unger, C., Habicht, G., Sauter, S. R. N., Hortschansky, P., Horn, U., Möllmann, U., Decker, M., Lehmann, J., & Fändrich, M. (2006). Alzheimer-like Plaque Formation by Human Macrophages Is Reduced by Fibrillation Inhibitors and Lovastatin. *Journal of Molecular Biology*, *360*(2), 251-257. https://doi.org/https://doi.org/10.1016/j.jmb.2006.05.026

Glenner, G. G., & Wong, C. W. (1984). Alzheimer's disease: initial report of the purification and characterization of a novel cerebrovascular amyloid protein. *Biochem Biophys Res Commun*, *120*(3), 885-890. https://doi.org/10.1016/s0006-291x(84)80190-4

Götz, J., Bodea, L.-G., & Goedert, M. (2018). Rodent models for Alzheimer disease. *Nature Reviews Neuroscience*, *19*(10), 583-598. https://doi.org/10.1038/s41583-018-0054-8

Gouras, G. K., Tampellini, D., Takahashi, R. H., & Capetillo-Zarate, E. (2010). Intraneuronal beta-amyloid accumulation and synapse pathology in Alzheimer's disease. *Acta Neuropathologica*, *119*(5), 523-541. https://doi.org/10.1007/s00401-010-0679-9

Grimm, M. O. W., Grimm, H. S., Tomic, I., Beyreuther, K., Hartmann, T., & Bergmann, C. (2008). Independent Inhibition of Alzheimer Disease β- and γ-Secretase Cleavage by Lowered Cholesterol Levels *. *Journal of Biological Chemistry*, *283*(17), 11302-11311. https://doi.org/10.1074/jbc.M801520200

Grubman, A., Choo, X. Y., Chew, G., Ouyang, J. F., Sun, G., Croft, N. P., Rossello, F. J., Simmons, R., Buckberry, S., Landin, D. V., Pflueger, J., Vandekolk, T. H., Abay, Z., Zhou, Y., Liu, X., Chen, J., Larcombe, M., Haynes, J. M., McLean, C., . . . Polo, J. M. (2021). Transcriptional signature in microglia associated with Abeta plaque phagocytosis. *Nat Commun*, *12*(1), 3015. https://doi.org/10.1038/s41467-021-23111-1

Haass, C., & Selkoe, D. J. (1993). Cellular processing of beta-amyloid precursor protein and the genesis of amyloid beta-peptide. *Cell*, *75*(6), 1039-1042. https://doi.org/10.1016/0092-8674(93)90312-e

Hagemeyer, N., Hanft, K. M., Akriditou, M. A., Unger, N., Park, E. S., Stanley, E. R., Staszewski, O., Dimou, L., & Prinz, M. (2017). Microglia contribute to normal myelinogenesis and to oligodendrocyte progenitor maintenance during adulthood. *Acta Neuropathol*, *134*(3), 441-458. https://doi.org/10.1007/s00401-017-1747-1

Hamilton, Laura K., Dufresne, M., Joppé, Sandra E., Petryszyn, S., Aumont, A., Calon, F., Barnabé-Heider, F., Furtos, A., Parent, M., Chaurand, P., & Fernandes, Karl J. L. (2015). Aberrant Lipid Metabolism in the Forebrain Niche Suppresses Adult Neural Stem Cell Proliferation in an Animal Model of Alzheimer's Disease. *Cell Stem Cell*, *17*(4), 397-411. https://doi.org/https://doi.org/10.1016/j.stem.2015.08.001

Hammond, T. R., Dufort, C., Dissing-Olesen, L., Giera, S., Young, A., Wysoker, A., Walker, A. J., Gergits, F., Segel, M., Nemesh, J., Marsh, S. E., Saunders, A., Macosko, E., Ginhoux, F., Chen, J., Franklin, R. J. M., Piao, X., McCarroll, S. A., & Stevens, B. (2019). Single-Cell RNA Sequencing of Microglia throughout the Mouse Lifespan and in the Injured Brain Reveals Complex Cell-State Changes. *Immunity*, *50*(1), 253-271 e256. https://doi.org/10.1016/j.immuni.2018.11.004

Hansson, O. (2021). Biomarkers for neurodegenerative diseases. *Nat Med*, *27*(6), 954-963. https://doi.org/10.1038/s41591-021-01382-x

Hardy, J., & Allsop, D. (1991). Amyloid deposition as the central event in the aetiology of Alzheimer's disease. *Trends Pharmacol Sci*, *12*(10), 383-388. https://doi.org/10.1016/0165-6147(91)90609-v

Harman, D. (2006). Alzheimer's disease pathogenesis: role of aging. *Ann N Y Acad Sci*, *1067*, 454-460. https://doi.org/10.1196/annals.1354.065

Hartz, A. M. S., Zhong, Y., Shen, A. N., Abner, E. L., & Bauer, B. (2018). Preventing P-gp Ubiquitination Lowers Abeta Brain Levels in an Alzheimer's Disease Mouse Model. *Front Aging Neurosci*, *10*, 186. https://doi.org/10.3389/fnagi.2018.00186

Hatami, A., Monjazeb, S., Milton, S., & Glabe, C. G. (2017). Familial Alzheimer's Disease Mutations within the Amyloid Precursor Protein Alter the Aggregation and Conformation of the Amyloid-β Peptide* *This work was supported by National Institutes of Health Grants AG033069 and AG00538 and a grant from the Cure Alzheimer's fund. The authors declare that they have no conflicts of interest with the contents of this article. The content is solely the responsibility of the authors and does not necessarily represent the official views of the National Institutes of Health. *Journal of Biological Chemistry*, *292*(8), 3172-3185. https://doi.org/https://doi.org/10.1074/jbc.M116.755264

Hawkins, N. A., Jurado, M., Thaxton, T. T., Duarte, S. E., Barse, L., Tatsukawa, T., Yamakawa, K., Nishi, T., Kondo, S., Miyamoto, M., Abrahams, B. S., During, M. J., & Kearney, J. A. (2021). Soticlestat, a novel cholesterol 24-hydroxylase inhibitor, reduces seizures and

premature death in Dravet syndrome mice. *Epilepsia*, *62*(11), 2845-2857. https://doi.org/10.1111/epi.17062

Hemonnot-Girard, A.-L., Meersseman, C., Pastore, M., Linck, N., Rey, C., Lachuer, J., Reynes, C., Rassendren, F., & Hirbec, H. (2021). *Relative Contribution of Amyloid-β Plaque Associated and Plaque Distant Microglia to Alzheimer'S Disease (AD) Progression*. https://doi.org/10.21203/rs.3.rs-876995/v2

Heneka, M. T., Nadrigny, F., Regen, T., Martinez-Hernandez, A., Dumitrescu-Ozimek, L., Terwel, D., Jardanhazi-Kurutz, D., Walter, J., Kirchhoff, F., Hanisch, U. K., & Kummer, M. P. (2010). Locus ceruleus controls Alzheimer's disease pathology by modulating microglial functions through norepinephrine. *Proc Natl Acad Sci U S A*, *107*(13), 6058-6063. https://doi.org/10.1073/pnas.0909586107

Hickman, S. E., Allison, E. K., & El Khoury, J. (2008). Microglial dysfunction and defective beta-amyloid clearance pathways in aging Alzheimer's disease mice. *J Neurosci*, *28*(33), 8354-8360. https://doi.org/10.1523/JNEUROSCI.0616-08.2008

Hippius, H., & Neundörfer, G. (2003). The discovery of Alzheimer's disease. *Dialogues in clinical neuroscience*, *5*(1), 101-108. https://doi.org/10.31887/DCNS.2003.5.1/hhippius

Hirsch-Reinshagen, V., Zhou, S., Burgess, B. L., Bernier, L., McIsaac, S. A., Chan, J. Y., Tansley, G. H., Cohn, J. S., Hayden, M. R., & Wellington, C. L. (2004). Deficiency of ABCA1 Impairs Apolipoprotein E Metabolism in Brain*. *Journal of Biological Chemistry*, *279*(39), 41197-41207. https://doi.org/https://doi.org/10.1074/jbc.M407962200

Hu, Y., Fryatt, G. L., Ghorbani, M., Obst, J., Menassa, D. A., Martin-Estebane, M., Muntslag, T. A. O., Olmos-Alonso, A., Guerrero-Carrasco, M., Thomas, D., Cragg, M. S., & Gomez-Nicola, D. (2021). Replicative senescence dictates the emergence of disease-associated microglia and contributes to Aβ pathology. *Cell Rep*, *35*(10), 109228. https://doi.org/10.1016/j.celrep.2021.109228

Huang, Y., Happonen, K. E., Burrola, P. G., O'Connor, C., Hah, N., Huang, L., Nimmerjahn, A., & Lemke, G. (2021). Microglia use TAM receptors to detect and engulf amyloid beta plaques. *Nat Immunol*, *22*(5), 586-594. https://doi.org/10.1038/s41590-021-00913-5

Hutton, M., Lendon, C. L., Rizzu, P., Baker, M., Froelich, S., Houlden, H., Pickering-Brown, S., Chakraverty, S., Isaacs, A., Grover, A., Hackett, J., Adamson, J., Lincoln, S., Dickson, D., Davies, P., Petersen, R. C., Stevens, M., de Graaff, E., Wauters, E., . . . Heutink, P. (1998). Association of missense and 5'-splice-site mutations in tau with the inherited dementia FTDP-17. *Nature*, *393*(6686), 702-705. https://doi.org/10.1038/31508

Huynh, K. K., Eskelinen, E.-L., Scott, C. C., Malevanets, A., Saftig, P., & Grinstein, S. (2007). LAMP proteins are required for fusion of lysosomes with phagosomes. *The EMBO journal*, *26*(2), 313-324. https://doi.org/10.1038/sj.emboj.7601511

Hyder, F., Rothman, D. L., & Bennett, M. R. (2013). Cortical energy demands of signaling and nonsignaling components in brain are conserved across mammalian species and activity levels. *Proceedings of the National Academy of Sciences*, *110*(9), 3549-3554. https://doi.org/10.1073/pnas.1214912110

Iliff, J. J., Wang, M., Liao, Y., Plogg, B. A., Peng, W., Gundersen, G. A., Benveniste, H., Vates, G. E., Deane, R., Goldman, S. A., Nagelhus, E. A., & Nedergaard, M. (2012). A paravascular pathway facilitates CSF flow through the brain parenchyma and the clearance of interstitial solutes, including amyloid β. *Sci Transl Med*, *4*(147), 147ra111. https://doi.org/10.1126/scitranslmed.3003748

Ingre, C., Chen, L., Zhan, Y., Termorshuizen, J., Yin, L., & Fang, F. (2020). Lipids, apolipoproteins, and prognosis of amyotrophic lateral sclerosis. *Neurology*, *94*(17), e1835-e1844. https://doi.org/10.1212/WNL.0000000000009322

Iwata, N., Mizukami, H., Shirotani, K., Takaki, Y., Muramatsu, S., Lu, B., Gerard, N. P., Gerard, C., Ozawa, K., & Saido, T. C. (2004). Presynaptic localization of neprilysin contributes to

efficient clearance of amyloid-beta peptide in mouse brain. *J Neurosci*, *24*(4), 991-998. https://doi.org/10.1523/jneurosci.4792-03.2004

Janelidze, S., Mattsson, N., Palmqvist, S., Smith, R., Beach, T. G., Serrano, G. E., Chai, X., Proctor, N. K., Eichenlaub, U., Zetterberg, H., Blennow, K., Reiman, E. M., Stomrud, E., Dage, J. L., & Hansson, O. (2020). Plasma P-tau181 in Alzheimer's disease: relationship to other biomarkers, differential diagnosis, neuropathology and longitudinal progression to Alzheimer's dementia. *Nature Medicine*, *26*(3), 379-386. https://doi.org/10.1038/s41591-020-0755-1

Jantzen, P. T., Connor, K. E., DiCarlo, G., Wenk, G. L., Wallace, J. L., Rojiani, A. M., Coppola, D., Morgan, D., & Gordon, M. N. (2002). Microglial Activation and β-Amyloid Deposit Reduction Caused by a Nitric Oxide-Releasing Nonsteroidal Anti-Inflammatory Drug in Amyloid Precursor Protein Plus Presenilin-1 Transgenic Mice. *The Journal of Neuroscience*, *22*(6), 2246-2254. https://doi.org/10.1523/jneurosci.22-06-02246.2002

Jay, T. R., Miller, C. M., Cheng, P. J., Graham, L. C., Bemiller, S., Broihier, M. L., Xu, G., Margevicius, D., Karlo, J. C., Sousa, G. L., Cotleur, A. C., Butovsky, O., Bekris, L., Staugaitis, S. M., Leverenz, J. B., Pimplikar, S. W., Landreth, G. E., Howell, G. R., Ransohoff, R. M., & Lamb, B. T. (2015). TREM2 deficiency eliminates TREM2+ inflammatory macrophages and ameliorates pathology in Alzheimer's disease mouse models. *J Exp Med*, *212*(3), 287-295. https://doi.org/10.1084/jem.20142322

Jongbloed, W., Bruggink, K. A., Kester, M. I., Visser, P. J., Scheltens, P., Blankenstein, M. A., Verbeek, M. M., Teunissen, C. E., & Veerhuis, R. (2015). Amyloid-β oligomers relate to cognitive decline in Alzheimer's disease. *J Alzheimers Dis*, *45*(1), 35-43. https://doi.org/10.3233/jad-142136

Jonsson, T., Atwal, J. K., Steinberg, S., Snaedal, J., Jonsson, P. V., Bjornsson, S., Stefansson, H., Sulem, P., Gudbjartsson, D., Maloney, J., Hoyte, K., Gustafson, A., Liu, Y., Lu, Y., Bhangale, T., Graham, R. R., Huttenlocher, J., Bjornsdottir, G., Andreassen, O. A., . . . Stefansson, K. (2012). A mutation in APP protects against Alzheimer's disease and age-related cognitive decline. *Nature*, *488*(7409), 96-99. https://doi.org/10.1038/nature11283

Kamboh, M. I., Demirci, F. Y., Wang, X., Minster, R. L., Carrasquillo, M. M., Pankratz, V. S., Younkin, S. G., Saykin, A. J., Jun, G., Baldwin, C., Logue, M. W., Buros, J., Farrer, L., Pericak-Vance, M. A., Haines, J. L., Sweet, R. A., Ganguli, M., Feingold, E., Dekosky, S. T., . . . Barmada, M. M. (2012). Genome-wide association study of Alzheimer's disease. *Transl Psychiatry*, *2*(5), e117. https://doi.org/10.1038/tp.2012.45

Kandutsch, A. A., & Russell, A. E. (1960). Preputial gland tumor sterols. 3. A metabolic pathway from lanosterol to cholesterol. *J Biol Chem*, *235*, 2256-2261.

Karasinska, J. M., Rinninger, F., Lütjohann, D., Ruddle, P., Franciosi, S., Kruit, J. K., Singaraja, R. R., Hirsch-Reinshagen, V., Fan, J., Brunham, L. R., Bissada, N., Ramakrishnan, R., Wellington, C. L., Parks, J. S., & Hayden, M. R. (2009). Specific Loss of Brain ABCA1 Increases Brain Cholesterol Uptake and Influences Neuronal Structure and Function. *The Journal of Neuroscience*, *29*(11), 3579-3589. https://doi.org/10.1523/jneurosci.4741-08.2009

Karran, E., Mercken, M., & Strooper, B. D. (2011). The amyloid cascade hypothesis for Alzheimer's disease: an appraisal for the development of therapeutics. *Nature Reviews Drug Discovery*, *10*(9), 698-712. https://doi.org/10.1038/nrd3505

Keren-Shaul, H., Spinrad, A., Weiner, A., Matcovitch-Natan, O., Dvir-Szternfeld, R., Ulland, T. K., David, E., Baruch, K., Lara-Astaiso, D., Toth, B., Itzkovitz, S., Colonna, M., Schwartz, M., & Amit, I. (2017). A Unique Microglia Type Associated with Restricting Development of Alzheimer's Disease. *Cell*, *169*(7), 1276-1290 e1217. https://doi.org/10.1016/j.cell.2017.05.018

Khan, S., Barve, K. H., & Kumar, M. S. (2020). Recent Advancements in Pathogenesis, Diagnostics and Treatment of Alzheimer's Disease. *Curr Neuropharmacol*, *18*(11), 1106-1125. https://doi.org/10.2174/1570159x18666200528142429

Kierdorf, K., Katzmarski, N., Haas, C. A., & Prinz, M. (2013). Bone marrow cell recruitment to the brain in the absence of irradiation or parabiosis bias. *PLoS One*, *8*(3), e58544. https://doi.org/10.1371/journal.pone.0058544

Kim, J., Castellano, J. M., Jiang, H., Basak, J. M., Parsadanian, M., Pham, V., Mason, S. M., Paul, S. M., & Holtzman, D. M. (2009). Overexpression of Low-Density Lipoprotein Receptor in the Brain Markedly Inhibits Amyloid Deposition and Increases Extracellular Aβ Clearance. *Neuron*, *64*(5), 632-644. https://doi.org/https://doi.org/10.1016/j.neuron.2009.11.013

Kim, J., Onstead, L., Randle, S., Price, R., Smithson, L., Zwizinski, C., Dickson, D. W., Golde, T., & McGowan, E. (2007). Aβ40 Inhibits Amyloid Deposition In Vivo. *The Journal of Neuroscience*, *27*(3), 627-633. https://doi.org/10.1523/jneurosci.4849-06.2007

Kiss, M., & Nagy, L. (2016). Nuclear Receptors in Immune Function. In M. J. H. Ratcliffe (Ed.), *Encyclopedia of Immunobiology* (pp. 146-156). Academic Press. https://doi.org/https://doi.org/10.1016/B978-0-12-374279-7.11012-4

Kojro, E., Gimpl, G., Lammich, S., Marz, W., & Fahrenholz, F. (2001). Low cholesterol stimulates the nonamyloidogenic pathway by its effect on the alpha -secretase ADAM 10. *Proc Natl Acad Sci U S A*, *98*(10), 5815-5820. https://doi.org/10.1073/pnas.081612998

Koo, E. H., & Squazzo, S. L. (1994). Evidence that production and release of amyloid beta-protein involves the endocytic pathway. *J Biol Chem*, *269*(26), 17386-17389.

Koper, J. W., Zeinstra, E. C., Lopes-Cardozo, M., & van Golde, L. M. (1984). Acetoacetate and glucose as substrates for lipid synthesis by rat brain oligodendrocytes and astrocytes in serum-free culture. *Biochim Biophys Acta*, *796*(1), 20-26. https://doi.org/10.1016/0005-2760(84)90233-9

Kraepelin, E. (1913). *Psychiatrie. Ein Lehrbuch* fuer *Studierende und* Aerzte. J.A. Barth.

Krasemann, S., Madore, C., Cialic, R., Baufeld, C., Calcagno, N., El Fatimy, R., Beckers, L., O'Loughlin, E., Xu, Y., Fanek, Z., Greco, D. J., Smith, S. T., Tweet, G., Humulock, Z., Zrzavy, T., Conde-Sanroman, P., Gacias, M., Weng, Z., Chen, H., . . . Butovsky, O. (2017). The TREM2-APOE Pathway Drives the Transcriptional Phenotype of Dysfunctional Microglia in Neurodegenerative Diseases. *Immunity*, *47*(3), 566-581.e569. https://doi.org/10.1016/j.immuni.2017.08.008

Kulkarni, B., Cruz-Martins, N., & Kumar, D. (2022). Microglia in Alzheimer's Disease: An Unprecedented Opportunity as Prospective Drug Target. *Molecular Neurobiology*. https://doi.org/10.1007/s12035-021-02661-x

Lanfranco, M. F., Ng, C. A., & Rebeck, G. W. (2020). ApoE Lipidation as a Therapeutic Target in Alzheimer's Disease. *Int J Mol Sci*, *21*(17). https://doi.org/10.3390/ijms21176336

Langness, V. F., van der Kant, R., Das, U., Wang, L., Chaves, R. d. S., Goldstein, L. S. B., & Olzmann, J. (2021). Cholesterol-lowering drugs reduce APP processing to Aβ by inducing APP dimerization. *Molecular Biology of the Cell*, *32*(3), 247-259. https://doi.org/10.1091/mbc.E20-05-0345

Lazarevic, V., Fieńko, S., Andres-Alonso, M., Anni, D., Ivanova, D., Montenegro-Venegas, C., Gundelfinger, E. D., Cousin, M. A., & Fejtova, A. (2017). Physiological Concentrations of Amyloid Beta Regulate Recycling of Synaptic Vesicles via Alpha7 Acetylcholine Receptor and CDK5/Calcineurin Signaling. *Frontiers in molecular neuroscience*, *10*, 221-221. https://doi.org/10.3389/fnmol.2017.00221

Lefterov, I., Wolfe, C. M., Fitz, N. F., Nam, K. N., Letronne, F., Biedrzycki, R. J., Kofler, J., Han, X., Wang, J., Schug, J., & Koldamova, R. (2019). APOE2 orchestrated differences in transcriptomic and lipidomic profiles of postmortem AD brain. *Alzheimers Res Ther*, *11*(1), 113. https://doi.org/10.1186/s13195-019-0558-0

Leoni, V., Mariotti, C., Nanetti, L., Salvatore, E., Squitieri, F., Bentivoglio, A. R., Bandettini di Poggio, M., Piacentini, S., Monza, D., Valenza, M., Cattaneo, E., & Di Donato, S. (2011). Whole body cholesterol metabolism is impaired in Huntington's disease. *Neurosci Lett*, *494*(3), 245-249. https://doi.org/10.1016/j.neulet.2011.03.025

Li, Q., & Barres, B. A. (2018). Microglia and macrophages in brain homeostasis and disease. *Nature Reviews Immunology*, *18*(4), 225-242. https://doi.org/10.1038/nri.2017.125

Liebmann, T., Renier, N., Bettayeb, K., Greengard, P., Tessier-Lavigne, M., & Flajolet, M. (2016). Three-Dimensional Study of Alzheimer's Disease Hallmarks Using the iDISCO Clearing Method. *Cell Rep*, *16*(4), 1138-1152. https://doi.org/10.1016/j.celrep.2016.06.060

Liu, C. C., Liu, C. C., Kanekiyo, T., Xu, H., & Bu, G. (2013). Apolipoprotein E and Alzheimer disease: risk, mechanisms and therapy. *Nat Rev Neurol*, *9*(2), 106-118. https://doi.org/10.1038/nrneurol.2012.263

Liu, P.-P., Xie, Y., Meng, X.-Y., & Kang, J.-S. (2019). History and progress of hypotheses and clinical trials for Alzheimer's disease. *Signal transduction and targeted therapy*, *4*, 29-29. https://doi.org/10.1038/s41392-019-0063-8

Love, S. (2004). Contribution of cerebral amyloid angiopathy to Alzheimer's disease. *J Neurol Neurosurg Psychiatry*, *75*(1), 1-4. https://doi.org/10.1136/jnnp.2003.034249

Luo, J., Yang, H., & Song, B. L. (2020). Mechanisms and regulation of cholesterol homeostasis. *Nat Rev Mol Cell Biol*, *21*(4), 225-245. https://doi.org/10.1038/s41580-019-0190-7

Mahan, T. E., Wang, C., Bao, X., Choudhury, A., Ulrich, J. D., & Holtzman, D. M. (2022). Selective reduction of astrocyte apoE3 and apoE4 strongly reduces Aβ accumulation and plaque-related pathology in a mouse model of amyloidosis. *Molecular Neurodegeneration*, *17*(1), 13. https://doi.org/10.1186/s13024-022-00516-0

Majumdar, A., Chung, H., Dolios, G., Wang, R., Asamoah, N., Lobel, P., & Maxfield, F. R. (2008). Degradation of fibrillar forms of Alzheimer's amyloid beta-peptide by macrophages. *Neurobiol Aging*, *29*(5), 707-715. https://doi.org/10.1016/j.neurobiolaging.2006.12.001

Marín-Teva, J. L., Dusart, I., Colin, C., Gervais, A., van Rooijen, N., & Mallat, M. (2004). Microglia Promote the Death of Developing Purkinje Cells. *Neuron*, *41*(4), 535-547. https://doi.org/https://doi.org/10.1016/S0896-6273(04)00069-8

Marquer, C., Devauges, V., Cossec, J. C., Liot, G., Lecart, S., Saudou, F., Duyckaerts, C., Leveque-Fort, S., & Potier, M. C. (2011). Local cholesterol increase triggers amyloid precursor protein-Bace1 clustering in lipid rafts and rapid endocytosis. *FASEB J*, *25*(4), 1295-1305. https://doi.org/10.1096/fj.10-168633

Marschallinger, J., Iram, T., Zardeneta, M., Lee, S. E., Lehallier, B., Haney, M. S., Pluvinage, J. V., Mathur, V., Hahn, O., Morgens, D. W., Kim, J., Tevini, J., Felder, T. K., Wolinski, H., Bertozzi, C. R., Bassik, M. C., Aigner, L., & Wyss-Coray, T. (2020). Lipid-droplet-accumulating microglia represent a dysfunctional and proinflammatory state in the aging brain. *Nat Neurosci*, *23*(2), 194-208. https://doi.org/10.1038/s41593-019-0566-1

Masters, C. L., Simms, G., Weinman, N. A., Multhaup, G., McDonald, B. L., & Beyreuther, K. (1985). Amyloid plaque core protein in Alzheimer disease and Down syndrome. *Proceedings of the National Academy of Sciences*, *82*(12), 4245-4249. https://doi.org/doi:10.1073/pnas.82.12.4245

McLean, C. A., Cherny, R. A., Fraser, F. W., Fuller, S. J., Smith, M. J., Beyreuther, K., Bush, A. I., & Masters, C. L. (1999). Soluble pool of Abeta amyloid as a determinant of severity of neurodegeneration in Alzheimer's disease. *Ann Neurol*, *46*(6), 860-866. https://doi.org/10.1002/1531-8249(199912)46:6<860::aid-ana8>3.0.co;2-m

Minichiello, L., Korte, M., Wolfer, D., Kühn, R., Unsicker, K., Cestari, V., Rossi-Arnaud, C., Lipp, H.-P., Bonhoeffer, T., & Klein, R. (1999). Essential Role for TrkB Receptors in Hippocampus-Mediated Learning. *Neuron*, *24*(2), 401-414. https://doi.org/https://doi.org/10.1016/S0896-6273(00)80853-3

Mitsche, M. A., McDonald, J. G., Hobbs, H. H., & Cohen, J. C. (2015). Flux analysis of cholesterol biosynthesis in vivo reveals multiple tissue and cell-type specific pathways. *Elife*, *4*, e07999. https://doi.org/10.7554/eLife.07999

Moulton, M. J., Barish, S., Ralhan, I., Chang, J., Goodman, L. D., Harland, J. G., Marcogliese, P. C., Johansson, J. O., Ioannou, M. S., & Bellen, H. J. (2021). Neuronal ROS-induced glial lipid droplet formation is altered by loss of Alzheimer’s disease–associated genes. *Proceedings of the National Academy of Sciences*, *118*(52), e2112095118. https://doi.org/doi:10.1073/pnas.2112095118

Muse, E. D., Yu, S., Edillor, C. R., Tao, J., Spann, N. J., Troutman, T. D., Seidman, J. S., Henke, A., Roland, J. T., Ozeki, K. A., Thompson, B. M., McDonald, J. G., Bahadorani, J., Tsimikas, S., Grossman, T. R., Tremblay, M. S., & Glass, C. K. (2018). Cell-specific discrimination of desmosterol and desmosterol mimetics confers selective regulation of LXR and SREBP in macrophages. *Proceedings of the National Academy of Sciences of the United States of America*, *115*(20), E4680-E4689. https://doi.org/10.1073/pnas.1714518115

Nag, S., Sarkar, B., Bandyopadhyay, A., Sahoo, B., Sreenivasan, V. K., Kombrabail, M., Muralidharan, C., & Maiti, S. (2011). Nature of the amyloid-beta monomer and the monomer-oligomer equilibrium. *J Biol Chem*, *286*(16), 13827-13833. https://doi.org/10.1074/jbc.M110.199885

Nirmalraj, P. N., List, J., Battacharya, S., Howe, G., Xu, L., Thompson, D., & Mayer, M. (2020). Complete aggregation pathway of amyloid β (1-40) and (1-42) resolved on an atomically clean interface. *Science Advances*, *6*(15), eaaz6014. https://doi.org/doi:10.1126/sciadv.aaz6014

Nugent, A. A., Lin, K., van Lengerich, B., Lianoglou, S., Przybyla, L., Davis, S. S., Llapashtica, C., Wang, J., Kim, D. J., Xia, D., Lucas, A., Baskaran, S., Haddick, P. C. G., Lenser, M., Earr, T. K., Shi, J., Dugas, J. C., Andreone, B. J., Logan, T., . . . Di Paolo, G. (2020). TREM2 Regulates Microglial Cholesterol Metabolism upon Chronic Phagocytic Challenge. *Neuron*, *105*(5), 837-854.e839. https://doi.org/10.1016/j.neuron.2019.12.007

O'Leary, E. I., Jiang, Z., Strub, M. P., & Lee, J. C. (2018). Effects of phosphatidylcholine membrane fluidity on the conformation and aggregation of N-terminally acetylated alpha-synuclein. *J Biol Chem*, *293*(28), 11195-11205. https://doi.org/10.1074/jbc.RA118.002780

Oakley, H., Cole, S. L., Logan, S., Maus, E., Shao, P., Craft, J., Guillozet-Bongaarts, A., Ohno, M., Disterhoft, J., Van Eldik, L., Berry, R., & Vassar, R. (2006). Intraneuronal beta-amyloid aggregates, neurodegeneration, and neuron loss in transgenic mice with five familial Alzheimer's disease mutations: potential factors in amyloid plaque formation. *J Neurosci*, *26*(40), 10129-10140. https://doi.org/10.1523/jneurosci.1202-06.2006

Oddo, S., Caccamo, A., Smith, I. F., Green, K. N., & LaFerla, F. M. (2006). A dynamic relationship between intracellular and extracellular pools of Abeta. *The American Journal of Pathology*, *168*(1), 184-194. https://doi.org/10.2353/ajpath.2006.050593

Ofengeim, D., Mazzitelli, S., Ito, Y., DeWitt, J. P., Mifflin, L., Zou, C., Das, S., Adiconis, X., Chen, H., Zhu, H., Kelliher, M. A., Levin, J. Z., & Yuan, J. (2017). RIPK1 mediates a disease-associated microglial response in Alzheimer's disease. *Proc Natl Acad Sci U S A*, *114*(41), E8788-e8797. https://doi.org/10.1073/pnas.1714175114

Ono, K., Condron, M. M., & Teplow, D. B. (2009). Structure-neurotoxicity relationships of amyloid beta-protein oligomers. *Proc Natl Acad Sci U S A*, *106*(35), 14745-14750. https://doi.org/10.1073/pnas.0905127106

Orth, M., & Bellosta, S. (2012). Cholesterol: its regulation and role in central nervous system disorders. *Cholesterol*, *2012*, 292598. https://doi.org/10.1155/2012/292598

Paolicelli, R. C., Bolasco, G., Pagani, F., Maggi, L., Scianni, M., Panzanelli, P., Giustetto, M., Ferreira, T. A., Guiducci, E., Dumas, L., Ragozzino, D., & Gross, C. T. (2011). Synaptic

Pruning by Microglia Is Necessary for Normal Brain Development. *Science*, *333*(6048), 1456-1458. https://doi.org/doi:10.1126/science.1202529

Parhizkar, S., Arzberger, T., Brendel, M., Kleinberger, G., Deussing, M., Focke, C., Nuscher, B., Xiong, M., Ghasemigharagoz, A., Katzmarski, N., Krasemann, S., Lichtenthaler, S. F., Muller, S. A., Colombo, A., Monasor, L. S., Tahirovic, S., Herms, J., Willem, M., Pettkus, N., . . . Haass, C. (2019). Loss of TREM2 function increases amyloid seeding but reduces plaque-associated ApoE. *Nat Neurosci*, *22*(2), 191-204. https://doi.org/10.1038/s41593-018-0296-9

Parkhurst, C. N., Yang, G., Ninan, I., Savas, J. N., Yates, J. R., 3rd, Lafaille, J. J., Hempstead, B. L., Littman, D. R., & Gan, W. B. (2013). Microglia promote learning-dependent synapse formation through brain-derived neurotrophic factor. *Cell*, *155*(7), 1596-1609. https://doi.org/10.1016/j.cell.2013.11.030

Pfrieger, F. W. (2003). Outsourcing in the brain: do neurons depend on cholesterol delivery by astrocytes? *Bioessays*, *25*(1), 72-78. https://doi.org/10.1002/bies.10195

Porsteinsson, A. P., Isaacson, R. S., Knox, S., Sabbagh, M. N., & Rubino, I. (2021). Diagnosis of Early Alzheimer's Disease: Clinical Practice in 2021. *J Prev Alzheimers Dis*, *8*(3), 371-386. https://doi.org/10.14283/jpad.2021.23

Porter, F. D., Scherrer, D. E., Lanier, M. H., Langmade, S. J., Molugu, V., Gale, S. E., Olzeski, D., Sidhu, R., Dietzen, D. J., Fu, R., Wassif, C. A., Yanjanin, N. M., Marso, S. P., House, J., Vite, C., Schaffer, J. E., & Ory, D. S. (2010). Cholesterol oxidation products are sensitive and specific blood-based biomarkers for Niemann-Pick C1 disease. *Sci Transl Med*, *2*(56), 56ra81. https://doi.org/10.1126/scitranslmed.3001417

Puzzo, D., Privitera, L., Fa, M., Staniszewski, A., Hashimoto, G., Aziz, F., Sakurai, M., Ribe, E. M., Troy, C. M., Mercken, M., Jung, S. S., Palmeri, A., & Arancio, O. (2011). Endogenous amyloid-β is necessary for hippocampal synaptic plasticity and memory. *Ann Neurol*, *69*(5), 819-830. https://doi.org/10.1002/ana.22313

Puzzo, D., Privitera, L., Leznik, E., Fà, M., Staniszewski, A., Palmeri, A., & Arancio, O. (2008). Picomolar amyloid-beta positively modulates synaptic plasticity and memory in hippocampus. *J Neurosci*, *28*(53), 14537-14545. https://doi.org/10.1523/jneurosci.2692-08.2008

Quan, G., Xie, C., Dietschy, J. M., & Turley, S. D. (2003). Ontogenesis and regulation of cholesterol metabolism in the central nervous system of the mouse. *Brain Res Dev Brain Res*, *146*(1-2), 87-98. https://doi.org/10.1016/j.devbrainres.2003.09.015

Ralhan, I., Chang, C.-L., Lippincott-Schwartz, J., & Ioannou, M. S. (2021). Lipid droplets in the nervous system. *Journal of Cell Biology*, *220*(7). https://doi.org/10.1083/jcb.202102136

Renier, N., Wu, Z., Simon, D. J., Yang, J., Ariel, P., & Tessier-Lavigne, M. (2014). iDISCO: a simple, rapid method to immunolabel large tissue samples for volume imaging. *Cell*, *159*(4), 896-910. https://doi.org/10.1016/j.cell.2014.10.010

Roberson, E. D., Halabisky, B., Yoo, J. W., Yao, J., Chin, J., Yan, F., Wu, T., Hamto, P., Devidze, N., Yu, G. Q., Palop, J. J., Noebels, J. L., & Mucke, L. (2011). Amyloid-β/Fyn-induced synaptic, network, and cognitive impairments depend on tau levels in multiple mouse models of Alzheimer's disease. *J Neurosci*, *31*(2), 700-711. https://doi.org/10.1523/jneurosci.4152-10.2011

Roberson, E. D., Scearce-Levie, K., Palop, J. J., Yan, F., Cheng, I. H., Wu, T., Gerstein, H., Yu, G. Q., & Mucke, L. (2007). Reducing endogenous tau ameliorates amyloid beta-induced deficits in an Alzheimer's disease mouse model. *Science*, *316*(5825), 750-754. https://doi.org/10.1126/science.1141736

Rodríguez, J. J., Olabarria, M., Chvatal, A., & Verkhratsky, A. (2009). Astroglia in dementia and Alzheimer's disease. *Cell Death & Differentiation*, *16*(3), 378-385. https://doi.org/10.1038/cdd.2008.172

Rogers, J., Strohmeyer, R., Kovelowski, C. J., & Li, R. (2002). Microglia and inflammatory mechanisms in the clearance of amyloid beta peptide. *Glia*, *40*(2), 260-269. https://doi.org/10.1002/glia.10153

Rogers, M. A., Liu, J., Song, B.-L., Li, B.-L., Chang, C. C. Y., & Chang, T.-Y. (2015). Acyl-CoA:cholesterol acyltransferases (ACATs/SOATs): Enzymes with multiple sterols as substrates and as activators. *The Journal of steroid biochemistry and molecular biology*, *151*, 102-107. https://doi.org/10.1016/j.jsbmb.2014.09.008

Saher, G., Brugger, B., Lappe-Siefke, C., Mobius, W., Tozawa, R., Wehr, M. C., Wieland, F., Ishibashi, S., & Nave, K. A. (2005). High cholesterol level is essential for myelin membrane growth. *Nat Neurosci*, *8*(4), 468-475. https://doi.org/10.1038/nn1426

Saher, G., & Stumpf, S. K. (2015). Cholesterol in myelin biogenesis and hypomyelinating disorders. *Biochim Biophys Acta*, *1851*(8), 1083-1094. https://doi.org/10.1016/j.bbalip.2015.02.010

Saito, M., Benson, E. P., Saito, M., & Rosenberg, A. (1987). Metabolism of cholesterol and triacylglycerol in cultured chick neuronal cells, glial cells, and fibroblasts: accumulation of esterified cholesterol in serum-free culture. *J Neurosci Res*, *18*(2), 319-325. https://doi.org/10.1002/jnr.490180208

Salter, M. W., & Stevens, B. (2017). Microglia emerge as central players in brain disease. *Nat Med*, *23*(9), 1018-1027. https://doi.org/10.1038/nm.4397

Sandbrink, R., Masters, C. L., & Beyreuther, K. (1996). APP gene family. Alternative splicing generates functionally related isoforms. *Ann N Y Acad Sci*, *777*, 281-287. https://doi.org/10.1111/j.1749-6632.1996.tb34433.x

Savonenko, A. V., Melnikova, T., Li, T., Price, D. L., & Wong, P. C. (2015). Chapter 21 - Alzheimer Disease. In M. J. Zigmond, L. P. Rowland, & J. T. Coyle (Eds.), *Neurobiology of Brain Disorders* (pp. 321-338). Academic Press. https://doi.org/https://doi.org/10.1016/B978-0-12-398270-4.00021-5

Schindelin, J., Arganda-Carreras, I., Frise, E., Kaynig, V., Longair, M., Pietzsch, T., Preibisch, S., Rueden, C., Saalfeld, S., Schmid, B., Tinevez, J.-Y., White, D. J., Hartenstein, V., Eliceiri, K., Tomancak, P., & Cardona, A. (2012). Fiji: an open-source platform for biological-image analysis. *Nature Methods*, *9*(7), 676-682. https://doi.org/10.1038/nmeth.2019

Selkoe, D. J. (1991). The molecular pathology of Alzheimer's disease. *Neuron*, *6*(4), 487-498. https://doi.org/10.1016/0896-6273(91)90052-2

Seubert, P., Vigo-Pelfrey, C., Esch, F., Lee, M., Dovey, H., Davis, D., Sinha, S., Schiossmacher, M., Whaley, J., Swindlehurst, C., McCormack, R., Wolfert, R., Selkoe, D., Lieberburg, I., & Schenk, D. (1992). Isolation and quantification of soluble Alzheimer's β-peptide from biological fluids. *Nature*, *359*(6393), 325-327. https://doi.org/10.1038/359325a0

Shibata, M., Yamada, S., Kumar, S. R., Calero, M., Bading, J., Frangione, B., Holtzman, D. M., Miller, C. A., Strickland, D. K., Ghiso, J., & Zlokovic, B. V. (2000). Clearance of Alzheimer's amyloid-ss(1-40) peptide from brain by LDL receptor-related protein-1 at the blood-brain barrier. *J Clin Invest*, *106*(12), 1489-1499. https://doi.org/10.1172/jci10498

Silvius, J. R. (2003). Role of cholesterol in lipid raft formation: lessons from lipid model systems. *Biochimica et Biophysica Acta (BBA) - Biomembranes*, *1610*(2), 174-183. https://doi.org/https://doi.org/10.1016/S0005-2736(03)00016-6

Simons, K., & Ehehalt, R. (2002). Cholesterol, lipid rafts, and disease. *The Journal of clinical investigation*, *110*(5), 597-603. https://doi.org/10.1172/JCI16390

Simons, M., Keller, P., De Strooper, B., Beyreuther, K., Dotti, C. G., & Simons, K. (1998). Cholesterol depletion inhibits the generation of beta-amyloid in hippocampal neurons. *Proc Natl Acad Sci U S A*, *95*(11), 6460-6464. https://doi.org/10.1073/pnas.95.11.6460

Simons, M., & Nave, K.-A. (2015). Oligodendrocytes: Myelination and Axonal Support. *Cold Spring Harbor perspectives in biology*, *8*(1), a020479-a020479. https://doi.org/10.1101/cshperspect.a020479

Sobue, A., Komine, O., Hara, Y., Endo, F., Mizoguchi, H., Watanabe, S., Murayama, S., Saito, T., Saido, T. C., Sahara, N., Higuchi, M., Ogi, T., & Yamanaka, K. (2021). Microglial gene signature reveals loss of homeostatic microglia associated with neurodegeneration of Alzheimer's disease. *Acta Neuropathologica Communications*, *9*(1), 1. https://doi.org/10.1186/s40478-020-01099-x

Sofroniew, M. V., & Vinters, H. V. (2010). Astrocytes: biology and pathology. *Acta Neuropathol*, *119*(1), 7-35. https://doi.org/10.1007/s00401-009-0619-8

Spangenberg, E., Severson, P. L., Hohsfield, L. A., Crapser, J., Zhang, J., Burton, E. A., Zhang, Y., Spevak, W., Lin, J., Phan, N. Y., Habets, G., Rymar, A., Tsang, G., Walters, J., Nespi, M., Singh, P., Broome, S., Ibrahim, P., Zhang, C., . . . Green, K. N. (2019). Sustained microglial depletion with CSF1R inhibitor impairs parenchymal plaque development in an Alzheimer's disease model. *Nat Commun*, *10*(1), 3758. https://doi.org/10.1038/s41467-019-11674-z

Spiteri, A. G., Wishart, C. L., Pamphlett, R., Locatelli, G., & King, N. J. C. (2022). Microglia and monocytes in inflammatory CNS disease: integrating phenotype and function. *Acta Neuropathol*, *143*(2), 179-224. https://doi.org/10.1007/s00401-021-02384-2

Stelzmann, R. A., Norman Schnitzlein, H., & Reed Murtagh, F. (1995). An english translation of alzheimer's 1907 paper, "über eine eigenartige erkankung der hirnrinde". *Clinical Anatomy*, *8*(6), 429-431. https://doi.org/https://doi.org/10.1002/ca.980080612

Streit, W. J., Sammons, N. W., Kuhns, A. J., & Sparks, D. L. (2004). Dystrophic microglia in the aging human brain. *Glia*, *45*(2), 208-212. https://doi.org/10.1002/glia.10319

Strittmatter, W. J., Weisgraber, K. H., Huang, D. Y., Dong, L. M., Salvesen, G. S., Pericak-Vance, M., Schmechel, D., Saunders, A. M., Goldgaber, D., & Roses, A. D. (1993). Binding of human apolipoprotein E to synthetic amyloid beta peptide: isoform-specific effects and implications for late-onset Alzheimer disease. *Proc Natl Acad Sci U S A*, *90*(17), 8098-8102. https://doi.org/10.1073/pnas.90.17.8098

Tajima, Y., Ishikawa, M., Maekawa, K., Murayama, M., Senoo, Y., Nishimaki-Mogami, T., Nakanishi, H., Ikeda, K., Arita, M., Taguchi, R., Okuno, A., Mikawa, R., Niida, S., Takikawa, O., & Saito, Y. (2013). Lipidomic analysis of brain tissues and plasma in a mouse model expressing mutated human amyloid precursor protein/tau for Alzheimer's disease. *Lipids in Health and Disease*, *12*(1), 68. https://doi.org/10.1186/1476-511X-12-68

Takahashi, R. H., Nagao, T., & Gouras, G. K. (2017). Plaque formation and the intraneuronal accumulation of β-amyloid in Alzheimer's disease. *Pathol Int*, *67*(4), 185-193. https://doi.org/10.1111/pin.12520

Tambini, M. D., Norris, K. A., & D'Adamio, L. (2020). Opposite changes in APP processing and human Aβ levels in rats carrying either a protective or a pathogenic APP mutation. *Elife*, *9*, e52612. https://doi.org/10.7554/eLife.52612

Tang, Y., & Le, W. (2016). Differential Roles of M1 and M2 Microglia in Neurodegenerative Diseases. *Molecular Neurobiology*, *53*(2), 1181-1194. https://doi.org/10.1007/s12035-014-9070-5

Terry, R. D., Masliah, E., Salmon, D. P., Butters, N., DeTeresa, R., Hill, R., Hansen, L. A., & Katzman, R. (1991). Physical basis of cognitive alterations in Alzheimer's disease: synapse loss is the major correlate of cognitive impairment. *Ann Neurol*, *30*(4), 572-580. https://doi.org/10.1002/ana.410300410

Tripathi, B. J., & Tripathi, R. C. (1974). Vacuolar transcellular channels as a drainage pathway for cerebrospinal fluid. *J Physiol*, *239*(1), 195-206. https://doi.org/10.1113/jphysiol.1974.sp010563

Ulland, T. K., & Colonna, M. (2018). TREM2 - a key player in microglial biology and Alzheimer disease. *Nat Rev Neurol*, *14*(11), 667-675. https://doi.org/10.1038/s41582-018-0072-1

Vance, J. E., Hayashi, H., & Karten, B. (2005). Cholesterol homeostasis in neurons and glial cells. *Seminars in Cell & Developmental Biology*, *16*(2), 193-212. https://doi.org/10.1016/j.semcdb.2005.01.005

vom Berg, J., Prokop, S., Miller, K. R., Obst, J., Kälin, R. E., Lopategui-Cabezas, I., Wegner, A., Mair, F., Schipke, C. G., Peters, O., Winter, Y., Becher, B., & Heppner, F. L. (2012). Inhibition of IL-12/IL-23 signaling reduces Alzheimer's disease–like pathology and cognitive decline. *Nature Medicine*, *18*(12), 1812-1819. https://doi.org/10.1038/nm.2965

Wahrle, S. E., Jiang, H., Parsadanian, M., Legleiter, J., Han, X., Fryer, J. D., Kowalewski, T., & Holtzman, D. M. (2004). ABCA1 Is Required for Normal Central Nervous System ApoE Levels and for Lipidation of Astrocyte-secreted apoE*. *Journal of Biological Chemistry*, *279*(39), 40987-40993. https://doi.org/https://doi.org/10.1074/jbc.M407963200

Wakselman, S., Bechade, C., Roumier, A., Bernard, D., Triller, A., & Bessis, A. (2008). Developmental neuronal death in hippocampus requires the microglial CD11b integrin and DAP12 immunoreceptor. *J Neurosci*, *28*(32), 8138-8143. https://doi.org/10.1523/JNEUROSCI.1006-08.2008

Wang, H. (2021). Microglia Heterogeneity in Alzheimer's Disease: Insights From Single-Cell Technologies [Review]. *Frontiers in Synaptic Neuroscience*, *13*. https://doi.org/10.3389/fnsyn.2021.773590

Wang, W. Y., Tan, M. S., Yu, J. T., & Tan, L. (2015). Role of pro-inflammatory cytokines released from microglia in Alzheimer's disease. *Ann Transl Med*, *3*(10), 136. https://doi.org/10.3978/j.issn.2305-5839.2015.03.49

Wang, Y., Rogers, P. M., Su, C., Varga, G., Stayrook, K. R., & Burris, T. P. (2008). Regulation of cholesterologenesis by the oxysterol receptor, LXRalpha. *The Journal of biological chemistry*, *283*(39), 26332-26339. https://doi.org/10.1074/jbc.M804808200

Warren, E. C., Walker, M. C., & Williams, R. S. B. (2018). All You Need Is Fats-for Seizure Control: Using Amoeba to Advance Epilepsy Research. *Front Cell Neurosci*, *12*, 199. https://doi.org/10.3389/fncel.2018.00199

Weller, R. O., Djuanda, E., Yow, H. Y., & Carare, R. O. (2009). Lymphatic drainage of the brain and the pathophysiology of neurological disease. *Acta Neuropathol*, *117*(1), 1-14. https://doi.org/10.1007/s00401-008-0457-0

Weller, R. O., Massey, A., Kuo, Y. M., & Roher, A. E. (2000). Cerebral amyloid angiopathy: accumulation of A beta in interstitial fluid drainage pathways in Alzheimer's disease. *Ann N Y Acad Sci*, *903*, 110-117. https://doi.org/10.1111/j.1749-6632.2000.tb06356.x

Wellington, C. L., Walker, E. K. Y., Suarez, A., Kwok, A., Bissada, N., Singaraja, R., Yang, Y.-Z., Zhang, L.-H., James, E., Wilson, J. E., Francone, O., McManus, B. M., & Hayden, M. R. (2002). ABCA1 mRNA and Protein Distribution Patterns Predict Multiple Different Roles and Levels of Regulation. *Laboratory Investigation*, *82*(3), 273-283. https://doi.org/10.1038/labinvest.3780421

Winchenbach, J., Düking, T., Berghoff, S. A., Stumpf, S. K., Hülsmann, S., Nave, K.-A., & Saher, G. (2016). Inducible targeting of CNS astrocytes in Aldh1l1-CreERT2 BAC transgenic mice. *F1000Research*, *5*, 2934-2934. https://doi.org/10.12688/f1000research.10509.1

Winkler, M. B. L., Kidmose, R. T., Szomek, M., Thaysen, K., Rawson, S., Muench, S. P., Wustner, D., & Pedersen, B. P. (2019). Structural Insight into Eukaryotic Sterol Transport through Niemann-Pick Type C Proteins. *Cell*, *179*(2), 485-497 e418. https://doi.org/10.1016/j.cell.2019.08.038

Wolozin, B. (2004). Cholesterol and the Biology of Alzheimer's Disease. *Neuron*, *41*(1), 7-10. https://doi.org/10.1016/S0896-6273(03)00840-7

Wolters, F. J., Yang, Q., Biggs, M. L., Jakobsdottir, J., Li, S., Evans, D. S., Bis, J. C., Harris, T. B., Vasan, R. S., Zilhao, N. R., Ghanbari, M., Ikram, M. A., Launer, L., Psaty, B. M., Tranah, G. J., Kulminski, A. M., Gudnason, V., & Seshadri, S. (2019). The impact of APOE genotype on survival: Results of 38,537 participants from six population-based cohorts

(E2-CHARGE). *PLoS One*, *14*(7), e0219668. https://doi.org/10.1371/journal.pone.0219668

World Alzheimer Report 2019. *Alzheimer´s Disease International*. https://www.alzint.org/u/WorldAlzheimerReport2019.pdf

Wyss-Coray, T. (2006). Inflammation in Alzheimer disease: driving force, bystander or beneficial response? *Nat Med*, *12*(9), 1005-1015. https://doi.org/10.1038/nm1484

Wyss-Coray, T., Lin, C., Yan, F., Yu, G.-Q., Rohde, M., McConlogue, L., Masliah, E., & Mucke, L. (2001). TGF-β1 promotes microglial amyloid-β clearance and reduces plaque burden in transgenic mice. *Nature Medicine*, *7*(5), 612-618. https://doi.org/10.1038/87945

Xiong, H., Callaghan, D., Jones, A., Walker, D. G., Lue, L. F., Beach, T. G., Sue, L. I., Woulfe, J., Xu, H., Stanimirovic, D. B., & Zhang, W. (2008). Cholesterol retention in Alzheimer's brain is responsible for high beta- and gamma-secretase activities and Abeta production. *Neurobiol Dis*, *29*(3), 422-437. https://doi.org/10.1016/j.nbd.2007.10.005

Zelcer, N., Hong, C., Boyadjian, R., & Tontonoz, P. (2009). LXR regulates cholesterol uptake through Idol-dependent ubiquitination of the LDL receptor. *Science*, *325*(5936), 100-104. https://doi.org/10.1126/science.1168974

Zhang, X., & Song, W. (2013). The role of APP and BACE1 trafficking in APP processing and amyloid-β generation. *Alzheimer's Research & Therapy*, *5*(5), 46. https://doi.org/10.1186/alzrt211

Zhang, Y. W., Thompson, R., Zhang, H., & Xu, H. (2011). APP processing in Alzheimer's disease. *Mol Brain*, *4*, 3. https://doi.org/10.1186/1756-6606-4-3

Zia, S., Rawji, K. S., Michaels, N. J., Burr, M., Kerr, B. J., Healy, L. M., & Plemel, J. R. (2020). Microglia Diversity in Health and Multiple Sclerosis [Review]. *Frontiers in Immunology*, *11*. https://doi.org/10.3389/fimmu.2020.588021

6 Appendix

6.1 List of tables

6.2 List of figures

6.3 List of abbreviations

ABC	ATP binding cassette
ABCA1	ATP binding cassette subfamily A member 1
ABCA7	ATP binding cassette subfamily A member 7
Aβ	Amyloid β
ACAT1	Acetyl-CoA Acetyltransferase 1
αCTF_{83}	α-C-terminal fragment 83 residue
AD	Alzheimer´s disease
ADAM10	A disintegrin and metalloproteinase domain-containing protein 10
ADE	Aβ-degrading enzymes
ALS	Amyotrophic lateral sclerosis
APOA1	Apolipoprotein A1
APOD	Apolipoprotein D
APOE	Apolipoprotein E
APOJ	Apolipoprotein J
APP	Amyloid precursor protein
AXL	Axl receptor tyrosine kinase
BACE 1	Beta-secretase 1
BBB	Blood brain barrier
β CTF_{99}	B-C-terminal fragment 99 residue
BIN1	Bridging integrator 1
BMDM	Bone marrow derived macrophages
BPSD	Behavioral and psychological symptoms of dementia
C83	C-terminal fragment with 83 residues
C99	C-terminal fragment with 99 residues
CAA	Cerebral amyloid angiopathy
CE	Cholesterol esters
CLU	Clusterin
CLEC7A	C-type lectin domain family 7 member A
CNS	Central nervous system
CSF	Cerebrospinal fluid
CT	Computerized tomography
CTF	C-terminal fragment, carboxyterminal fragment
CR1	Complement C3b/C4b receptor 1

CYP46	24S-hydroxylase
CYP51	14-alpha-demethylase
DAM	Disease associated microglia
DGE	Differential Gene Expression
DHCR7	7-dehydrocholesterol reductase
DHCR24	24-dehydrocholesterol reductase
DNA	Desoxyribonucleic acid
EAE	Experimental autoimmune encephalomyelitis
ECE1	Endothelin Converting Enzyme 1
ER	Endoplasmatisches Riticulum
EOAD	Early-onset Alzheimer´s disease
DMAPP	Dimethylallyl pyrophosphate
FAD	Familial Alzheimer´s disease
FDA	U.S. Food and Drug Administration
FDFT1	Farnesyl-diphosphate farnesyltransferase 1
FPP	Farnesyl pyrophosphate
GCPII	Glutamate carboxypeptidase II
GFAP	Glial fibrillary acidic protein
GPP	Geranyl pyrophosphate
HDL	High-density lipoprotein
HMG-CoA	Acetyl-CoA to 3-hydroxy-3-methylglutaryl-CoA
HMGCS	HMG-CoA synthase
HMGCR	HMG-CoA reductase
IDE	Insulysin, insulin-degrading enzyme
INSIG	Insulin-induced gene
IPP	Isopentenyl pyrophosphate
iPSC	Induced pluripotent stem cells
ITGAX	Integrin Subunit Alpha X
LAMP1	Lysosomal-associated membrane protein 1
LD	Lipid droplets
LDLR	Low density lipoprotein receptor
LOAD	Late-onset Alzheimer´s disease
LRP	LDL receptor-related protein
MACS	Magnetic-activated cell sorting
MMP9	Matrix metallopeptidase 9
MRI	Magnetic resoanace imaging
mRNA	Messenger ribonucleic acid
NEP	Neprilysin
OPC	Oligodendrocyte progenitor cell
PET	Positron emission tomography
PICALM	Phosphatidylinositol-binding clatherin assembly protein

PSEN 1	Presenilin 1
PSEN 2	Presenilin 2
RXR	Retinoid X receptor
RNA	Ribonucleic acid
SAD	Sporadic Alzheimer´s disease
SCAP	SREBP cleavage-activating protein
SPIA	Single primer isothermal amplification
SOAT1	Sterol O-Acyltransferase 1
SPP1	Secreted Phosphoprotein 1
SQLE	Squalene epoxidase
SRE	Sterol regulatory element
SREBP-2	Sterol regulatory element-binding protein 2
TGN	Trans-Golgi network
TJ	Tight junctions
TPM	Transcripts Per Millions
TREM2	Triggering Receptor Expressed On Myeloid Cells 2
TYROBP	Tyro protein tyrosine kinase-binding protein
24-OHC	24S-hydroxycholesterol

6.4 Publications

Stefan A. Berghoff, Tim Düking, **Lena Spieth**, Jan Winchenbach, Sina K. Stumpf, Nina Gerndt, Kathrin Kusch, Torben Ruhwedel, Wiebke Möbius & Gesine Saher. Blood-brain barrier hyperpermeability precedes demyelination in the cuprizone model
Acta Neuropathologica Communications, 2017 Dec, 01

Sina K. Stumpf, Stefan A. Berghoff, Andrea Trevisiol, **Lena Spieth**, Tim Düking, Lennart V. Schneider, Lennart Schlaphoff, Steffi Dreha-Kulaczewski, Annette Bley, Dinah Burfeind, Kathrin Kusch, Miso Mitkovski, Torben Ruhwedel, Philipp Guder, Heiko Röhse, Jonas Denecke, Jutta Gärtner, Wiebke Möbius, Klaus-Armin Nave & Gesine Saher. Ketogenic diet ameliorates axonal defects and promotes myelination in Pelizaeus–Merzbacher disease
Acta Neuropathologica, 2019 Mar, 27

Sergey Kalinin, Gordon P. Meares, Shao Xia Lin, Elizabeth A. Pietruczyk, Gesine Saher, **Lena Spieth**, Klaus-Armin Nave, Anne I. Boullerne, Sarah E. Lutz, Etty N. Benveniste, Douglas L. Feinstein. Liver kinase B1 depletion from astrocytes worsens disease in a mouse model of multiple sclerosis
Glia, 2019 Oct, 30

Berghoff SA, **Spieth L**, Sun T, Hosang L, Schlaphoff L, Depp C, Düking T, Winchenbach J, Neuber J, Ewers D, Scholz P, van der Meer F, Cantuti-Castelvetri L, Sasmita AO, Meschkat M, Ruhwedel T, Möbius W, Sankowski R, Prinz M, Huitinga I, Sereda MW, Odoardi F, Ischebeck T, Simons M, Stadelmann-Nessler C, Edgar JM, Nave KA, Saher G. Microglia facilitate repair of demyelinated lesions via post-squalene sterol synthesis.
Nature Neuroscience, 2021 Jan, 24

Depp C, Sun T, Sasmita AO, **Spieth L**, Berghoff SA, Steixner-Kumar AA, Subramanian S, Möbius W, Göbbels S, Saher G, Zampar S, Wirths O, Thalmann M, Saito T, Saido T, Krueger-Burg D, Kawaguchi R, Willem M, Haass C, Geschwind D, Ehrenreich H, Stassart R, Nave K. Ageing-associated myelin dysfunction drives amyloid deposition in mouse models of Alzheimer's disease
BioRxiv, 2021 Aug, 02

Lena Spieth, Stefan A Berghoff, Sina K Stumpf, Jan Winchenbach, Thomas Michaelis, Takashi Watanabe, Nina Gerndt, Tim Düking, Sabine Hofer, Torben Ruhwedel, Ali H Shaib, Katrin Willig, Katharina Kronenberg, Uwe Karst, Jens Frahm, Jeong Seop Rhee, Susana Minguet, Wiebke Möbius, Niels Kruse, Christian von der Brelie, Peter Michels, Christine Stadelmann, Petra Hülper, Gesine Saher. Anesthesia triggers drug delivery to experimental glioma in mice by hijacking caveolar transport
Neuro-Oncology Advances, 2021 Sep, 20

Berghoff SA*, **Spieth L***, Sun T, Hosang L, Depp C, Sasmita AO, Vasileva MH, Scholz P, Zhao Y, Krueger-Burg D, Wichert S, Brown ER, Michail K, Nave KA, Bonn S, Odoardi F, Rossner M, Ischebeck T, Edgar JM, Saher G. Neuronal cholesterol synthesis is essential for repair of chronically demyelinated lesions in mice.
Cell Reports, 2021 Oct, 26

Sahab Arinrad, Justus B. H. Wilke, Anna Seelbach, José Doeren, Martin Hindermann, Umer Javed Butt, Agnes A. Steixner-Kumar, **Lena Spieth**, Anja Ronnenberg, Hong Pan, Stefan A. Berghoff, Michael Hollmann, Fred Lühder, Klaus-Armin Nave, Karl Bechter & Hannelore Ehrenreich. NMDAR1 autoantibodies amplify behavioral phenotypes of genetic white matter inflammation: a mild encephalitis model with neuropsychiatric relevance
Molecular Psychiatry, 2021 Dec, 06

Stefan A. Berghoff, **Lena Spieth**, Gesine Saher. Local cholesterol metabolism orchestrates remyelination
Trends in Neuroscience, 2022 Feb, 10

Tim Düking, **Lena Spieth**, Stefan A Berghoff, Lars Piepkorn, Annika M Schmidke, Miso Mitkovski, Nirmal Kannaiyan, Leon Hosang, Patricia Scholz, Ali H Shaib, Lennart V Schneider, Dörte Hesse, Torben Ruhwedel, Ting Sun, Lisa Linhoff, Andrea Trevisiol, Susanne Köhler, Adrian Marti Pastor, Thomas Misgeld, Michael Sereda, Imam Hassouna, Moritz J Rossner, Francesca Odoardi, Till Ischebeck, Livia de Hoz, Johannes Hirrlinger, Olaf Jahn, Gesine Saher. Ketogenic diet uncovers differential metabolic plasticity of brain cells.
Science Advances, 2022 Sep, 16.

7 Acknowledgements

First of all, I want to thank my supervisor Dr. Gesine Saher for giving me the opportunity to work on this great project. Furthermore, I would like to thank her for all the scientific input and support during the whole time of my PhD and the possibility to develop a broad-range of skills by working on several projects. It is a pleasure to be part of this successful team.

Secondly I thank Prof. Dr. Klaus-Armin Nave for the opportunity to work in his department, for critical advises and contribution of scientific expertise.

Moreover, I want to thank my thesis advisory committee members, Prof. Thomas Bayer and Prof. Dr. Hannelore Ehrenreich for fruitful discussions during my TAC meetings and helpful advices how to proceed with my project.

In addition, I would like to thank all members of my examination committee Prof. Rüdiger Behr, Prof Susann Boretius and Dr. Nico Posnien for taking the time to attend my thesis defense.

I am sincerely grateful to Dr. Stefan Berghoff, Dr. Constanze Depp, Dr. Ting Sun and Andrew Sasmita for all the inspiring discussions and great contribution to this project.

A big thank you also to our collaborators Dr. Francesca Odoardi and Dr. Leon Hosang for their help with flow cytometry and their contribution towards this project. I further want to thank Dr. Gabriela Salinas-Riester, Fabian Ludewig and Susanne Luthin of the NGS Facility.

I would especially like to thank previous and recent members of the AG Saher: Dr. Tim Düking for introducing me to a really helpful laboratory technique and a joyful environment in the lab. Dr. Jan Winchenbach for a short but great time and the contribution to this project. Dr. Sina Stumpf for a great start in the lab and a wonderful time working together. A big thank you to Annika Schmidke for the support, especially during the last months. Special thanks to Dr. Stefan Berghoff for all the inspiring discussions, scientific advice and supportive contributions towards this project. I really appreciate it!

I am grateful to the outstanding students I had the pleasure to supervise: Annika Schmidke, Taisiia Nazarenko, Henrike Jungeblut and Hoang Duy Nguyen for their contributions to this project and beyond during your lab rotation and bachelor thesis.

My deepest gratitude goes to Lisa for always supporting me on a scientific and personal level, to Sophie for all the help and the fun time in and outside the lab and Theresa for fruitful discussions and the wonderful time. I am thankful for every minute we spent together!

I am grateful to all the colleagues that got friends during the last years. Stefan for the amazing teamwork and for being reachable all the time. Ting for the cake breaks, massages and the time we spent together. Constanze for funny lab times and bouldering trips. Leon for always making me laugh and the good Safran Sours. Tobi for the good food and the joyful time. Tim for the fun time in the lab and the calls even after you left. Swati for the lovely care and amazing naan. Maria for always making me realize that there is more than science. Andrew for all the funny moment and your help. Alejandro for your sense of humor, especially in the last weeks. Silya for your help in busy times.
It was a pleasure to meet you!

I would like to express my gratitude to various people for their constant support and help:

Michaela Schmalstieg for the administrative support and the wonderful coffee breaks.

Annette Fahrenholz, without you, handling all experiments would have been hard to manage.

Ulli Bode, Ramona Jung, Uschi Kutzke and Dr. Kathrin Kusch for your technical support.

Dr. Wiebke Möbius, Torben Ruhwedel and Boguslawa Sadowski for their constant support the friendly working relationship, and a coffee now and then.

Our animal caretakers Tanja Freerk, Conny Casper, Sarah Schulze, Marion Peine, Ines Gremmes, Kathrin Wilke, Ute Bornemann, Dennis Funk, Nadja Hoffmeister, Stefan Röglin and Nadine Asmus for always keeping an eye on my mice and for your good teamwork.

Dr. Sarah Kimmina, Dr. Ursula Fünfschilling and Dr. Anke Schräpler for providing an excellent mouse house, transgenic animal facility and support when it comes to animal licences.

Martin, Rolf, Hajo and Lothar for their continuous support when something technical did not work as expected.

Miso and Heiko for making the great Light Microscopy Facility available and for support with data generation and analysis.

Finally, I would like to thank my family and friends for their loving support and for enabling me to finish my PhD-studies.

Thanks to Sotirios Pavlidis and Enzymel for supporting me in the last weeks and for helping me with the graphics.

Thanks to Jana Vieten for making the Bachelor easier and more fun and for your friendship since.

An enormous thank you to Miriam Steimmig, my best friend and for always being there, in good and bad times.

The biggest thank you goes to my mother Andrea, my father Udo and my sister Janina for being my greatest supporter and making me the person I am today.

Curriculum Vitae

Lena Spieth

CONTACT

lena.spieth@dzne..de

https://www.linkedin.com/in/lena-spieth-1b2730b0/

https://www.researchgate.net/profile/Lena-Spieth

LANGUAGES

German

English

Spanish

RESEARCH INTERESTS

Neuropathology

Lipids

Genetics

Glial biology

ACTIVITIES

2018-2020 MPI-EM
Internal PhD representative

2019 MPG
N^2 event - organizor

SOFT SKILLS

Communication
Organization
Collaboration
Supervision
Teamwork
Creative Thinking

Signature and Date:

Spieth 24.10.2022

EDUCATION

2022 - present **Postdoctoral fellow**
Technical University of Munich
Institute of Neuronal Cell Biology
Munich, Germany

2018 - 2022 **PhD thesis**
Max Planck Institute for Multidisciplinary Sciences
Department of Neurogenetics
Göttingen, Germany
Thesis title: Cell specific cholesterol synthesis ablation affects cerebral β-amyloidosis

2016 - 2018 **Master of Science**
Georg-August University
Molecular Medicine
Göttingen, Germany
Thesis: Max Planck Institute of Experiemntal Medicine, Göttingen

2013 - 2016 **Bachelor of Science**
Hochschule Furtwangen University
Molecular and Technical Medicine
Schwenningen, Germany
Thesis: Charité Univerity Medicine, Berlin

2009 - 2013 **Medical lab technician**
Klinikum Stuttgart

PROFESSIONAL EXPERIENCE

2016 - 2018 **Student assistant**
Institute of Pharmacology and Toxicology
University Medical Center, Göttingen, Germany

2016 **Student assistant**
Multi-Organ-Chip development
TissUse GmbH, Berlin, Germany

2015 **Research internship**
Department of Research and Development
IDEXX Laboratories Inc., Westbrook, Main, USA

2013 - 2015 **Student assistant**
IDEXX Laboratories Inc., Ludwigsburg, Germany

2012 - 2013 **Medical lab technician**
Department of Next-generation sequencing
Münchner Leukämielabor, München, Germany

CONFERENCES

27-28th October, 2021 **New Horizons in Alzheimer´s Disease**
Poster presentation: *Cell-specific choelsterol synthesis ablation affects cerebral β-amyloidosis*

07-10th July, 2021 **European Glia Meeting**
Poster presentation: *Cell-specific choelsterol synthesis ablation affects cerebral β-amyloidosis*

List of publications

Tim Düking*, **Lena Spieth***, Stefan A Berghoff*, ... Gesine Saher. (2022) Ketogenic diet uncovers differential metabolic plasticity of brain cells. *Science Advances*

Stefan A. Berghoff, **Lena Spieth**, Gesine Saher. (2022) Local choelsterol metabolism orchestrates remyelination. *Trends in Neuroscience*

Sahab Arinrad, Justus B. H. Wilke, Anna Seelbach, José Doeren, Martin Hindermann, Umer Javed Butt, Agnes A. Steixner-Kumar, **Lena Spieth**, … Karl Bechter & Hannelore Ehrenreich. (2021) NMDAR1 autoantibodies amplify behavioral phenotypes of genetic white matter inflammation: a mild encephalitis model with neuropsychiatric relevance. *Molecular Psychiatry*

Berghoff SA*, **Spieth L***, Sun T*, … Saher G. (2021) Neuronal cholesterol synthesis is essential for repair of chronically demyelinated lesions in mice. *Cell Reports*

Lena Spieth*, Stefan A Berghoff*, Sina K Stumpf*, … Gesine Saher. (2021) Anesthesia triggers drug delivery to experimental glioma in mice by hijacking caveolar transport. *Neuro-Oncology Advances*

Depp C, Sun T, Sasmita AO, **Spieth L**, … Nave K. (2021) Ageing-associated myelin dysfunction drives amyloid deposition in mouse models of Alzheimer's disease. *BioRxiv*

Berghoff SA, **Spieth L.**, … Nave KA, Saher G. (2021) Microglia facilitate repair of demyelinated lesions via post-squalene sterol synthesis. *Nature Neuroscience*

Sergey Kalinin, Gordon P. Meares, Shao Xia Lin, Elizabeth A. Pietruczyk, Gesine Saher, **Lena Spieth**, … Douglas L. Feinstein. (2019) Liver kinase B1 depletion from astrocytes worsens disease in a mouse model of multiple sclerosis. *Glia*

Sina K. Stumpf, Stefan A. Berghoff, Andrea Trevisiol, **Lena Spieth**, … Klaus-Armin Nave & Gesine Saher. (2019) Ketogenic diet ameliorates axonal defects and promotes myelination in Pelizaeus–Merzbacher disease. *Acta Neuropathologica*

Stefan A. Berghoff, Tim Düking, **Lena Spieth**, … Wiebke Möbius & Gesine Saher. (2017) Blood-brain barrier hyperpermeability precedes demyelination in the cuprizone

*shared first authorship

Signature and Date: